University of Massachusetts Medical School
eScholarship@UMMS

GSBS Dissertations and Theses | Graduate School of Biomedical Sciences

2020-08-31

Investigating the Role of Phox2B-expressing Glutamatergic Parafacial Zone Neurons in Sleep Wake Control

Evelyn T. M. Erickson
University of Massachusetts Medical School

Let us know how access to this document benefits you.
Follow this and additional works at: https://escholarship.umassmed.edu/gsbs_diss

Part of the Behavioral Neurobiology Commons

Repository Citation

Erickson ET. (2020). Investigating the Role of Phox2B-expressing Glutamatergic Parafacial Zone Neurons in Sleep Wake Control. GSBS Dissertations and Theses. https://doi.org/10.13028/tsyw-vr44. Retrieved from https://escholarship.umassmed.edu/gsbs_diss/1100

Creative Commons License

This work is licensed under a Creative Commons Attribution 4.0 License.
This material is brought to you by eScholarship@UMMS. It has been accepted for inclusion in GSBS Dissertations and Theses by an authorized administrator of eScholarship@UMMS. For more information, please contact Lisa.Palmer@umassmed.edu.

INVESTIGATING THE ROLE OF PHOX2B-EXPRESSING GLUTAMATERGIC PARAFACIAL ZONE NEURONS IN SLEEP WAKE CONTROL

A Master's Thesis Presented

By

Evelyn Erickson

Submitted to the faculty of the

University of Massachusetts Graduate School of Biomedical Sciences, Worcester

In partial fulfillment of the requirements for the degree of

MASTER OF SCIENCE

August 31, 2020

NEUROSCIENCE

INVESTIGATING THE ROLE OF PHOX2B-EXPRESSING GLUTAMATERGIC PARAFACIAL ZONE NEURONS IN SLEEP WAKE CONTROL

A Master's Thesis Presented

By

Evelyn Erickson

This work was undertaken in the Graduate School of Biomedical Sciences

Neuroscience Program

The signatures of the Master's Thesis Committee signify completion and approval as to style and content of the Thesis

____
Mary Ellen Lane, Ph.D.
Dean of the Graduate School of Biomedical Sciences

____
Daryl Bosco, Ph.D.
Chair of Committee

____
David Weaver, Ph.D.
Member of Committee

The signature of the Dean of the Graduate School of Biomedical Sciences signifies that the student has met all Master's degree graduation requirements of the school

____
Mary Ellen Lane, Ph.D.
Dean of the Graduate School of Biomedical Sciences

August 31, 2020

Acknowledgements

Thank you to the members of my Master's Thesis Committee: Mary Ellen Lane, Daryl Bosco, David Weaver, and additionally to Morgan Thompson, for their valuable guidance, support, and especially patience even in the midst of this global pandemic.

Thank you to Christelle Anaclet, my PI, for the opportunity to perform this research. Additionally, I would like to thank everyone in the lab: Loris Ferrari, Heinrich Gompf, and Oghomwen Igiesuorobo. Thank you to the Department of Neurobiology and Brudnick Neuropsychiatric Research Institute for the strong sense of scientific pursuit and student success. A special thank you to the wonderful administrators whose tireless efforts keep everything together.

Also thank you to Brian Lewis and Michelle Morrison, who took me into the IMSD program where I benefited greatly from having such support. It is a great program thanks to your caring and persistence.

Finally, I would like to thank those people who have been with me. To my coach, Brittany Smith, whose advice, guidance, and unwavering support gave me the strength to make it through. To my great friend Andrea Kingler, always understanding and sympathetic no matter how long we went between texts. I greatly appreciate the care and support of the kind friends over the years, and especially to Pablo Abrante who is simply one of the most caring people I know. And to Micah Young, for always being very enthusiastic and imbued with the power to renew my excitement for science.

Last but not least, thank you to Vitali and Shinobi, for being their hilarious, comforting, attention-demanding selves.

Abstract

Inhibitory GABAergic neurons in the parafacial zone (PZ^{GABA}) are essential for slow wave sleep (SWS). Since existing literature about the heterogenous population of PZ neurons is lacking, questions remain regarding the non-GABAergic sleep active PZ neurons. This study seeks to determine if glutamatergic PZ neurons expressing the transcription factor Phox2B (PZ^{Phox2B}) participate in sleep-wake control. Phox2B-*IRES*-Cre mice received injections of adeno-associated virus containing Cre-dependent diphtheria toxin subunit A (DTA) DNA into the PZ ($PZ^{Phox2B\text{-}DTA}$). Analysis of injection sites revealed transfection covering the PZ and the locus coeruleus, also known to express Phox2B. We recorded the sleep-wake cycle of $PZ^{Phox2B\text{-}DTA}$ mice and compared them with control mice, analyzing their sleep-wake quantity, fragmentation, and power spectral distribution.

We found total amounts and cortical power for wakefulness, SWS, and REM sleep of $PZ^{Phox2B\text{-}DTA}$ mice were unaffected. There was fragmentation in wakefulness during the active period for $PZ^{Phox2B\text{-}DTA}$ mice, seen as a significant reduction in the amount of time and number of episodes spent in the longest bout; however, wakefulness during the rest period was not significantly altered. No significant change was found in the bout numbers and amounts for SWS and REM sleep of $PZ^{Phox2B\text{-}DTA}$ mice. I was unable to confirm targeted ablation of $PZ^{Phox2B\text{-}DTA}$ neurons due to a lack of reliable antibody staining. Therefore, it remains possible that ablation of PZ^{Phox2B} neurons was incomplete and the wakeful

fragmentation is due to neuronal ablation outside of the PZ, such as in the neighboring LC.

Table of Contents

Signature Page ii
Acknowledgements iii
Abstract iv
Table of Contents vi
List of Figures vii
List of Tables viii
List of Copyrighted Materials Produced by the Author ix
List of Third Party Copyrighted Material x
Preface xi
Chapter 1 Introduction 1
  Understanding sleep 1
  Sleep Research 4
  Sleep-wake circuitry 10
  Project Summary 30
Chapter 2 Investigating the Role of Phox2B-expressing Glutamatergic Parafacial Zone Neurons in Sleep-Wake Control 34
  Abstract 34
  Introduction 36
  Materials and Methods 38
  Results 49
Chapter 3 Discussion 60
Appendix 1 Erickson et al., 2019 68
Bibliography 85

List of Figures

Figure 1.1: Wake-promoting Nuclei and Projections. 27

Figure 1.2: NREM Sleep-promoting Nuclei and Projections. 28

Figure 1.3: REM Sleep-promoting Nuclei and Projections. 29

Figure 2.1: Viral construct for neuronal ablation 45

Figure 2.2: Transduced Neurons at the Injection Site for $PZ^{Phox2B\text{-}DTA}$ mice 46

Figure 2.3: Sleep-wake Amounts 54

Figure 2.4: Sleep Architecture During the Rest Period (07:00-19:00) 55

Figure 2.5: Sleep Architecture of the Active Period (19:00-07:00) 56

Figure 2.6: Cortical EEG Power Distribution 57

Figure 2.7: Phox2B Immunofluorescence 58

Figure 2.8: Phox2B Immunohistochemistry 59

List of Tables

Table 2.1: Primary and Secondary Antibodies Used for Immunostaining........... 47

Table 2.2: List of Parameters During Troubleshooting 48

List of Copyrighted Materials Produced by the Author

Appendix 1 represents work previously published and is presented in accordance with copyright permissions from *Frontiers in Neuroscience* (Creative Commons CC-BY 4.0): Erickson, E. T. M., Ferrari, L. L., Gompf, H. S., & Anaclet, C. (2019). Differential Role of Pontomedullary Glutamatergic Neuronal Populations in Sleep-Wake Control. *Front Neurosci*, *13*, 755. https://doi.org/10.3389/fnins.2019.00755

List of Third Party Copyrighted Material

Figure 1.1, figure 1.2, and figure 1.3 represents work previously published and is presented in accordance with copyright permissions from *Elsevier* (license number 4896850820077): Gompf, H. S., & Anaclet, C. (2020). The neuroanatomy and neurochemistry of sleep-wake control. *Curr Opin Physiol*, *15*, 143-151. https://doi.org/10.1016/j.cophys.2019.12.012

Figure 2.1 represents work previously published and is presented in accordance with copyright permissions from *Elsevier* (license number 4895600663136): Kaur, S., Wang, J. L., Ferrari, L., Thankachan, S., Kroeger, D., Venner, A., Lazarus, M., Wellman, A., Arrigoni, E., Fuller, P. M., & Saper, C. B. (2017). A Genetically Defined Circuit for Arousal from Sleep during Hypercapnia. *Neuron*, *96*(5), 1153-1167.e1155. https://doi.org/10.1016/j.neuron.2017.10.009

Preface

The work presented in Chapter 2 represents unpublished experimental results conducted within the Anaclet Lab at University of Massachusetts Medical School, Graduate School of Biomedical Sciences. Genotyping was performed by Kawai So, Adwoa Sefah and Samantha Belculfine. Lab supplies were obtained, and lab reagents were prepared by Kawai So, Loris Ferrari, Adwoa Sefah and Samantha Belculfine. Manuscript preparation guidance was provided by Christelle Anaclet, Daryl Bosco and David Weaver. Mice were maintained at University of Massachusetts Medical School, Graduate School of Biomedical Sciences and cared for by Animal Medicine personnel and by Kawai So, Adwoa Sefah and Christelle Anaclet. Remaining experimental work, analysis, figures, tables, diagram, and manuscript preparation was provided by myself.

Appendix 1 represents work previously published and is presented in accordance with copyright permissions from *Frontiers in Neuroscience* (Creative Commons CC-BY 4.0).

Chapter 1

Introduction

Understanding sleep

A vital part of life

Sleep is one of the more highly evolutionarily conserved behaviors among living organisms. Every animal species studied to date, from jellyfish to humans, has exhibited a sleep-like state despite the vulnerability of doing so (Lesku & Ly, 2017; Lima et al., 2005). Humans spend about one-third of their lives asleep, totaling about 28 years. No other single activity has so much time dedicated to it, suggesting sleep plays a vital role throughout human life. As such, sleep is an important field of scientific inquiry.

Sleep appears as a period of inactivity due to relative unresponsiveness to external stimuli, but is a highly organized, complex, and dynamic state that is naturally occurring, periodic, and reversible (Neckelmann & Ursin, 1993). The cooperative interplay of many neuronal networks generates and regulates the sleep-wake cycle (Gompf & Anaclet, 2020). The brain's overall electrical activity changes significantly between wakefulness and sleep, cycling through several discrete states with corresponding alterations to the neural, endocrine, and somatic systems (Aldabal & Bahammam, 2011; Fink et al., 2018). A massive reorganization of gene expression takes place upon transitioning from wake to sleep, altering molecular and cellular biology of the brain (Cirelli, 2005; Cirelli et

al., 2004). Additionally, an organism's overall physiology undergoes significant changes in heart rate, body temperature, and muscle activity (Siegel, 2005).

Sleep in health and disease

While the exact physiological purpose remains a mystery, there are many functions known to be affected by the lack of sleep (Imeri & Opp, 2009; Lesku et al., 2011). The importance of this highly regulated process is evidenced by the presence of a sleep rebound mechanism designed to help ensure an organism recovers from too little sleep (Tobler & Borbély, 1985). Sleep's essential role has been most dramatically demonstrated through rats when after three to four weeks of being deprived of all sleep, the rats died due to the breakdown of metabolic processes (Everson et al., 1989).

Similar to nutrition and exercise, sleep is crucial for health and well-being, having far-reaching effects on many different physiological and cognitive functions. This includes the regulation of respiration rates, the regulation of hormone levels, thought processes, and emotional states (Arnal et al., 2015; Baglioni et al., 2010). Healthy sleep requires sufficient duration, good quality, appropriate timing, appropriate regularity, and the absence of sleep disturbances and disorders (Arnal et al., 2015; Blunden & Galland, 2014).

Disrupted sleep correlates with many negative health consequences and is comorbid with a variety of diseases. Adults who experience sleep disruption but are otherwise healthy, report increased likelihood of accidents and poor balance (Tobler & Borbély, 1985; Van Dongen et al., 2003), increased emotional distress

and mood changes (Babson et al., 2010), trouble thinking and concentration (Killgore, 2010), and increased proinflammatory responses and weakened immunity (Imeri & Opp, 2009). Notably, sleep disruption has detrimental effects on learning and memory (Wagner et al., 2001)

Longer-term consequences of sleep disruption include cardiovascular disease, hypertension, weight gain, diabetes, depression, and increased incidences of mortality (Cappuccio et al., 2011; Cappuccio et al., 2010). Additionally, sleep disruption can be a symptom of diseases such as Parkinson’s disease and epilepsy (Loddo et al., 2017; Méndez & Radtke, 2001).

Poor sleep does not affect just the one individual. The impairment of poor sleep can bring harm to others, as seen with the increased prevalence of automobile crashes and surgery errors in sleep deprived individuals (Eastridge et al., 2003; Landrigan, 2008). Sleep has become an ever-increasing health issue for modern society (Rajaratnam & Arendt, 2001; Roth et al., 2011). In an effort to identify sleep problems, official publications are categorizing them based on the behavioral and physiological phenotypes patients display (American Academy of Sleep, 2014; American Psychiatric Association, 2013). Insomnias, disorders involving the inability to fall asleep or stay asleep, are an increasingly reported struggle and could lead to increased risk of other diseases (Fernandez-Mendoza & Vgontzas, 2013; Roth et al., 2011). Hypersomnias, disorders of excessive sleepiness, include conditions where an individual experiences sleep onset inappropriately such as narcolepsy (Burgess & Scammell, 2012). Sleep health

impacts the daily lives of millions of people, making sleep research a vast and important field of investigation.

Sleep Research

Experimental measures of sleep

These shifts in an organism's physiology, accompanied by changes in alertness and consciousness, are called vigilance states, as detailed later. It is important that differences between wakefulness and sleep be definable, identifiable, and measurable to study the vigilance states of the sleep-wake cycle. While various technologies facilitate researching sleep and wakefulness in humans, model organisms such as rodents facilitate studying vigilance states because it is so highly evolutionarily conserved (Dringenberg, 2019; Lesku et al., 2019). Model organisms allow for additional dimensions in conducting research, such as genetic manipulation, organism alteration, variable isolation, and direct measurements of internal processes. Measurement and identification of vigilance states often utilizes electroencephalogram (EEG) recording of the brain, electromyogram (EMG) recording of muscles, electrooculogram (EOG) recording of eye movement, video recording, or changes in physiology such as breathing rate or body temperature.

Electrodes placed on the head detect the brain's electrical activity generated by neuronal firing. EEG is the difference of electrical potential measured between two electrodes, and is represented as a continuous waveform with variable amplitude and frequency (Timofeev et al., 2012). Amplitude, a measure

of electrical energy, is the distance from equilibrium to the wave peak or trough. (Dang-Vu et al., 2008). Frequency, measured in Hertz (Hz), is how many neuronal firing cycles occur in one second. High frequency reflects desynchronized activity of the neuronal assembly while low frequency indicates cortical synchronization (Moruzzi & Magoun, 1949). The waveform's amplitude and frequency patterns are typical to each vigilance state, as detailed later.

To reflect the different vigilance states of brain activity, EEG waveforms get classified into five frequency bands (Abo-Zahhad et al., 2015). The delta band ranges from 0 to 4 Hz. The theta band ranges from 4 to 9 Hz. The alpha band ranges from 9 to 15 Hz and the beta band ranges from 15 to 30 Hz. The remaining frequencies above 30 Hz are the gamma band. EEG machines recording the electrical activity of the brain provide a direct measurement of vigilance states (Hernan et al., 2017; Moruzzi & Magoun, 1949).

Muscle activity and muscle tone recorded by EMG fluctuate from high activity to no activity across different vigilance states. The EOG records eye movement, which changes between vigilance states. Video cameras record physical behavior and body posture which can be used in complementation with other measures to facilitate identification and classification of vigilance state. Measuring multiple parameters increases confidence in classifying vigilance state. Many mouse-based experiments utilize EEG, EMG, and video methods, although it depends on what is being manipulated and what resources are available.

Vigilance states in humans

Humans are diurnal so their wakeful activity occurs primarily during the daytime with resting at night. Wakefulness is one vigilance state and is characterized by conscious and responsive behavior, high motility, and high frequency activity on the cortical EEG reflecting the cortical desynchronization of conscious cognition (Hernan et al., 2017; Moruzzi & Magoun, 1949). In wakefulness, there is high muscle activity and high muscle tone on the EMG.

Since it progresses through a cycle of identifiable changes, sleep gets divided into the two vigilance states non-rapid eye movement (NREM) and rapid eye movement (REM). NREM sleep precedes REM sleep but does not require it, while REM sleep requires NREM sleep and is followed by wakefulness. NREM sleep in humans gets further subdivided into three stages based on distinct physiological changes and progressive alterations in recordable brain activity.

At the first stage of NREM sleep, the transition between waking and sleeping, awaking a person is still easy (Neckelmann & Ursin, 1993). The EEG power distribution shifts from the high-frequency EEG activity associated with wakefulness to lower frequency alpha and theta waves.

In the second stage of human NREM sleep, a person is much less responsive to external stimuli (Neckelmann & Ursin, 1993). While brain waves begin slowing, there are sudden higher frequency waves known as sleep spindles, and higher-amplitude slow waves called K-complexes (Forget et al., 2011). Sleep spindles occur at 7 to 15 Hz for 1 to 2 seconds and subjects woken right after a

sleep spindle occurrence report they were dreaming (Siclari et al., 2018). A K-complex occurs in response to environmental stimuli, producing a high-amplitude biphasic wave composed of an initial sharply negative upward wave followed by a slower positive downward wave on the EEG (Forget et al., 2011). Gradual inactivation of wake-promoting neural networks leads to slower, more synchronized oscillation of neuronal and synaptic activity as the thalamus and cerebral cortex neurons generate lower frequency slow-wave patterns (David et al., 2013; Funk et al., 2017). On the EMG, muscle tone decreases while respiration slows, and body temperature begins to decrease (Darwent et al., 2010; Okada et al., 1991).

Deep sleep of stage three, also called slow wave sleep (SWS), is characterized by increasing amounts of delta waves, reflecting increased synchronization of cortical and thalamic activity (Dijk, 1995; Timofeev et al., 2012). High amplitude, low frequency activity primarily below 4 Hertz (Hz) is known as slow wave activity (SWA) and is used as an indicator of deep sleep (Abo-Zahhad et al., 2015). Decreased responsiveness to outside stimuli, due to a reduction in neural arousal processes, makes it harder to wake a person (Neckelmann & Ursin, 1993). On the EMG there is very little to no muscle activity, although low muscle tone is present (Okada et al., 1991). Respiration is slow and regular while the heart rate decreases, and the body temperature continues to diminish (Ma et al., 2018).

In order to transition into REM sleep, NREM sleep must sequentially pass through all three stages and then back to stage two sleep (Carskadon & Dement,

2005). REM sleep's cortical EEG contains an abundance of theta activity produced by the neurons in the hippocampus, the brain region beneath the cortex primarily responsible for memories. These hippocampal theta waves are seen during motor activity and during REM sleep, which makes them stand out since REM sleep is uniquely marked by the loss of muscle tone, a state known as muscle atonia, with intermittent muscle twitches and rapid movement of the eyes (Abo-Zahhad et al., 2015; Chen et al., 2017; Peever & Fuller, 2017: Valencia Garcia et al., 2018). Intermittent muscle twitches may activate brain regions not activated by waking motor activity and may function to aid sensorimotor system development (Peever & Fuller, 2017; Sokoloff et al., 2015). Fluttering eye movements, as recordable by an EOG, are a way to immediately distinguish between NREM sleep and REM sleep since NREM sleep does not have eye movement. Heart rate speeds up but body temperature falls even further as temperature regulation decreases (Darwent et al., 2010). REM sleep then transitions to wakefulness before the sleep-wake cycle can start over (Carskadon & Dement, 2005).

Overall, these changes, progressing from wakefulness to NREM sleep to REM sleep, comprise the sleep-wake cycle (Steriade et al., 2001). The first half of a person's sleep cycle consists mostly of NREM sleep. This time spent in deep sleep appears to be the restful and restorative portion of sleep. Humans then progress to increasingly longer REM sleep bouts in the latter half of the night where the average NREM-REM sleep cycle duration is about 90 minutes with four to six REM cycles a night (Carskadon & Dement, 2005). Across development, the ratio

of REM sleep to NREM sleep decreases, then with aging the ratio of deep sleep to light sleep decreases even though total time spent sleeping remains the same through adulthood (Scullin & Bliwise, 2015).

Vigilance states in mice

Research utilizes rats and mice for investigations more targeted than human experimental designs can accommodate. In rodents, EEG electrodes get placed in the skull, above the cortex, thus providing improved recording as the skull is no longer a barrier filtering out higher frequencies. A mouse's thinner cortex allows recording of the theta rhythms from the hippocampus. Mice also offer both genetic manipulation and higher throughput, which are not possible with humans.

Although mice have three sleep states like humans, there are some important differences. NREM in rats and mice is not as easily distinguished into sub-stages. Since the slow waves in NREM on the EEG are most distinguishable, this state is sometimes called slow wave sleep (SWS). Mice are nocturnal and in lab housing, do not sleep in one large continuous length of time. Instead, lab-housed mice sleep in several bouts across the day, interspersed with wakeful activity.

EEG recordings are the primary method used to determine a mouse's vigilance state and measure the amount and quality of sleep. The EMG serves to further confirm vigilance states such as REM sleep. If needed, video recordings can provide visual determination to supplement the analysis.

In mice, the wakeful state, characterized by engaging with the environment, occurs primarily during the night. Cortical EEG recordings are rich in low amplitude, high-frequency beta and gamma waves, characteristics of perception and cognition. The EMG shows high muscle activity, reflective of the locomotor activity level. Conversely, high amplitude, low-frequency delta waves in the EEG characterizes SWS. The EMG records low muscle tone as the mouse relaxes into the stereotypical posture for sleeping. Lastly, hippocampal theta rhythms dominate the EEG during REM sleep in mice. During REM sleep, the EMG recording goes flat, indicative of muscle atonia. An awakening always follows REM sleep, which may last only one to two seconds.

Sleep-wake circuitry

Anatomy and neurochemistry

The anatomy and neurochemistry of sleep-wake control is diverse and widely distributed throughout the brain (Figure 1.1 - 1.3 on pages 27 - 29). Recent technological advancements allow for better specific selection of targeted neurons and more diverse ways of manipulating the neuronal activity to interrogate their function and to determine their neural circuitry (Drew et al., 2018; Fuller et al., 2015; Shiromani & Peever, 2017). This has facilitated revealing the control of sleep and wakefulness are established by a complex array of interconnected activation and inhibition.

Wakefulness

The first identified wake-promoting brain region, the reticular activating system, was discovered by stimulating the brain between the pons and the midbrain. This reticular activating system projects to the cortex mainly through a ventral ascending pathway via the basal forebrain (BF), posterior and lateral hypothalamus (LH) and the medial forebrain bundle, and a dorsal ascending pathway through the thalamus (Jones & Yang, 1985). Subsequent investigation shows the wake-promoting brain regions are populated by a variety of neural subtypes that often contribute to cognition beyond sleep-wake control. For example, cholinergic innervation of the cortex and hippocampus are critical parts of cognitive processes such as selective attention and emotional processing (Bentley et al., 2003; Butcher et al., 1993; Dautan et al., 2016; Li et al., 2018). Dopaminergic neural activity plays a large role in learning and many motivation-based behaviors such as eating and drug seeking (Corbit & Janak, 2010; Ostlund et al., 2011; Salamone, 1994; Salamone & Correa, 2009; Smith et al., 2011; Steinberg et al., 2013). Noradrenergic neurons activate in response to novelty and stress (Pudovkina et al., 2001; Ronzoni et al., 2016), contributing to cognitive processes such as shifts in attention, memory consolidation and retrieval, and decision making (Borodovitsyna et al., 2017; Sara, 2009). Orexinergic neurons are involved in arousal and response to homeostatic challenges such as food seeking (Sakurai et al., 1998; Yamanaka et al., 2003). Investigation has also identified additional neuronal populations that contribute to wakefulness.

One of the most prominent wake-promoting brain regions is the basal forebrain (BF). Cholinergic neurons in the BF project to the hippocampus, hypothalamus, amygdala, and cerebral cortex (Henny & Jones, 2008; Mesulam et al., 1983). Chemogenetic activation and selective inhibition of cholinergic BF neurons revealed they contribute to wakefulness by inhibiting cortical synchronization (Anaclet et al., 2015; Chen et al., 2016). GABAergic neurons in the BF project to the hypothalamus, amygdala, and cerebral cortex (Gritti et al., 1993, 1994; Gritti et al., 1997; McDonald et al., 2011). Chemogenetic activation and selective inhibition of GABAergic BF neurons demonstrated they play an essential role in wake-promotion and desynchronization of the cortex (Anaclet et al., 2015; Kim et al., 2015).

The glutamatergic neurons in the parabrachial nucleus (PB) reciprocally provide excitatory projections with the cerebral cortex to promote wakefulness, and extensively innervate the BF, lateral hypothalamus (LH), and central nucleus of the amygdala (Kaur et al., 2017; Saper, 1982; Saper & Loewy, 1980). Furthermore, both activating and inhibiting, or bidirectional, optogenetic and chemogenetic manipulation of glutamatergic lateral PB neurons expressing the calcitonin gene-related peptide demonstrated their essential role in promoting wakefulness during sleep in response to elevated CO_2 levels (Kaur et al., 2017).

Several portions of the hypothalamus are involved in sleep-wake control. The orexinergic neurons in the lateral hypothalamus (LH) have widespread projections throughout the brain, including to the LC, tuberomammillary nucleus

(TMN), BF, ventral tegmental area (VTA), midline thalamus, and cortex (Jones & Yang, 1985; Peyron et al., 1998; Yu et al., 2019). Intracerebroventricular injection, and optogenetic and chemogenetic activation of orexinergic LH neurons demonstrated their role in consolidating wakefulness into long bouts in opposition to accumulating sleep pressure (Adamantidis et al., 2007; de Lecea et al., 1998). Furthermore, orexinergic signaling was found to establish transition boundaries between sleeping and waking, the loss of which caused narcolepsy (Carter et al., 2009; Lin et al., 1999). Histaminergic neurons in the TMN of the posterior hypothalamus project to a widespread and diffuse array of various sleep and wake regulating brain regions such as the neocortex, hippocampal formation, amygdala, basal ganglia, thalamus, superior colliculus, and cerebellum (Köhler et al., 1985). Histaminergic TMN innervation of the forebrain was shown to promote wakefulness and arousal (Garbarg et al., 1974; Liu et al., 2010). Histaminergic release on the ventrolateral preoptic area (VLPO) suppresses the sleep promotion action of the VLPO to increase wakefulness (Liu et al., 2010; Sherin et al., 1998). The GABAergic neurons in the ventral LH project to the TMN, ventrolateral periaqueductal gray, and LC (Venner et al., 2016). Chemogenetic activation of the GABAergic ventral LH neurons demonstrated their important role in promoting wakefulness (Venner et al., 2016). There are glutamatergic neurons in the supramammillary region of the caudal hypothalamus which also express nitric oxide synthase (NOS) (Pedersen et al., 2017). Bidirectional, chemogenetic manipulation of glutamatergic supramammillary neurons demonstrated their

significant role in promoting wakefulness (Pedersen et al., 2017). Furthermore, manipulations including NOS-expressing supramammillary neurons were found to not only drive wakefulness but also contribute to REM theta rhythms on EEG (Pedersen et al., 2017). The GABAergic neurons in the bed nucleus of the stria terminalis (BNST) project to the VTA (Kodani et al., 2017; Kudo et al., 2014). Optogenetic and chemogenetic stimulation of GABAergic BNST neurons demonstrated their contribution to transitioning from NREM sleep to wakefulness and to longer bouts of waking facilitated through orexinergic signaling (Kodani et al., 2017; Kudo et al., 2014).

Noradrenergic neurons in the LC innervates and receives descending projections from the anterior cingulate cortex to promote wakefulness (Gompf et al., 2010; Jones & Yang, 1985; Luppi et al., 1995; Schwarz et al., 2015). Optogenetic interrogation and CRISPR/cas9 genetic editing of noradrenergic LC neurons demonstrated their role in promoting wakefulness and orexinergic mediated transitioning from sleep to wake (Carter et al., 2012; Yamaguchi et al., 2018). Furthermore, noradrenergic LC neurons project to and activate neural circuitry known as REM-off neurons to inhibit REM sleep (Lu et al., 2006).

The dopaminergic neurons in the VTA project to the striatum, medial prefrontal cortex, nucleus accumbens (NAc), and central amygdala (Eban-Rothschild et al., 2016; Qiu et al., 2019). Bidirectional chemogenetic and optogenetic manipulations of the dopaminergic VTA innervations on the ventral striatum demonstrated dopaminergic VTA neurons promote wakefulness during

salient activities and facilitates transition from REM sleep to wakefulness (Eban-Rothschild et al., 2016; Qiu et al., 2019; Yang et al., 2018). Additionally, dopaminergic neurons in the dorsal raphe nucleus support wakefulness during environmental salience (Cho et al., 2017). The glutamatergic neurons in the VTA project to the NAc and the LH (Taylor et al., 2014; Yu et al., 2019). Lesion and chemogenetic activation of glutamatergic VTA neurons demonstrated how they consolidate wakefulness through stimulation of the NAc and the LH (Yu et al., 2019). GABAergic neurons in the NAc of the ventral striatum project back to the VTA (Luo et al., 2018). Optogenetic and chemogenetic stimulation of GABAergic NAc neurons demonstrated their contribution to induction and maintenance of wakefulness (Luo et al., 2018). Additionally, GABAergic neurons in the superior colliculus project to the VTA to facilitate induction of wakefulness during transition to darkness (Ze Zhang et al., 2019).

Glutamatergic neurons in the pedunculopontine tegmental nuclei (PPT) project to the caudal basal forebrain, ventral part of the BNST, subthalamic nucleus, substantia nigra (SNc), and VTA (Kroeger et al., 2017). Bidirectional chemogenetic manipulation of glutamatergic PPT neurons demonstrated their contribution to promoting quiet wakefulness (Kroeger et al., 2017). Cholinergic neurons in the PPT project to the reticular nucleus of the thalamus, anterior pretectal nucleus and superior colliculus (Kroeger et al., 2017). Chemogenetic activation of cholinergic PPT neurons demonstrated their role in reducing NREM

sleep by reducing cortical slow waves during NREM sleep and increasing transitions to wakefulness (Kroeger et al., 2017).

While the reticular formation's ascending ventral pathway projects directly to the forebrain, the cortex reciprocally innervates the wake promoting systems, such as the LC and PB, demonstrating the possibility of exerting executive control over sleep-wake regulation (Breton-Provencher & Sur, 2019; Saper, 1982). The reticular formation's ascending dorsal pathway projects to the thalamus which then relays the arousal signals through thalamocortical neurons. Glutamatergic neurons in the paraventricular thalamus (PVT) project to the NAc and receive projection from the LH (Ren et al., 2018). This network has been shown to be essential for sustained, time-of-day dependent wakefulness (Ren et al., 2018). Matrix cells in the ventromedial thalamic nucleus (VM) project to almost the entire cortex (Honjoh et al., 2018). Optogenetic stimulation and chemogenetic inhibition of matrix cells in the VM demonstrated they contribute to transitioning from NREM sleep to wakefulness (Honjoh et al., 2018). Additionally, both glutamatergic PVT and VM matrix cells have been shown to contribute to emergence from isoflurane induced unconsciousness (Honjoh et al., 2018; Ren et al., 2018). Glutamatergic neurons in the dorsomedial thalamus (DMT) project throughout the forebrain, including to prelimbic cortices, the NAc, and the central amygdala (Mátyás et al., 2018). Glutamatergic DMT neuronal activity transitions the cortical state from NREM sleep to arousal with a drop in delta power, achieved by the unique characteristic

of each neuron having multiple axon arbors branching out to multiple brain areas so one neuron can affect a wide region across the brain (Mátyás et al., 2018).

NREM sleep

The NREM sleep system is also distributed throughout the brain and much like with wakefulness, some of the sleep-promoting neuronal populations are part of the hypothalamus. The ventrolateral preoptic area (VLPO) of the anterior hypothalamus was the first NREM sleep-promoting region found. GABAergic and galaninergic neurons in the VLPO project to wake-promoting regions such as the tuberomammillary nucleus (TMN), locus coeruleus (LC), and raphe nuclei (Sherin et al., 1998). Optogenetic and chemogenetic activation of the inhibitory GABAergic and galaninergic VLPO neurons demonstrate their role in facilitating transition to NREM sleep by inhibiting wakefulness and maintaining NREM sleep (Kroeger et al., 2018). GABAergic and galaninergic neurons in the dorsomedial hypothalamus (DMH) project to the preoptic area (Chen et al., 2018). Bilateral optogenetic manipulation of galaninergic DMH neurons demonstrated their role in suppressing REM sleep (Chen et al., 2018).

Adenosine is a sleep factor produced by neuronal metabolism, increasing in accumulation during prolonged wakefulness, and believed to play a role in sleep pressure (Basheer et al., 2000; Basheer et al., 2004; Porkka-Heiskanen et al., 1997). Of the four adenosine receptor (AR) types, A_1 AR and A_3 AR inhibit neuronal signaling while A_{2A} AR and A_{2B} AR are excitatory (Borea et al., 2016; Sheth et al., 2014).

Microdialysis and cellular recordings demonstrated the role of A_1 AR in inhibiting wake-promoting brain areas such as the BF cholinergic neurons, LH orexinergic neurons, and TMN histaminergic neurons (Alam et al., 1999; Liu & Gao, 2007; Oishi et al., 2008; Rainnie et al., 1994; Thakkar et al., 2003). Also, A_1 AR disinhibits sleep-active neurons such as the VLPO and the anterior hypothalamic area (Chamberlin et al., 2003; Gallopin et al., 2005; Morairty et al., 2004). Use of agonists and antagonists demonstrated A_1 AR's role in increasing NREM consolidation and SWA response following acute sleep deprivation (Benington et al., 1995; Gass et al., 2009; Methippara et al., 2005; Radulovacki et al., 1984; Thakkar et al., 2008; Virus et al., 1990). Like with adenosine levels, A_1 AR expression increases with prolonged wakefulness and resolves during sleep (Basheer et al., 2007; Elmenhorst et al., 2017; Elmenhorst et al., 2007).

A_2 AR is expressed in the VLPO and NAc. Sleep promoting neuronal sub-population within the VLPO express A_{2A} receptors and are activated by adenosine (Kumar et al., 2013). Use of agonists demonstrated A_2 AR's role in initiating sleep through activation of the VLPO and the NAc (Gallopin et al., 2005; Satoh et al., 1999; Scammell et al., 2001). NAc neurons with A_{2A} receptors project to the ventral pallidum (Oishi et al., 2017; Reppert et al., 1991). Optogenetic activation and bidirectional chemogenetic manipulation of these neurons revealed their contribution to sleep induction and how motivational stimuli suppresses their signaling (Oishi et al., 2017). Caffeine's wakefulness effect is mediated through antagonism of A_2 AR expressed in the NAc (Huang et al., 2005; Lazarus et al.,

2011). A_2 AR expressing neurons in the rostral striatum project to the globus pallidus to form inhibitory synapses with inhibitory globus pallidus parvalbumin interneurons (Yuan et al., 2017). Bidirectional chemogenetic manipulation of these striatal neurons demonstrated their contribution to promoting NREM sleep (Yuan et al., 2017).

GABAergic neurons in the ventral zona incerta (VZI) have widespread connectivity throughout the brain and project to such neuronal populations as the orexinergic LH (Liu et al., 2017; Mitrofanis, 2005). Bidirectional optogenetic and chemogenetic manipulations and conditional deletion of GABAergic VZI neurons demonstrated their essential role in NREM sleep control through orexinergic neurons (Liu et al., 2017).

GABAergic neurons in the parafacial zone (PZ) project to the PB (Anaclet et al., 2014; Anaclet & Fuller, 2017). Lesion, optogenetic and chemogenetic activation, and knockdown of neurotransmission of GABAergic PZ neurons demonstrated their critical role in promoting NREM sleep by induction and maintenance of NREM sleep as well as stimulating SWA (Anaclet et al., 2014; Anaclet, Griffith, et al., 2018; Anaclet et al., 2012).

GABAergic neurons in the rostromedial tegmental nucleus (RMTg) project to the midbrain dopaminergic system containing the VTA and the SNc (Yang et al., 2018). Lesion, and optogenetic and chemogenetic stimulation of GABAergic RMTg neurons demonstrated their essential role in inducing NREM sleep and SWA (Yang et al., 2018).

Glutamatergic neurons in the perioculomotor region of the midbrain project to the sleep-promoting preoptic hypothalamus and posterior ventromedial medulla (Zhe Zhang et al., 2019). Ablation and bidirectional optogenetic and chemogenetic manipulation of the glutamatergic perioculomotor neurons demonstrated their contribution to induction and maintenance of NREM and to sleep recovery following deprivation (Zhe Zhang et al., 2019).

Dopaminergic neurons in the SNc project to the dorsal striatum (Qiu et al., 2019). Selective chemogenetic activation of the dopaminergic SNc innervation to the dorsal striatum demonstrated their contribution to promoting sleep (Qiu et al., 2019). GABAergic neurons in the VTA project to the LH and innervate locally within the VTA (Chowdhury et al., 2019; Taylor et al., 2014; Yu et al., 2019). Lesion, bidirectional optogenetic and chemogenetic manipulation, and cellular recording of GABAergic VTA neurons demonstrated their essential role in inducing and maintaining NREM sleep by inhibiting the wake-promoting activity from the LH and VTA (Chowdhury et al., 2019; Takata et al., 2018; Yu et al., 2019).

GABAergic neurons of the ventrolateral periaqueductal gray (vlPAG) project to the REM-promoting sublaterodorsal nucleus (SLD) neurons, establishing reciprocal connection for mutual inhibition (Boissard et al., 2003; Kroeger et al., 2019; Lu et al., 2006; Sapin et al., 2009). Optogenetic activation of the GABAergic vlPAG neurons demonstrated their essential role in stabilizing NREM sleep by suppressing REM sleep (Hsieh et al., 2011; Sakai, 2018; Weber et al., 2018).

Glutamatergic neurons in the deep mesencephalic nuclei (DpMe) project to the SLD (Liang et al., 2014). Chemogenetic activation of glutamatergic DpMe neurons demonstrated their prominent role in promoting NREM sleep by suppressing transition to REM sleep (Hayashi et al., 2015; Sakai, 2018). GABAergic neurons of the DpMe project to REM-promoting SLD neurons, establishing reciprocal connection for mutual inhibition (Liang et al., 2014; Lu et al., 2006). Lesion, optogenetic and pharmacological inactivation of GABAergic DpMe neurons demonstrated their role in suppressing transition into REM sleep (Hayashi et al., 2015; Lu et al., 2006; Sakai, 2018).

Much like with wakefulness, the cortex participates in sleep promotion. Slow wave activity seems to be propagated by inhibitory cortical interneurons (Funk et al., 2017; Neske & Connors, 2016). Somatostatin GABAergic interneurons provide critical regulation to decreased neuronal excitability in the cortex to achieve slow wave firing patterns while parvalbumin GABAergic interneuron activity increases NREM sleep duration (Funk et al., 2017; Neske & Connors, 2016). Somatostatin GABAergic interneuron activity is also essential for SWA (Funk et al., 2017; Neske & Connors, 2016). Cortical neurons expressing neuronal NOS are activated by sleep and provide critical signaling for increasing SWA in response to sleep deprivation (Dittrich et al., 2015; Morairty et al., 2013). Pyramidal neurons from the prefrontal cortex innervate the LC, contributing to the inhibition exerted by GABAergic interneurons upon the LC (Breton-Provencher & Sur, 2019).

Interestingly, the cerebral cortex can produce slow oscillations without the thalamus (Timofeev & Steriade, 1996).

However, optogenetic activation and microdialysis injections demonstrated the thalamus' role in finely tuning slow waves in NREM sleep (David et al., 2013). Glutamatergic neurons expressing neurotensin in the posterior thalamus innervate the neurotensin-expressing GABAergic neurons in the central nucleus of the amygdala (Ma et al., 2019). Bidirectional optogenetic manipulation of the glutamatergic neurons in the posterior thalamus demonstrated their role in promoting sleep (Ma et al., 2019). Bidirectional optogenetic manipulation of the GABAergic central nucleus of the amygdala neurons demonstrated their role of broadly inhibiting multiple wake-promoting populations (Ma et al., 2019).

REM sleep

REM sleep is always preceded by NREM sleep and followed by wakefulness except in disorders like narcolepsy. REM sleep is accompanied by the unique phenomenon of muscle atonia, where muscle activity is abolished by silencing neuronal input.

Neuronal populations that promote REM sleep are called REM-on while those that inhibit REM sleep are called REM-off. The main anatomical region for REM sleep control is the SLD, and REM-off regions include the vlPAG, the dorsal raphe, the PPT, and the DpMe (Peever & Fuller, 2017). Mutual inhibition between REM-on neurons and REM-off neurons has been investigated as the method controlling REM sleep state switching to prevent inappropriate shifts between

wakefulness and REM sleep, as seen with narcolepsy (Burgess & Scammell, 2012; Chen et al., 2018; Lu et al., 2006).

GABAergic neurons in the SLD project to many REM-off regions and are mutually inhibited by projections from those regions (Boissard et al., 2003; Hayashi et al., 2015; Kroeger et al., 2019; Liang et al., 2014; Lu et al., 2006; Sakai, 2018; Weber et al., 2018). Lesions of GABAergic neurons demonstrated their essential role for the inhibition of REM-off neuronal populations (Lu et al., 2006; Sapin et al., 2009). Glutamatergic neurons in the SLD project to the vM and to the BF (Lu et al., 2006). Chemogenetic activation of glutamatergic SLD neurons demonstrated their prominent role in being able to drive all features of REM sleep (Erickson et al., 2019). Lesion and optogenetic inhibition of glutamatergic SLD neurons projecting to the medial septum demonstrated their critical role in generating REM sleep cortical activation and hippocampal theta rhythms (Boyce et al., 2016; Lu et al., 2006; Valencia Garcia et al., 2018).

GABAergic neurons in the vM project to motor neurons in the spinal ventral horn (Chen et al., 2017; Lu et al., 2006; Valencia Garcia et al., 2018). Knockdown of neurotransmission of GABAergic vM neurons demonstrated their essential role in establishing REM sleep muscle atonia.

As with wakefulness and NREM sleep, the hypothalamus is involved in REM sleep control. GABAergic and galaninergic neurons of the DMH project to the raphe pallidus (Chen et al., 2018). Optogenetic manipulation demonstrated their role in promoting REM sleep while suppressing NREM sleep (Chen et al., 2018).

Neurons in the LH expressing melanin-concentrating hormone (MCH) innervate the lateral pontine tegmentum (LPT) and the vlPAG (Kroeger et al., 2019). Dual optogenetic and chemogenetic manipulations of MCH neurons demonstrated their essential role in inhibiting the REM sleep suppression from vlPAG and LPT (Kroeger et al., 2019).

Sleep-wake timing

Many structured and cyclically rhythmic changes occur during the sleep-wake cycle (Waterhouse et al., 2012). The coordination and timing of these changes create the framework for healthy sleep. A person's circadian rhythm (process C) and homeostatic sleep pressure (process S) interact during the sleep-wake cycle to determine sleep-wake timing (Borbély, 1982; Borbély et al., 2016).

Circadian rhythm is an approximately 24-hour repeating cycle of changing genetic expression that impacts an organism from the molecular level to the behavioral level (Okamura et al., 2002; Reppert & Weaver, 2002). While cells contain this rhythm on their own, the suprachiasmatic nucleus (SCN) of the hypothalamus, known as the master clock, synchronizes the body (Shi et al., 2019). The SCN signals the body, able to maintain synchronous circadian rhythmicity on its own, but light cycles can entrain it. The SCN follows the day-night cycle by responding to light in the environment as detected by retinal ganglion cells (RGC), specialized neurons in the eye. RGCs detect and respond to blue light, signaling to the SCN directly (Brzezinski et al., 2005; Hattar et al., 2002). The SCN maintains coordinated oscillations even in the absence of lighting cycles

Process C represents the SCN signaling time of day information to the brain and body, synchronizing many physical, mental, and behavioral activities (Dibner et al., 2010).

Process S represents homeostatic sleep pressure, a drive to sleep that increases with more time spent awake and only decreases by sleeping (Friedman et al., 1979). Sleep pressure is thought to be produced in part by the build-up of small molecules such as adenosine and nitric oxide and requiring galanin signaling (Basheer et al., 2000; Dittrich et al., 2015; Dworak et al., 2017; Reichert et al., 2019). Sleep pressure diminishes with time spent asleep and with the quality of sleep (Friedman et al., 1979).

Process S and process C typically work in tandem as understood through the two-process model of sleep regulation (Borbély et al., 2016). In humans, during the day, process C provides progressively stronger activating signaling to remain awake even as process S increases during wakefulness. As part of the SCN continuing to maintain synchronized circadian rhythmicity, process C decreases and the built-up sleep pressure finally begins to reduce with the onset of sleep (Borbély et al., 2016). However, if the person does not go to sleep, process S continues to build instead (Borbély et al., 2016). The increased sleep pressure results in sleep rebound where excessive sleeping occurs in the next sleep episode to offset the previous sleep loss (Friedman et al., 1979). With continued sleep deprivation, sleep pressure can degrade the SCN's synchrony since sleep

pressure is not controlled by the SCN (Dijk & Archer, 2010; Tobler et al., 1983; Wyatt et al., 1999).

The interaction of circadian rhythm and homeostatic sleep pressure are important for overall sleep-wake timing (Daan et al., 1984). Sleeping at the time established by circadian rhythms increases quality of sleep (Zitting et al., 2018). When sleep quality is high, sleep pressure is more effectively removed (Friedman et al., 1979). These two processes individually signal to the neural circuitry that establishes sleep-wake control (Tobler et al., 1983). In this way, the interactions of process C and process S provide important structure to sleep timing (Daan et al., 1984; Fang & Rao, 2017).

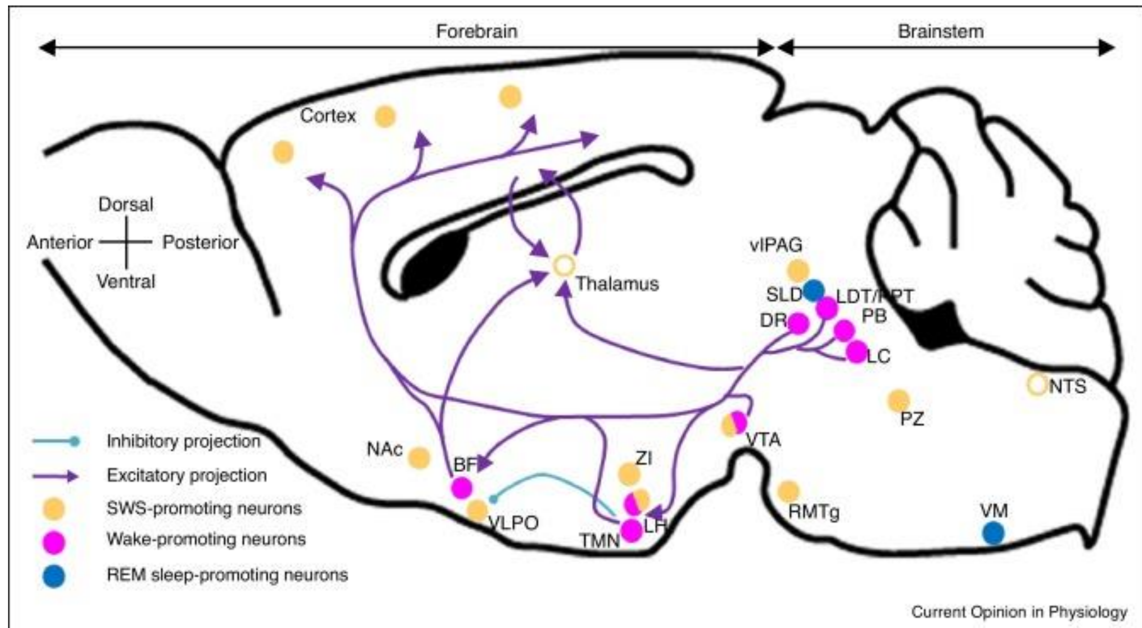

Figure 1.1: Wake-promoting Nuclei and Projections.

Sagittal plane of a mouse brain showing that wake-promoting neurons are located in the brainstem and in the forebrain, and project to the cortex to actively promote cortical activation and wakefulness. Histaminergic neurons located in the TMN actively inhibit VLPO sleep-promoting neurons. Open circles, brain areas contributing to sleep control but not sleep-promoting per se. Dash line, functional connectivity to be confirmed; BF, basal forebrain; DR, dorsal raphe; LDT/PPT, laterodorsal and pedunculopontine tegmental nuclei; LH, lateral hypothalamus; LC, locus coeruleus; NAc, nucleus accumbens; NTS, nucleus of the solitary tract; PB, parabrachial nucleus; PZ, parafacial zone; RMTg, rostromedial tegmental nucleus; SLD, sublaterodorsal nucleus; TMN, tuberomamillary nucleus; vlPAG, ventrolateral periaqueductal gray; VLPO, ventrolateral preoptic area; VM, ventral medulla; VTA, ventral tegmental area; ZI, zona incerta. Modified from Gompf and Anaclet, 2020 with authorization.

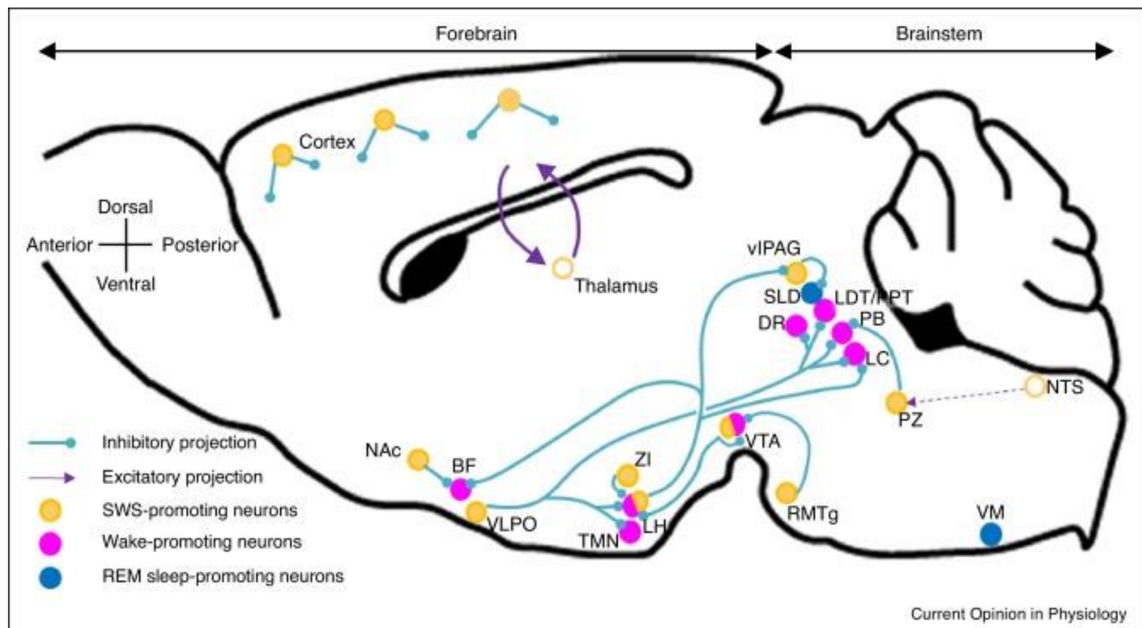

Figure 1.2: NREM Sleep-promoting Nuclei and Projections.

Sagittal plane of a mouse brain showing that NREM-promoting neurons are distributed along the neural axis and also in the cortex. They are mainly GABAergic and inhibit wake-promoting systems. Cortical interneurons and the thalamo-cortico-thalamic feedback loop actively promote cortical synchronization. Open circles, brain areas contributing to sleep control but not sleep-promoting per se. BF, basal forebrain; DR, dorsal raphe; LDT/PPT, laterodorsal and pedunculopontine tegmental nuclei; LH, lateral hypothalamus; LC, locus coeruleus; Nac, nucleus accumbens; NTS, nucleus of the solitary tract; PB, parabrachial nucleus; PZ, parafacial zone; RMTg, rostromedial tegmental nucleus; SLD, sublaterodorsal nucleus; TMN, tuberomamillary nucleus; vlPAG, ventrolateral periaqueductal gray; VLPO, ventrolateral preoptic area; VM, ventral medulla; VTA, ventral tegmental area; ZI, zona incerta. Modified from Gompf and Anaclet, 2020 with authorization.

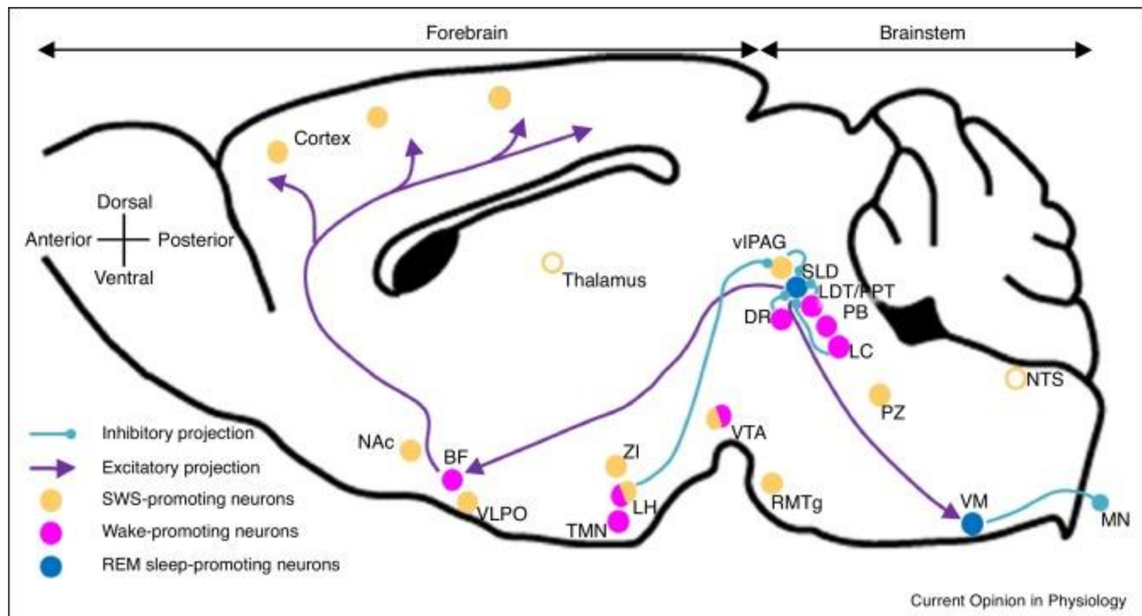

Figure 1.3: REM Sleep-promoting Nuclei and Projections.

Sagittal plane of a mouse brain showing that REM sleep is driven by the SLD which projects rostrally to promote cortical activation and caudally to actively drive muscle atonia. SLD REM sleep-promoting neurons are glutamatergic and receive inhibitory inputs from the pontine wake-promoting neurons. The LH contributes to REM sleep by inhibiting the vlPAG REM-off neurons. Open circles, brain areas contributing to sleep control but not sleep-promoting per se. BF, basal forebrain; DR, dorsal raphe; LDT/PPT, laterodorsal and pedunculopontine tegmental nuclei; LH, lateral hypothalamus; LC, locus coeruleus; MN, motoneurons; Nac, nucleus accumbens; NTS, nucleus of the solitary tract; PB, parabrachial nucleus; PZ, parafacial zone; RMTg, rostromedial tegmental nucleus; SLD, sublaterodorsal nucleus; TMN, tuberomamillary nucleus; vlPAG, ventrolateral periaqueductal gray; VLPO, ventrolateral preoptic area; VM, ventral medulla; VTA, ventral tegmental area; ZI, zona incerta. Modified from Gompf and Anaclet, 2020 with authorization.

Project Summary

Discovering sleep promoting neurons in the parafacial zone

Investigating brain regions to discover the circuitry behind sleep-wake control is an ongoing endeavor. Even with the many sleep and wake brain regions that have been uncovered, their interaction and overall coordination require further study. While the wake-promoting reticular formation was revealed seventy years ago (Moruzzi & Magoun, 1949), the SWS-promoting regions have taken longer to find. Several SWS-promoting populations were located in the midbrain and even cortex, but less than a decade ago, a long sought-after population of neurons was finally located in the brainstem (Anaclet et al., 2012). These neurons are located in the parafacial zone (PZ), named for its location adjacent to the facial nerve, and are the subject of active scrutiny since there was very little pre-existing literature on the region. While the VLPO, the first identified SWS-promoting region, promotes SWS by inhibiting wake-promoting brain regions, the PZ exhibits the additional ability to increase SWA (Anaclet et al., 2014; Anaclet, Griffith, et al., 2018).

The GABAergic neurons in the PZ (PZ^{GABA}) are essential for the onset and maintenance of SWS (Anaclet et al., 2014; Anaclet & Fuller, 2017; Anaclet et al., 2012). Research indicates the PZ^{GABA} seems to be particularly powerful among the currently known SWS promoting systems since they promote SWA (Anaclet et al., 2014; Anaclet & Fuller, 2017). This has sparked a new abundance of study into this once poorly characterized region (Anaclet, et al., 2018; Erickson et al., 2019; Sakai, 2017; Venner et al., 2019). The boundaries of this sleep active neuronal

population remain undefined but are being investigated (Sakai, 2017). The parvocellular reticular nucleus part alpha exhibited no sleep-active neurons upon recording individual cell activity, thus establishing a boundary on the ventral side from the PZ (Sakai, 2017). The current understanding of the PZ is that it is a heterogeneous population of excitatory and inhibitory sleep active neurons (Anaclet et al., 2012; Erickson et al., 2019). Since PZ^{GABA} plays a critical part in sleep-wake control, and PZ sleep active neurons are not all GABAergic (Anaclet et al., 2012), we investigated the role of PZ non-GABAergic neurons in sleep-wake control.

Characterizing PZ Neurons

Previous research demonstrated that the GABAergic neurons in the PZ (PZ^{GABA}) are necessary for SWS (Anaclet et al., 2014; Anaclet et al., 2012). Inhibition of GABAergic transmission in PZ^{GABA} neurons resulted in insomnia, significantly reducing the amount of SWS compared to the control group (Anaclet et al., 2012). Utilizing the Designer Receptors Exclusively Activated by Designer Drugs system (DREADDs) demonstrated chemogenetic activation of PZ^{GABA} neurons is sufficient to induce SWS (Anaclet et al., 2014). Additionally, EEG measurements show that activation of PZ^{GABA} neurons by DREADDs produced a significant increase in SWS amount and SWA (Anaclet et al., 2014).

Double immunohistochemistry labeling of both sleep active neurons and GABAergic neurons showed there were sleep active neurons not labeled as GABAergic (Anaclet et al., 2012). The Allen Mouse Brain Atlas from the Allen

Institute for Brain Science contains *in situ* hybridization data available at https://mouse.brain-map.org/experiment/show/73818754 indicating there are glutamatergic neurons in the PZ specifically expressing the vesicular-glutamate transporter 2 (Vglut2) gene (PZ^{Vglut2}). Targeting Vglut2 expression in the PZ^{Vglut2} neurons provided the ability to manipulate, label, and test glutamatergic neurons in the PZ for their possible involvement in sleep-wake control (Erickson et al., 2019).

DREADDs activation of PZ^{Vglut2} showed a significant increase in wakefulness (Erickson et al., 2019). However, the wake-promoting parabrachial nucleus is adjacent to the PZ and also contains Vglut2 expressing neurons. Imaging of DREADDs expression showed these wake-promoting neurons were possibly transfected, making it difficult to interpret if the recorded behavior was due to PZ^{Vglut2} neurons (Erickson et al., 2019). Therefore, to target PZ^{Vglut2} neurons more precisely, we used a specific marker of PZ^{Vglut2}, the transcription factor called Paired Like Homeobox 2B (Phox2B). Labeling showed colocalization between PZ^{Vglut2} neurons and Phox2B-expressing neurons in the PZ [PZ^{Phox2B}; (Erickson et al., 2019)]. EEG recordings showed that activation of PZ^{Phox2B} neurons by the DREADDs system did not produce a significant change in the amount of sleep or wakefulness (Erickson et al., 2019). In conclusion, activation of PZ^{Phox2B} neurons is not sufficient to affect sleep-wake control (Erickson et al., 2019).

Despite this, it remained unclear if they were necessary. We then sought to determine if physiological sleep-wake behavior requires the connection and function of these neurons as documented in the following research.

Chapter 2

Investigating the Role of Phox2B-expressing Glutamatergic Parafacial Zone Neurons in Sleep-Wake Control

Abstract

The parafacial zone (PZ) is a brain area that contains a heterogenous neuronal population currently under investigation for its role in sleep-wake control. PZ GABAergic neurons play an essential role in slow-wave-sleep, a characteristic of non-rapid eye movement sleep. Using the homeodomain transcription factor Phox2B as a specific marker for PZ glutamatergic neurons (PZ^{Phox2B}), chemogenetic activation of PZ^{Phox2B}-neurons was not sufficient to affect sleep-wake phenotypes. However, it is not known if PZ^{Phox2B} neurons play a necessary role in sleep-wake control. We hypothesize that PZ^{Phox2B} neurons are required for normal sleep-wake phenotypes. We tested the hypothesis by injecting Phox2B-*IRES*-Cre mice with an adeno-associated virus containing Cre-dependent diphtheria toxin subunit-A DNA to ablate PZ^{Phox2B} ($PZ^{Phox2B\text{-}DTA}$) neurons. Injection site mapping revealed transfection covering the PZ as well as the locus coeruleus (LC) which is known to express Phox2B. This research found that $PZ^{Phox2B\text{-}DTA}$ mice did not have significantly altered amounts or quality of sleep-wake states. $PZ^{Phox2B\text{-}DTA}$ mice did have fragmented wakefulness during the active period but no changes in SWS or REM sleep, and no changes in any sleep-wake states during the rest period. Since targeted ablation of $PZ^{Phox2B\text{-}DTA}$ neurons was not able to be confirmed, we cannot conclude that PZ^{Phox2B} neurons are necessary in sleep-wake

control. The limited sleep-wake phenotype could be due to partial lesion of Phox2B neurons or lesion in adjacent regions such as the LC.

Introduction

It is widely understood that a restful night's sleep is an important part of being healthy. Sleep amount and quality impacts a person's physiology, psychology, and cognitive function (Grandner, 2017; Shi et al., 2018). Multiple neuronal populations have been discovered to be involved in wakefulness, slow wave sleep (SWS), and rapid eye movement (REM) sleep, as well as in the transitions between vigilance states. Recent discoveries revealing the complexity of interaction within and between the systems that establish dynamic regulation of sleeping and waking states are due to advances in more selective targeting and manipulation of specific neuronal populations (Gompf & Anaclet, 2020). Modern research makes use of powerful molecular and genetic tools available to investigate neurophysiological functions by targeted manipulation of defined neuronal subtypes within the targeted neuroanatomy of interest (Shiromani & Peever, 2017). However, our understanding of the neural networks and regulative processes behind sleeping and waking remains incomplete.

Within the past decade, the medullary parafacial zone (PZ) has been identified and characterized as an essential and strong sleep promoting brain area (Anaclet et al., 2014; Anaclet, Griffith, et al., 2018; Anaclet et al., 2012). Located dorsal and lateral from the facial nerve, the boundaries of the PZ are still under investigation. Currently, the ventral border has begun to take shape by definitive exclusion of the parvicellular reticular nucleus part alpha (Sakai, 2017). It is also

known that the PZ contains sleep active neuronal populations of both GABAergic and non-GABAergic subtypes (Anaclet et al., 2012).

The GABAergic neurons in the PZ have been found to be sufficient and necessary for SWS amount, consolidation, and sleep depth (Anaclet et al., 2014; Anaclet et al., 2012). Investigation into the sleep active non-GABAergic neurons in the PZ has begun by using the homeodomain transcription factor Phox2B (PZ^{Phox2B}) to target glutamatergic neurons (Erickson et al., 2019). Research sought to determine if PZ^{Phox2B} neurons were involved in sleep-wake control and acted synergistically with the PZ^{GABA} neurons. Chemogenetic activation of PZ^{Phox2B} neurons did not produce any alterations in sleep-wake amount, structure, or quality, suggesting they are not sufficient to affect the sleep-wake cycle. However, the necessity of PZ^{Phox2B} neurons remains to be determined.

In this research, we hypothesized that PZ^{Phox2B} neurons are required for physiologically normal sleep and wakefulness. We tested this hypothesis by lesioning PZ^{Phox2B} neurons. We injected a cre-dependent AAV containing DTA into the PZ of Phox2B-*IRES*-cre mice ($PZ^{Phox2B\text{-}DTA}$). This research found that $PZ^{Phox2B\text{-}DTA}$ mice had fragmentation in waking during the active period but did not have significantly altered sleep-wake amount or quality during any time of day.

Materials and Methods

Mice

The study used twelve adult male Phox2B-IRES-cre [Jackson Laboratory #016223 (Rossi et al., 2011)] mice (8-12 weeks, 20-25 g) to target parafacial zone (PZ) neurons expressing Phox2B (PZ^{Phox2B}). Phox2B-IRES-Cre mice were crossed with a cre-dependent reporter mouse Flox-L10-GFP [Jackson Laboratory #24750 (Liu et al., 2014)] producing a Phox2B-GFP mouse line. Sixteen adult male Phox2B-GFP mice were used in attempts to label Phox2B. Genotyping was performed within the lab both before and after experiments. The mice were bred at the University of Massachusetts Medical School animal facility in a 12-hour light/dark cycle with lights on at 07:00 local time and lights off at 19:00 local time. The Institutional Animal Care and Use Committee of the University of Massachusetts Medical School approved all procedures (Protocol #A-2574).

Surgery

Naïve mice were intraperitoneally injected with ketamine/xylazine anesthetic (100 and 10 mg/kg, respectively). Once unresponsive to toe pinch, mice were subcutaneously injected with a preoperative nonsteroidal anti-inflammatory drug (Meloxicam, 5mg/kg) and securely placed in the Kopf stereotaxic apparatus (Germany). To selectively ablate PZ^{Phox2B} neurons, bilateral injections of an adeno-associated virus (AAV; serotype 10) containing diphtheria toxin subunit-A (DTA) in a cre-dependent configuration [DTA-AAV, titer = $1.6x10^{13}$ viral genome copies per ml; Figure 2.1 on page 45; (Anaclet, et al., 2018; Kaur et al., 2017, Kaur et al.,

2013)] was injected into the PZ [coordinates from Bregma: Antero-posterior = -5.6 mm, Lateral = ± 1.0 mm, Dorso-ventral = 4.2 mm, as per The Mouse Brain in Stereotaxic Coordinates (Paxinos & Franklin, 2001)] of *Phox2B-IRES-cre* ($PZ^{Phox2B\text{-}DTA}$) experimental mice and littermate control mice not expressing Cre ($PZ^{Phox2B\text{-}WT}$). By placing the DNA sequence of DTA in an inverted fashion within a FLEX cassette, DTA cannot be transcribed except in the presence of cre-recombinase, conferring absolute expression selectivity (Anaclet, et al., 2018; Kaur et al., 2017). With mCherry located on the construct but external to the FLEX switch, mCherry is expressed in all non-cre-recombinase cells within the injection field, thereby the anatomical extent of the injection to be ascertained and demonstrates quantitatively the “survival” of non-cre-recombinase cells intermingled with cre-recombinase cells targeted by DTA (Anaclet, et al., 2018; Kaur et al., 2017).

For brain injection, the Neurostar Wireless Capillary Nanoinjector (Germany) was used to inject DTA-AAV (50 nl) with a borosilicated capillary pipette into the PZ bilaterally of mice. Dissolving surgical sutures were used to close the scalp wound and postoperative analgesic was administered subcutaneously (Buprenorphine, 0.05 mg/kg). Mice were kept in a clean, warm environment until resuming normal activity as previously described (Anaclet et al., 2015).

After two weeks for recovery, mice were prepared for a second surgery with the same anesthetic, stereotaxic apparatus, and preoperative NSAID protocols. For EEG/EMG implantation surgery, mice were implanted with four EEG screw

electrodes (Pinnacle Technology Inc., Catalog #8403) placed snugly in holes drilled into the skull with a Dremel 105 round engraving cutter bit (1/32 inch) in the frontal and parietal bones on each side, and two flexible EMG wire electrodes (Plastics One, catalog #E363/76/SPC) tucked under the trapezius muscle. Electrodes were previously soldered to a 6-pin connector (Heilind Electronics, catalog #853-43-006-10-001000). Dental cement was used to secure the assembly to the scalp. The mouse was given the same post-operative analgesic protocol and again placed in a clean, warm environment until resuming normal activity as previously described (Anaclet et al., 2015). Mice were individually housed after EEG/EMG implantation so the mice do not damage each other's headsets.

Sleep-wake monitoring

One week after EEG/EMG implantation surgery, mice were relocated to transparent barrels placed in an insulated, sound-proofed recording chamber maintained at the ambient temperature of 22 ± 1°C and on a 12-hour light/dark cycle (lights on at 07:00 local time) with food and water available *ad libitum*. Mice were habituated to the recording cable for 5-7 days before the start of polygraphic recording. Vital Recorder (Kissei, Japan) was used to detect amplified (A-M System 3500, United States) and digitalized cortical EEG (ipsilateral frontoparietal leads) and EMG signals with a resolution of 256 Hz. Up to eight mice were simultaneously recorded for a 48-hour period with an equal number of $PZ^{Phox2B\text{-}WT}$ and $PZ^{Phox2B\text{-}DTA}$ mice.

Sleep scoring and analysis

Polygraphic records were scored in 10 second epochs for wakefulness, slow wave sleep (SWS), and rapid eye movement (REM) sleep using SleepSign for Animal (Kissei, Japan) assisted by spectral analysis utilizing fast Fourier transform. Data from each group were analyzed as the percentages of time spent in wakefulness, SWS, and REM sleep hourly.

To assess sleep-wake fragmentation, vigilance state bouts were separated into eight bout lengths [<30, 40-70, 80-150, 160-310, 320-630, 640-1270, 1280-2550, and >2550 seconds; (Kantor et al., 2013; Mochizuki et al., 2004)]. For each vigilance state, a time-weighted frequency histogram was produced using the number of episodes and the percentage of each vigilance state occurring in each bout length and compared between $PZ^{Phox2B\text{-}DTA}$ mice to $PZ^{Phox2B\text{-}WT}$ mice.

Sleep-wake power density was assessed by rescoring 3-hours of recording early in the rest period (10:00–13:00) and at the start of the active period (19:00-22:00) into 4-second epochs of wakefulness, SWS, and REM sleep. Assessment included visually identifying epochs containing artifacts occurring during active wake (with large movements) or containing two vigilance states and omitting them from the spectral analysis. Mice were excluded from spectral analysis if more than 20% of their 3-hour recording was omitted. Fast Fourier transform routine (FFT) was applied to the EEG to generate the power spectrum by computing consecutive 4-second epochs within a frequency range of 0.5-120 Hz and 0.5 Hz bins. The data was normalized by expressing each frequency bin as a percentage of the

epoch total power. For analyzing the EEG frequency bands, the power bins were normalized as a percentage of total power then summed into delta (δ, 0.5 – 4 Hz), theta (θ, 4 – 9 Hz), alpha (α, 9 – 15 Hz), beta (β, 15 – 30 Hz), low gamma (lγ, 30 – 60 Hz), and high gamma (hγ, 60 – 120 Hz) bands. The difference was analyzed between each band for each sleep-wake state comparing $PZ^{Phox2B\text{-}DTA}$ mice to $PZ^{Phox2B\text{-}WT}$ mice for the 3-hours during the rest period (10:00-13:00) and for the 3-hours during the active period (19:00-22:00).

Prism v6 (Graphpad Software, San Diego, CA, United States) was used to perform statistical analyses. After confirming the data met the parameters for the ANOVA model, two-way repeated-measures ANOVA followed by a *post hoc* Bonferroni test were performed to determine significant differences in sleep-wake amount, fragmentation, and cortical EEG power density between $PZ^{Phox2b\text{-}DTA}$ mice and $PZ^{Phox2B\text{-}WT}$ mice. Welch's t-test was performed to assess significant changes in 24-hour sleep-wake amount between $PZ^{Phox2b\text{-}DTA}$ mice to $PZ^{Phox2B\text{-}WT}$ mice.

Injection site mapping

At the end of the behavioral experiments, mice received ketamine/xylazine (200 and 20 mg/kg, respectively) intraperitoneal injections. Once the mice were deeply anesthetized and unresponsive to toe pinch, they were perfused transcardially with 20 ml of saline, followed by 100 ml of neutral phosphate-buffered formalin (4%, Thermo Fisher Scientific). After extraction from the skull, brains were incubated in neutral phosphate-buffered formalin (4%, Thermo Fisher Scientific) for two hours, followed by 20% sucrose in 1x PBS until they sank.

Brains were sectioned at 40 μm into 3 series using a sliding, freezing microtome. To determine the region containing transfected cells, one series was mounted on slides, cover slipped using ProLong antifade Glass (Life Technologies #P36984) and viewed with a fluorescent microscope (Keyence BZ-X710, Japan). The boundary of the transfected area was mapped using mCherry native fluorescence expressed in all non-cre-recombinase expressing cells at the injection site, indicating the anatomic extent of transfection (Figure 2.2).

Immunolabeling

Since the homeodomain transcription factor Phox2B is expressed transiently during development in some neurons, GFP expression in Phox2B-GFP mice reflects developmental expression rather than adult expression of Phox2B-cre (Kang et al., 2007; Pattyn et al., 1997). Therefore, GFP expression is not a reliable proxy for Phox2B-cre expressing neurons. To confirm the lesion of PZ^{Phox2B} neurons following DTA-AAV injection, we attempted immunolabeling of Phox2B.

Series from sixteen Phox2B-GFP mice were immunostained for Phox2B using either monoclonal recombinant rabbit anti-Phox2B antibody (ab183741; Table 2.1 A) or polyclonal rabbit anti-Phox2B antibody (pa5-35044; Table 2.1 A) at varying concentrations (Table 2.2). Slices were then labeled with a secondary antibody conjugated to either a red fluorophore (CY1300, 1:1000; Table 2.1 B), or biotinylated (BA-1000, 1:1000; Table 2.1 B) and followed by either a far-red fluorophore (016-650-084, 1:1000; Table 2.1 C) or ABC (#PK-4000, Vectorlabs) followed by diaminobenzidine (DAB) reaction (Table 2.1 C).

Standard immunofluorescence and immunohistochemistry protocols were performed with parameters optimized during troubleshooting which included primary antibody concentration, antigen retrieval, and length of time incubating in the primary antibody [Table 2.2; (Venner et al., 2016)]. Antigen retrieval was attempted by incubating slices in 1x phosphate buffer saline (PBS, ph7.4) at 90°C in an oven for 10 minutes, or by incubating slices in Tris-EDTA buffer at 90°C in a water bath for 10 minutes. Primary antibodies were tested between a concentration of 1:5000 and 1:250 with incubation normally lasting two nights but some were extended to three nights. The parameters optimized are detailed in Table 2.2.

To test if the absence of labeling was due to insufficient signal amplification, we use the DAB labeling technique which allow further amplification of the signal. This technique is appropriate for double labeling of cell cytoplasm and nucleus. In previous experiments, GFP has been shown to have a cytoplasmic localization while the transcription factor Phox2B has been shown to be nuclear (Liu et al., 2014; Rossi et al., 2011). In Phox2B-GFP brain slices double-labeling using rabbit anti-Phox2B (Table 2.1 A) and chicken anti-GFP (Table 2.1 A), the appropriate biotinylated secondary antibody followed be Avidin/Biotin complex. GFP was labeled in brown and Phox2B in black using DAB staining. GFP expressing neurons are seen in brown (Figure 2.8) however, black labeling was not seen, in contrast to a previous report (Tiveron et al., 1996).

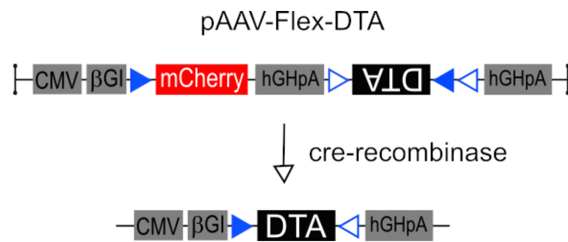

Figure 2.1: Viral construct for neuronal ablation

Diagram depicting the AAV-Flex-DTA construct to express diphtheria toxin subunit A (DTA) in a cre-dependent configuration to genetically produce cell death in cre-expressing neurons with mCherry to be expressed in transfected cre-negative cells. Abreviations: CMV, cytomegalovirus promoter; betaGI, beta glucosidase; hGHpA = the human growth hormone gene polyadenylation signal. Modified from Kaur et al., 2017 with authorization.

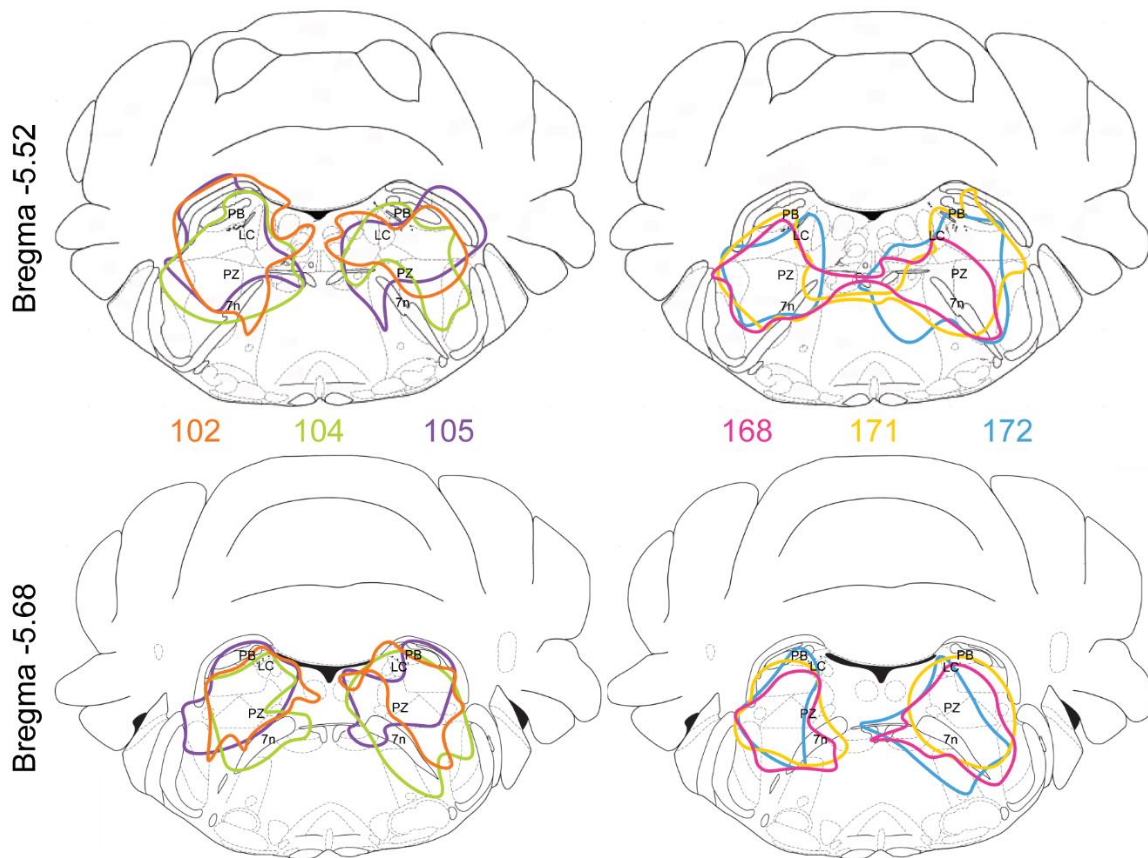

Figure 2.2: Transduced Neurons at the Injection Site for $PZ^{Phox2B\text{-}DTA}$ mice

Extent of transduced neurons with mCherry-positive somas is displayed for six individual Phox2B-*IRES*-cre mice that received bilateral injections of AAV-lox-mCherry-lox-DTA-lox2 into the PZ ($PZ^{Phox2B\text{-}DTA}$). Boundaries of transduced neurons are mapped and represented on diagrams of mouse brain slices from The Mouse Brain in Stereotaxic Coordinates (Franklin & Paxinos, 2001) at anatomic locations Bregma -5.52 and -5.68 to display the PZ. Abreviations: 7n, seventh (facial) nerve; LC, locus coeruleus; PB, parabrachial nucleus; PZ, parafacial zone.

A) Primary Antibodies

Antigen	Host	Source	Catalog#	Type
Phox2B	Rabbit	abcam	ab183741	Monoclonal, recombinant
Phox2B	Rabbit	Invitrogen	PA5-35044	Polyclonal
GFP	Chicken	Invitrogen	Ab262	-

B) Secondary Antibodies

Antigen	Host	Source	Catalog#	Labeling Marker Name
Rabbit	Goat	Vector Labs	BA-1000	Biotin
Rabbit	Goat	Vector Labs	CY-1300	Cy3
Chicken	Goat	Vector Labs	BA-90110	Biotin

C) Labeling Method for Biotinilated Secondary Antibodies

Antigen	Host	Source	Catalog#	Labeling Marker Name
Biotin	-	Vector Labs	PK-4000	ABC kit
Biotin	-	Invitrogen	016-650-084	Alexa 790

Table 2.1: Primary and Secondary Antibodies Used for Immunostaining

Details for A) primary and B) secondary antibodies and C) the method used to visualize labeling of biotin secondary antibodies.

A) Rabbit anti-Phox2B (ab183741, abcam)

<table>
<tr><th># of mice</th><th>Antibody Concentration</th><th>Antigen Retrieval</th><th>Incubation Length</th><th>Labeling Marker</th><th>Result</th></tr>
<tr><td>1</td><td>1:250</td><td rowspan="5">None</td><td rowspan="8">2 days</td><td rowspan="4">Cy3</td><td rowspan="4">No label</td></tr>
<tr><td>2</td><td>1:500</td></tr>
<tr><td>3</td><td>1:1000</td></tr>
<tr><td>2</td><td>1:5000</td></tr>
<tr><td>2</td><td>1:1000</td><td>DAB</td><td>No label</td></tr>
<tr><td>2</td><td>1:500</td><td rowspan="7">Oven 90°C</td><td rowspan="2">Cy3</td><td rowspan="2">No overlap with Phox2B-GFP</td></tr>
<tr><td>3</td><td>1:1000</td></tr>
<tr><td>1</td><td>1:500</td><td>Alexa 790</td><td>No label</td></tr>
<tr><td>1</td><td>1:250</td><td rowspan="4">3 days</td><td rowspan="3">Cy3</td><td rowspan="3">No overlap with Phox2B-GFP</td></tr>
<tr><td>1</td><td>1:500</td></tr>
<tr><td>1</td><td>1:1000</td></tr>
<tr><td>10</td><td>1:500</td><td>DAB</td><td>High background, unclear if nuclear staining</td></tr>
</table>

B) Rabbit anti-Phox2B (PA5-35044, Invitrogen)

<table>
<tr><th># of mice</th><th>Antibody Concentration</th><th>Antigen Retrieval</th><th>Incubation Length</th><th>Labeling Marker</th><th>Result</th></tr>
<tr><td>1</td><td>1:1000</td><td rowspan="2">Water Bath 100°C</td><td rowspan="2">2 days</td><td>Alexa 790</td><td>Tissue damaged</td></tr>
<tr><td>2</td><td>1:1000</td><td>DAB</td><td>High background, unclear if nuclear staining</td></tr>
</table>

Table 2.2: List of Parameters During Troubleshooting

Combinations of optimized parameters for A) monoclonal Phox2B antibody and B) polyclonal Phox2B antibody labeling. Results are for best series outcome.

Results

Transfection of Phox2B-cre neurons in the parafacial zone

To test the necessity of PZ^{Phox2B} neurons in sleep-wake control, Phox2B-IRES-Cre mice received bilateral injections into the PZ of DTA-AAV (Figure 2.1). The constitutive expression of mCherry encoded by the virus allowed us to see the anatomical extent of transduction at the injection site. Fluorescent visualization of the transduced neurons was used to map the transduction boundary. Six cre-expressing mice used for behavioral state analysis displayed full coverage of mCherry labeling bilaterally in the PZ with some transduction in the parabrachial nucleus and locus coeruleus (Figure 2.2).

$PZ^{Phox2B\text{-}DTA}$ mice have unaltered sleep-wake amounts

We analyzed sleep-wake phenotypes after bilateral injection of DTA-AAV into the PZ of Phox2B-IRES-cre mice. Cre-expressing mice ($PZ^{Phox2B\text{-}DTA}$) were compared with non-cre-expressing littermates ($PZ^{Phox2B\text{-}WT}$). We found that genotype did not affect the distribution of wakefulness (two-way ANOVA, $F(23,207) = 1.03$, $p = 0.43$; Figure 2.3 A1), SWS (two-way ANOVA, $F(23,207) = 1.059$, $p = 0.39$; Figure 2.3 A2), or REM sleep (two-way ANOVA, $F(23,207) = 0.74$, $p = 0.80$; Figure 2.3 A3). To see if there may be a difference in overall amount of sleep-wake behavior during either the rest period (07:00-19:00) or the active period (19:00-07:00), we assessed the twelve hours of each period and the full 24 hours (07:00-07:00) of sleep-wake amount in $PZ^{Phox2B\text{-}DTA}$ mice as compared with $PZ^{Phox2B\text{-}WT}$ mice. There was no significant effect of the mouse genotype in the

amount of wakefulness (two-way ANOVA, $F(1,9) = 1.84$, $p = 0.21$; Figure 2.3 B1), SWS (two-way ANOVA, $F(1,9) = 2.16$, $p = 0.18$; Figure 2.3 B2), or REM sleep (two-way ANOVA, $F(1,9) = 0.41$, $p = 0.54$; Figure 2.3 B3) for the rest and active period in $PZ^{Phox2B\text{-}DTA}$ mice as compared to $PZ^{Phox2B\text{-}WT}$ mice. There was also no significant difference in the 24 hour total amount for wakefulness (Welch's t-test, $p = 0.091$; Figure 2.3 B1), SWS (Welch's t-test, $p = 0.108$; Figure 2.3 B2), or REM sleep (Welch's t-test, $p = 0.166$; Figure 2.3 B3) in $PZ^{Phox2B\text{-}DTA}$ mice as compared to $PZ^{Phox2B\text{-}WT}$ mice.

$PZ^{Phox2B\text{-}DTA}$ mice display increased wake fragmentation during the active period

To determine if $PZ^{Phox2B\text{-}DTA}$ mice have changes in sleep architecture, we evaluated the number of bouts and bout durations for each vigilance state. During the rest period, the mouse genotype did not have a significant effect on the number of wake bouts (two-way ANOVA, $F(7,63) = 0.13$, $p = 0.99$; Figure 2.4 A1), SWS bouts (two-way ANOVA, $F(7,63) = 0.36$, $p = 0.92$; Figure 2.4 A2), or REM sleep bouts (two-way ANOVA, $F(7,63) = 0.73$, $p = 0.65$; Figure 2.4 A3). Additionally, the percentage of wakefulness spent in each bout length (two-way ANOVA, $F(7,63) = 0.31$, $p = 0.95$; Figure 2.4 B1), the percentage of SWS spent in each bout length (two-way ANOVA, $F(7,63) = 0.04$, $p = 0.99$; Figure 2.4 B2), and the percentage of REM sleep spent in each bout length (two-way ANOVA, $F(7,63) = 0.79$, $p = 0.60$; Figure 2.4 B3) was not affected by the mouse genotype.

During the active period, the number of bouts was significantly affected by the mouse genotype (two-way ANOVA, $F(7,63) = 4.09$, $p = 0.0009$; Figure 2.5 A1). PZ$^{Phox2B\text{-}DTA}$ mice had a significant increase in the number of wakefulness bouts lasting 70 - 150 seconds (18.83 ± 2.6 vs 8.8 ± 1.7 in PZ$^{Phox2B\text{-}WT\ mice}$, $p = 0.013$; Figure 2.5 A1). This correlates with the significant effect of the mouse genotype on the proportion of wakefulness from various bout length (two-way ANOVA, $F(7,63) = 3.12$, $p = 0.007$; Figure 2.5 B1). PZ$^{Phox2B\text{-}DTA}$ mice spent significantly less of their total wake time in bouts longer than 40 minutes (5.5 ± 4.2 vs 23.4 ± 6.4% in PZ$^{Phox2B\text{-}WT\ mice}$, $p = 0.012$; Figure 2.5 B1). While there was a trend towards increased proportion of wakefulness spent in the shorter bouts between 40 seconds and 10 minutes. However, there was no effect of the mouse genotype in the number of SWS bouts (two-way ANOVA, $F(7,63) = 0.93$, $p = 0.49$; Figure 2.5 A2) or in the percentage of total SWS time spent in each bout length (two-way ANOVA, $F(7,63) = 0.97$, $p = 0.46$; Figure 2.5 B2). Likewise, the mouse genotype did not affect the number of REM sleep bouts (two-way ANOVA, $F(7,63) = 0.60$, $p = 0.759$; Figure 2.5 A3) or the percentage of total REM sleep spent in each bout (two-way ANOVA, $F(7,63) = 0.54$, $p = 0.80$; Figure 2.5 B3).

Cortical power distribution was not significantly affected in PZ$^{Phox2B\text{-}DTA}$ mice

To assess if PZ$^{Phox2B\text{-}DTA}$ mice have altered cortical power distribution, vigilance states were analyzed for three hours during the rest period (10:00-13:00), and at the start of the active period (19:00-21:00). The mouse genotype did not significantly affect cortical EEG power distribution during wakefulness (two-way

ANOVA, $F(5,24) = 0.23$, $p = 0.945$; Figure 2.6 A1), SWS (two-way ANOVA, $F(5,24) = 0.80$, $p = 0.559$; Figure 2.6 A2), and REM sleep (two-way ANOVA, $F(5,24) = 0.44$, $p = 0.813$; Figure 2.6 A3) during the rest period. Similarly, the mouse genotype did not significantly affect cortical EEG power distribution during wakefulness (two-way ANOVA, $F(5,24) = 0.78$, $p = 0.572$; Figure 2.6 B1), SWS (two-way ANOVA, $F(5,24) = 0.13$, $p = 0.984$; Figure 2.6 B2), or REM sleep (two-way ANOVA, $F(5,24) = 0.14$, $p = 0.983$; Figure 2.6 B3) during the active period.

Phox2B antibody immunostaining was unsuccessful

To determine whether PZ^{Phox2B} neurons were successfully ablated by DTA-AAV, we planned to utilize a rabbit anti-Phox2B antibody (Table 2.1 A) to label Phox2B-expressing neurons in adult mice. Initial labeling attempts were unsuccessful, and troubleshooting failed to produce a solution. Despite several methodological alterations (Table 2.2), we were not able to achieve successful labeling (Table 2.2; Figure 2.7, 2.8). In endogenously labeled Phox2B-GFP brain slices (Figure 2.7 A, D), immunolabeling of rabbit anti-Phox2B (Table 2.1 A) by the red fluorophore Cy3 (CY-13000; Table 2.1 B) did not successfully label Phox2B (Figure 2.7 C, F).

Since GFP is located in the cytoplasm while the transcription factor Phox2B is localized to the nucleus, we used the DAB labeling technique to amplify the signal (Liu et al., 2014; Rossi et al., 2011). Phox2B-GFP brain slices were double-labeled using rabbit anti-Phox2B (Table 2.1 A) and chicken anti-GFP (Table 2.1 A), with the appropriate biotinylated secondary antibody followed by Avidin/Biotin

complex. GFP was labeled in brown using standard DAB staining, and Phox2B in black using DAB staining with Cobalt and Nickel. GFP expressing neurons are seen in brown (Figure 2.8) however, black labeling was not seen, in contrast to a previous report (Tiveron et al., 1996).

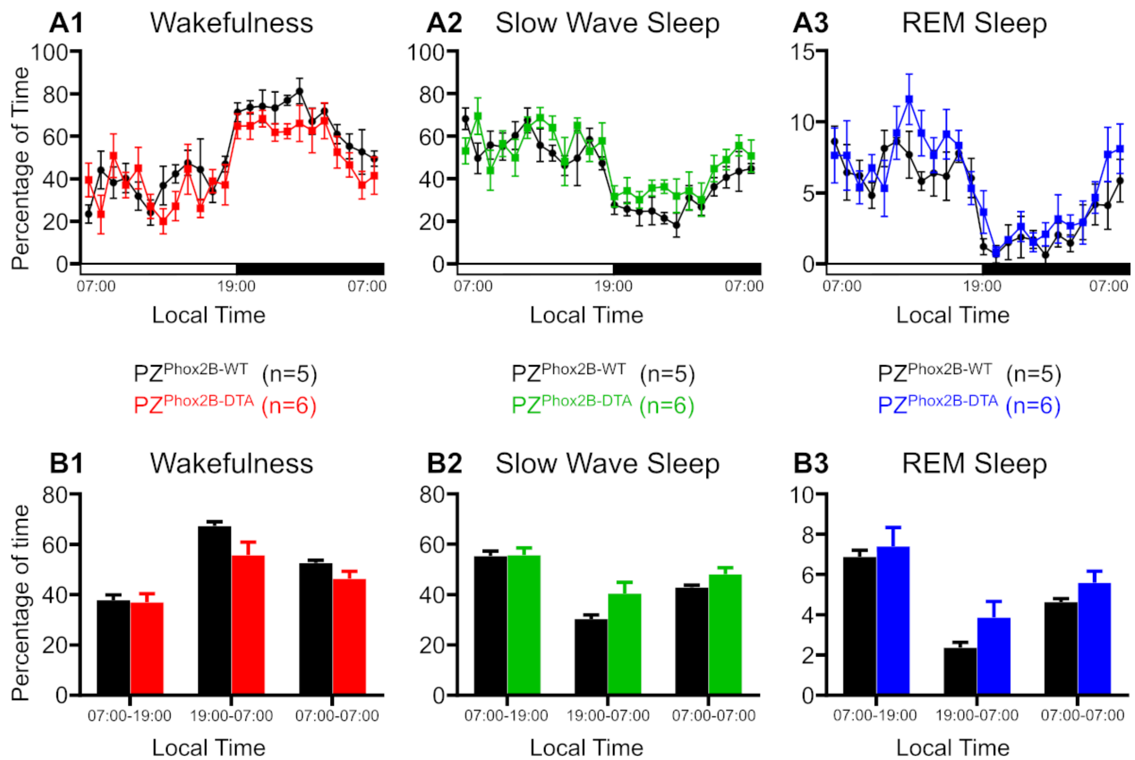

Figure 2.3: Sleep-wake Amounts

(A) Hourly percentage of time (± S.E.M.) $PZ^{Phox2B-DTA}$ mice spent in wakefulness (A1), slow-wave-sleep (A2), and REM sleep (A3) during a 24-hour period as compared with control ($PZ^{Phox2B-WT}$) mice. (B) The percentage of each sleep-wake state (±S.E.M.) in $PZ^{Phox2B-DTA}$ mice as compared to $PZ^{Phox2B-WT}$ mice during the rest period (07:00-19:00), the active period (19:00-07:00), and the entire 24-hour period (07:00-07:00). $PZ^{Phox2B-WT}$ mice (n = 5) in black, $PZ^{Phox2B-DTA}$ mice (n = 6) in color; no significant change, Welch's t-test and two-way ANOVA for repeated-measures (factor: hour).

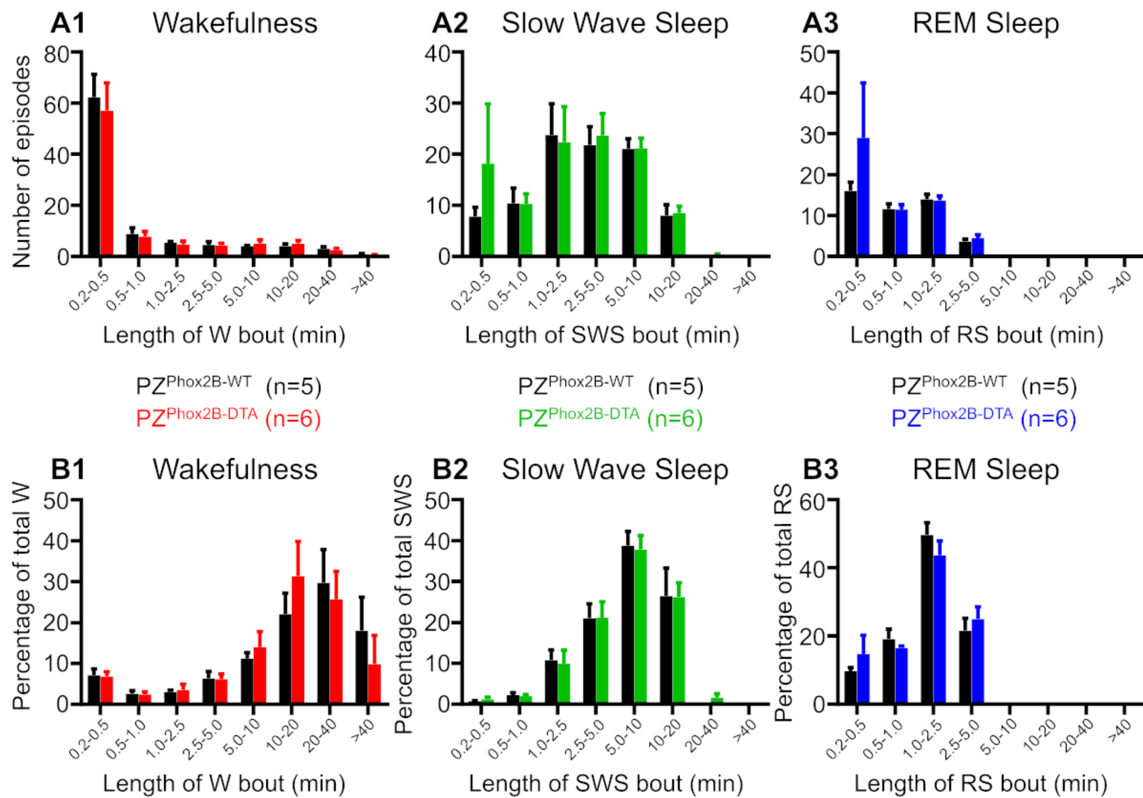

Figure 2.4: Sleep Architecture During the Rest Period (07:00-19:00)

(A) Number of episodes (±S.E.M.) spent in each bout length of wakefulness (W; A1), slow wave sleep (SWS; A2), and REM sleep (RS; A3) for $PZ^{Phox2B\text{-}DTA}$ mice as compared to control ($PZ^{Phox2B\text{-}WT}$) mice during the rest period (07:00-19:00). (B) Time-weighted frequency histograms showing the portion (±S.E.M.) of wakefulness (B1), slow wave sleep (B2), or REM sleep (B3) amounts in each bout length as a percentage of the total amount of the vigilance stage in $PZ^{Phox2B\text{-}DTA}$ mice as compared to $PZ^{Phox2B\text{-}WT}$ mice during the rest period (07:00-19:00). $PZ^{Phox2B\text{-}WT}$ mice (n=5) in black, $PZ^{Phox2B\text{-}DTA}$ mice (n=6) in color; no significance, two-way ANOVA for repeated-measures (factor: bout length).

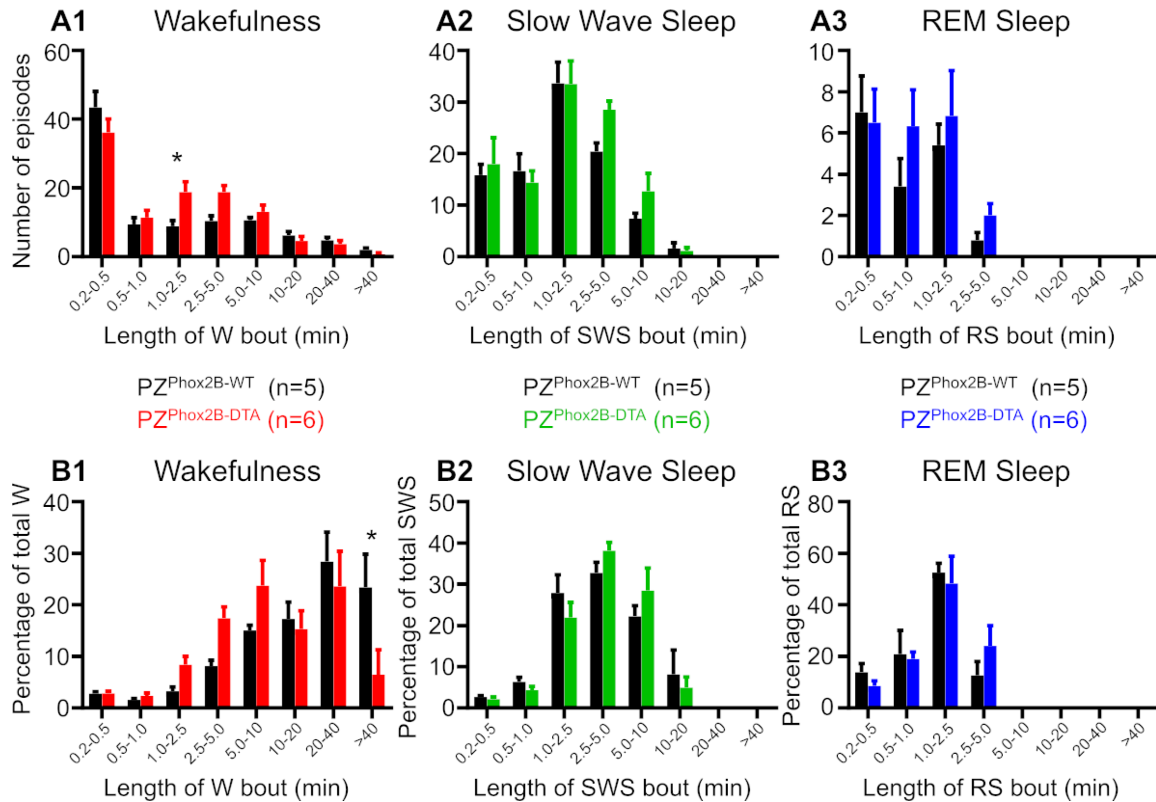

Figure 2.5: Sleep Architecture of the Active Period (19:00-07:00)

(A) Number of episodes (±S.E.M.) spent in each bout length of wakefulness (W; A1), slow wave sleep (SWS; A2), and REM sleep (RS; A3) in PZ$^{Phox2B-DTA}$ mice as compared to PZ$^{Phox2B-WT}$ mice during the active period (19:00-07:00). (B) Time-weighted frequency histograms showing the portion (±S.E.M.) of wakefulness (B1), slow wave sleep (B2), or REM sleep (B3) amounts in each bout length as a percentage of the total amount of the vigilance stage in PZ$^{Phox2B-DTA}$ mice as compared to PZ$^{Phox2B-WT}$ mice during the active period (19:00-07:00). PZ$^{Phox2B-WT}$ mice (n=5) in black, PZ$^{Phox2B-DTA}$ mice (n=6) in color; *$p < 0.05$, two-way ANOVA for repeated-measures (factor: bout length) followed by *post hoc* Bonferroni test.

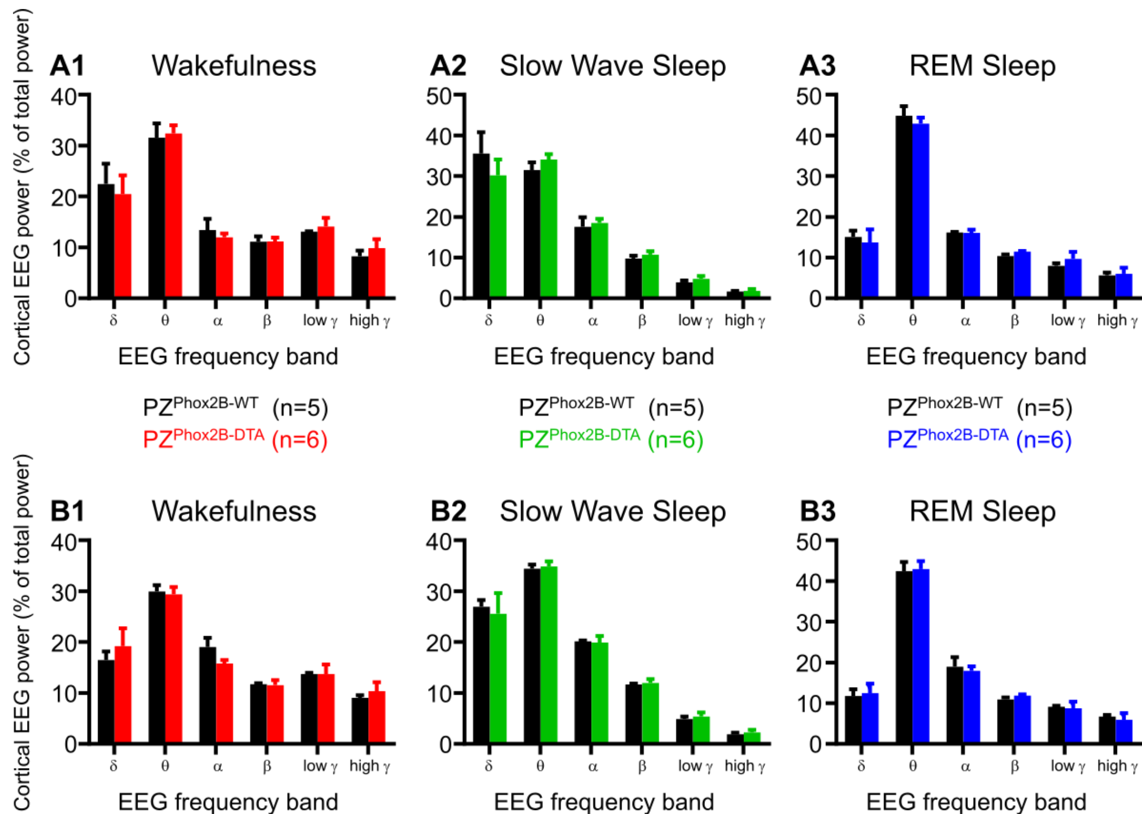

Figure 2.6: Cortical EEG Power Distribution

(A) The quantitative measures (±S.E.M.) of sleep-wake cortical EEG power in $PZ^{Phox2B\text{-}DTA}$ mice as compared with $PZ^{Phox2B\text{-}WT}$ mice for wakefulness (A1), slow wave sleep (A2), and REM sleep (A3) during 3 hours of the rest period (07:00-19:00). (B) The quantitative measures (±S.E.M.) of sleep-wake cortical EEG power for wakefulness (B1), slow wave sleep (B2), and REM sleep (B3) during 3 hours of the active period (19:00-07:00) for $PZ^{Phox2B\text{-}DTA}$ mice as compared with $PZ^{Phox2B\text{-}WT}$ mice. Power bands reported as delta (δ, 0.5-4 Hz), theta (θ, 4-9 Hz), alpha (α, 9-15 Hz), beta (β, 15-30 Hz), low gamma (lγ, 30-60 Hz), and high gamma (hγ, 60-120 Hz) frequency bands. Control mice (n=3) in black, DTA injected mice (n=3) in color; no significance, two-way ANOVA for repeated-measures (factor: power band).

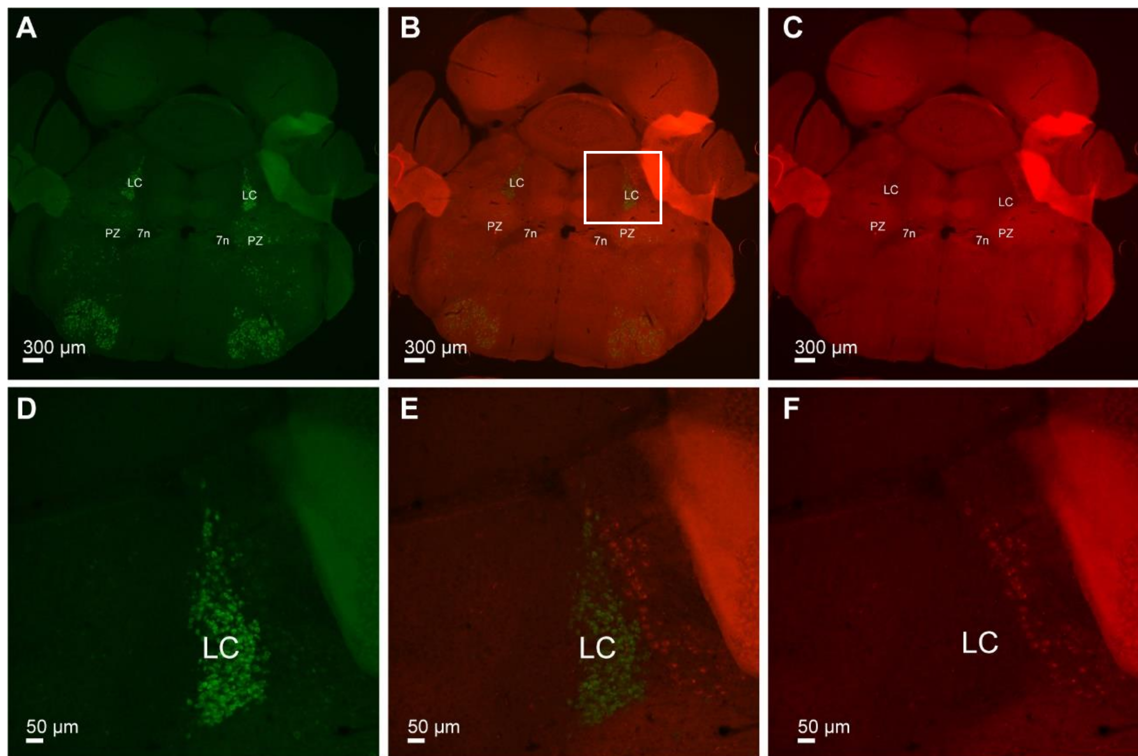

Figure 2.7: Phox2B Immunofluorescence

(A-C) Photomicrograph images of a Phox2B-GFP mouse brain showing GFP-expressing neurons (A) in the PZ and LC, merged to show overlap (B) with attempted immunolabeling of Phox2B in red (Cy3; C). Scale bar: 300 μm. (D-F) Higher magnification of the box in (B). Photomicrograph images of Phox2B-expressing GFP neurons (D) in the LC, merged to show overlap (E) with attempted immunolabeling of Phox2B in red (Cy3; F). Scale bar: 50 μm. Abbreviations: 7n, seventh (facial) nerve; LC, locus coeruleus; PZ, parafacial zone.

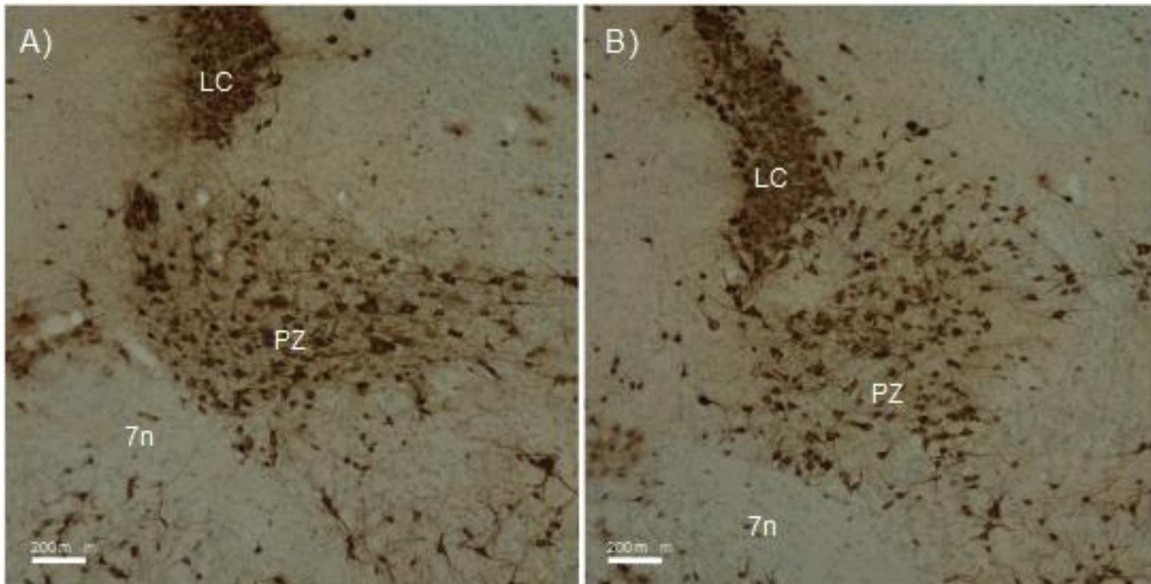

Figure 2.8: Phox2B Immunohistochemistry

(A-B) Photomicrograph from a Phox2B-GFP mouse brain on different levels showing GFP DAB staining (cell bodies in brown) in the PZ and LC and attempted DAB immunolabeling of Phox2B which would be in black. Scale bar: 100 µm. Abbreviations: 7n, seventh facial nerve; LC, locus coeruleus; PZ, parafacial zone.

Chapter 3

Discussion

PZ$^{Phox2B\text{-}DTA}$ mice phenotype

Previous research showed that GABAergic neurons in the PZ (PZ^{GABA}) are both sufficient and necessary for SWS (Anaclet et al., 2014; Anaclet et al., 2012). The PZ contains a heterogeneous population of neurons. Staining for c-fos, a neuronal marker for activity, found non-GABAergic sleep-active neurons in a region of the PZ containing glutamatergic neurons. Research investigating glutamatergic PZ neurons using Phox2B (PZ^{Phox2B}) as a marker found no significant sleep-wake effect when chemogenetically stimulated (Erickson et al., 2019). That showed PZ^{Phox2B} neurons are not sufficient to affect sleep-wake phenotype, but it remained unclear if they were required for normal sleep-wake phenotypes.

Based on this previous research (Erickson et al., 2019), we sought to determine the necessity of glutamatergic PZ^{Phox2B} neurons in sleep-wake control. The results here document the sleep-wake phenotype of mice after DTA-AAV injection into the PZ of Phox2B-*IRES*-cre (PZ$^{Phox2B\text{-}DTA}$) mice to ablate PZ^{Phox2B} neurons. Anatomical mapping confirmed coverage of the PZ by viral transfection using mCherry labeling (Figure 2.2). PZ$^{Phox2B\text{-}DTA}$ mice had no significant difference in sleep-wake amount (Figure 2.3) nor in sleep-wake quality as measured by cortical power distribution (Figure 2.6) when compared to control mice (PZ$^{Phox2B\text{-}}$

^{WT}) for wakefulness, SWS, or REM sleep during the active and inactive periods. Additionally, PZ$^{Phox2B\text{-}DTA}$ mice did not experience a change in sleep architecture as measured by proportion of the vigilance stage spent in different bout lengths during the rest period (Figure 2.4). There was not a change in sleep architecture for SWS and REM sleep during the active period either (Figure 2.5). PZ$^{Phox2B\text{-}DTA}$ mice displayed a significant decrease in the amount of wakefulness spent in bouts longer than 40 minutes with a trend of increased amounts of wakefulness in bouts shorter than 10 minutes (Figure 2.5). This corresponds with the significant increase in the number of bouts that lasted 1 to 2.5 minutes and the trend of increased number of wakefulness bouts up to 10 minutes long in PZ$^{Phox2B\text{-}DTA}$ mice as compared with PZ$^{Phox2B\text{-}WT}$ mice. This suggests wake fragmentation during the active period; however, confirmation of the lesion was not possible.

PZ^{Phox2B} neuronal lesion

Phox2B-*IRES*-Cre mice have been shown to reliably mediate expression of cre-dependent factors (Rossi et al., 2011). DTA-AAV has been shown to reliably transfect and selectively ablate cre-expressing neurons (Anaclet, et al., 2018; Kaur et al., 2017). Therefore, transfected cre-expressing neurons at the PZ injection site were likely ablated. However, it needs to be confirmed both that only PZ^{Phox2B} neurons and all PZ^{Phox2B} neurons were ablated.

The cre-dependent reporter mouse Flox-L10-GFP [Jackson Laboratory #24750 (Liu et al., 2014)] was crossed with the Phox2B-*IRES*-Cre mouse line, resulting in GFP labeling of Phox2B-expressing neurons (Phox2B-GFP). The GFP

expression is cre-dependent so it is persistent once turned on. As such, cells only need to express Phox2B once, at which time the Cre from the Phox2B locus facilitates recombination of GFP, resulting in persistent expression of GFP for the lifetime of the cell and in its progeny even if Phox2B is no longer being produced within the cell. For this reason, GFP expression in Phox2B-GFP mice may not accurately identify neurons expressing Phox2B in adulthood since Phox2B is a neurodevelopmentally important transcription factor. As such, it was necessary to identify Phox2B in adult mice through a different method, such as immunolabeling. The Phox2B antibody previously published (Kang et al., 2007) did not result in specific labeling here for Phox2B-GFP mice (Figure 2.7, 2.8). Due to this, it cannot be said that the experimental results are due to lesion of PZ^{Phox2B} neurons, since lesion may be incomplete or may have occurred in nearby populations that also expressed Phox2B, such as the wake-promoting LC.

Phox2B Relationship with Glutamatergic Neurons in the PZ

The PHOX2B gene codes for a homeodomain transcription factor expressed exclusively in the nervous system. Prior research on Phox2B indicates that it plays a specific role in autonomic neuronal development and more specifically in neurons involved with breathing (Moreira et al., 2016). This transcription factor is essential for the differentiation of sympathetic neurons involved in the peripheral autonomic nervous system as Phox2B mutations are implicated in congenital central hypoventilation syndrome (Moreira et al., 2016).

Since this transcription factor is developmentally important, it may be expressed transiently in neurons that do not express it in adulthood. As such, a Phox2B-GFP mouse would display fluorescent labeling of all neurons that expressed the transcription factor at any time, even just during development, rather than only the neurons expressing it in adulthood. Therefore, in this study, Phox2B-GFP mice were not used to identify Phox2B-expressing neurons in adult brains.

Phox2B labeling in adult rats showed expression in the PZ (Kang et al., 2007), although the physiological function of these PZ neurons had not been experimentally explored. These neurons became a new focus in sleep research with the revelation that some PZ neurons are more active during sleep as compared with wakefulness (Anaclet et al., 2012). Previous research found Phox2B highly colocalized with Vglut2 expression in the PZ but not in the nearby PB, making it an ideal marker for targeting PZ^{Vglut2} neurons while excluding the strongly wake-promoting PB^{Vglut2} neurons (Erickson et al., 2019). However, Phox2B is a critical part of neurodevelopment for the neighboring LC and has been shown to be expressed in adulthood (Fan et al., 2018; Liu et al., 2020; Nobuta et al., 2015). Additionally, the LC contributes to wakefulness and when disrupted results in a decrease in wakefulness (Yamaguchi et al., 2018). This creates a need to confirm lesion specificity before the observed phenotype can be attributed to ablation of PZ^{Phox2B} neurons.

PZ^{Phox2B} neuron continuing investigation

Since the ablation of PZ^{Phox2B} neurons remains unconfirmed, obtaining a reliable Phox2B antibody will be important for any further inquiries or conclusions with these neurons. The brains of PZ$^{Phox2B-DTA}$ mice used in this research have been sectioned and stored for long-term preservation; confirmation of lesion could still be performed on these slices. Alternatively, a mouse line with Phox2B tagged by GFP directly (e.g. Phox2B-*IRES*-GFP) would make identification of adult expressing Phox2B neurons, and efficacy of ablation, much easier.

Additionally, since the antibody for labeling Phox2B neurons did not reliably function, it remains to be confirmed whether these are the non-GABAergic sleep active neurons previously found (Anaclet et al., 2012). As previously published (Anaclet et al., 2012), brain sections from sleeping mice can be labeled with c-fos, a marker of neuronal activity, and double-labeled for Phox2B to look for colocalization. Comparing the anatomical mapping of these Phox2B sleep active neurons with mapping for Phox2B lesion will confirm that they occur in the same neuronal population. Phox2B-GFP mice labeled for c-fos may sufficiently demonstrate this.

If neuronal ablation occurred within the LC, the wake fragmentation phenotype may be due to loss of those neurons (Yamaguchi et al., 2018) and not due to disrupting the functionality of PZ^{Phox2B} neurons. In this case, PZ^{Phox2B} neurons may not be involved in sleep-wake control and would no longer be of interest for a research group studying sleep. It remains to be considered, though,

that if the LC is affected, then the phenotype from the LC neurons and the phenotype from the PZ^{Phox2B} neurons may be masking each other. In this case, finding an even more specific neuronal marker for the glutamatergic PZ neurons of interest would be required. Single cell genomics of the PZ already underway may assist in doing so. If ablation of PZ^{Phox2B} neurons were complete and contained to only the PZ, then the reduction in wakefulness, while significant, does not prove these neurons are necessary for sleep-wake control since overall sleep and wake amounts were unaffected.

Continuing to characterize PZ sleep-wake control

While glutamatergic neurons are the only known non-GABAergic neuronal population in the PZ, it remains open for investigation if other types of sleep active neurons are present that are neither GABAergic nor glutamatergic. Future research can explore the *in-situ* hybridization data made available at the Allen Brain Atlas, although no candidates of interest were identified at this time. To confirm if there are additional sleep active neuronal population to identify, a Vgat^{Cre+} Phox2B^{Cre+} tdTomato mouse could be generated and immunostained for c-fos, a marker of neuronal activity, in mice sacrificed during the rest period. If there is a substantial population of c-fos labeled neurons that are not labeled by the endogenously expressed Tomato, then the PZ brain region can be sorted to remove the fluorescent cells, providing a pure population for single cell genomic analysis to determine their neuronal subtype identity. The research contained here

provides a starting point for characterization of the PZ's heterogeneous neuronal population.

In making progress on better understanding the many recently identified sleep control regions, future endeavors would benefit the most by consolidating efforts on the PZ^{GABA} neurons. Efferent tracing has identified projections to the wake-promoting parabrachial nucleus (Anaclet et al., 2014), but it remains to be seen if there are additional targets. Afferent projections are also still unknown, leaving as a mystery the regions that inform and control the PZ for sleep activity.

Potential interest for Phox2B

Since research implicates Phox2B mutations in breathing control (Moreira et al., 2016; Nobuta et al., 2015), alteration in breathing may have occurred in $PZ^{Phox2B\text{-}DTA}$ mice. No overt or dramatic phenotype was noticed; however, a lab with the resources and expertise for studying breathing in rodents would be best situated to conduct this investigation.

Conclusion

Using Phox2B as a specific neuronal marker facilitated investigation of PZ glutamatergic neurons' role in sleep-wake control. Chemogenetic activation of PZ^{Phox2B} neurons demonstrated no evidence they are sufficient for sleep-wake control (Erickson et al., 2019). Cre-mediated ablation of PZ^{Phox2B} neurons, if confirmed, provide no evidence they are necessary for sleep-wake control. Altogether, our results provide no evidence that PZ glutamatergic neurons are essential for sleep-wake control and thus no evidence these neurons are of interest

for further investigations into sleep-wake control. Future lines of inquiry into sleep-wake control in the PZ should focus on the GABAergic sleep-promoting neurons. This research combined with the previous study was important for establishing that glutamatergic PZ neurons do not contribute to sleep-wake control. Additionally, the documentation of these neurons provides new information about this previously uncharacterized region of the brain for future researchers to work with.

Appendix 1

Erickson et al., 2019

The following chapter is a manuscript published in the *Frontiers of Neuroscience*. Loris Ferrari performed *in vitro* experiments and provided the corresponding data for the figures and text. Heinrich Gompf performed RNAscope experiments and provided the corresponding images for the figures and data in the text. My contributions to this manuscript included analysis and manuscript preparation of all other data in Figures 1 through 5, 7, and 8. Christelle Anaclet planned and performed all other experiments and prepared all other elements of the manuscript.

frontiers in Neuroscience

ORIGINAL RESEARCH
published: 30 July 2019
doi: 10.3389/fnins.2019.00755

Differential Role of Pontomedullary Glutamatergic Neuronal Populations in Sleep-Wake Control

Evelyn T. M. Erickson, Loris L. Ferrari, Heinrich S. Gompf and Christelle Anaclet*

Department of Neurobiology, University of Massachusetts Medical School, Worcester, MA, United States

Parafacial zone (PZ) GABAergic neurons play a major role in slow-wave-sleep (SWS), also called non-rapid eye movement (NREM) sleep. The PZ also contains glutamatergic neurons expressing the vesicular transporter for glutamate, isoform 2 (Vglut2). We hypothesized that PZ Vglut2-expressing (PZ^{Vglut2}) neurons are also involved in sleep control, playing a synergistic role with PZ GABAergic neurons. To test this hypothesis, we specifically activated PZ^{Vglut2} neurons using the excitatory chemogenetic receptor hM3Dq. Anatomical inspection of the injection sites revealed hM3Dq transfection in PZ, parabrachial nucleus (PB), sublaterodorsal nucleus (SLD) or various combinations of these three brain areas. Consistent with the known wake- and REM sleep-promoting role of PB and SLD, respectively, chemogenetic activation of PB^{Vglut2} or SLD^{Vglut2} resulted in wake or REM sleep enhancement. Chemogenetic activation of PZ^{Vglut2} neurons did not affect sleep-wake phenotype during the mouse active period but increased wakefulness and REM sleep, similar to PB^{Vglut2} and SLD^{Vglut2} activation, during the rest period. To definitively confirm the role of PZ^{Vglut2} neurons, we used a specific marker for PZ^{Vglut2} neurons, Phox2B. Chemogenetic activation of PZ^{Phox2B} neurons did not affect sleep-wake phenotype, indicating that PZ glutamatergic neurons are not sufficient to affect sleep-wake cycle. These results indicate that PZ glutamatergic neurons are not involved in sleep-wake control.

Keywords: neuronal circuitry, DREADDs, brainstem, parafacial zone, sleep-wake control, sublaterodorsal nucleus, parabrachial nucleus

OPEN ACCESS

Edited by:
Takeshi Sakurai,
University of Tsukuba, Japan

Reviewed by:
Radhika Basheer,
Harvard Medical School,
United States
Hiromasa Funato,
Toho University, Japan

Correspondence:
Christelle Anaclet
Christelle.Anaclet@umassmed.edu

Specialty section:
This article was submitted to Sleep and Circadian Rhythms, a section of the journal Frontiers in Neuroscience

Received: *30 March 2019*
Accepted: *08 July 2019*
Published: *30 July 2019*

Citation:
Erickson ETM, Ferrari LL, Gompf HS and Anaclet C (2019) Differential Role of Pontomedullary Glutamatergic Neuronal Populations in Sleep-Wake Control. Front. Neurosci. 13:755. doi: 10.3389/fnins.2019.00755

INTRODUCTION

Over the past few years, the medullary parafacial zone (PZ) has been identified as a strong sleep-promoting brain area (Anaclet and Fuller, 2017). Both disruption of PZ GABAergic transmission (Anaclet et al., 2012) and chemogenetic inhibition of PZ GABAergic (PZ^{GABA}) neurons (Anaclet et al., 2014) result in insomnia. More importantly, chemogenetic activation of PZ^{GABA} neurons strongly increases SWS amount and consolidation and enhances cortical EEG slow-wave activity (SWA), a marker of SWS depth (Anaclet et al., 2014). Finally, chemogenetic activation of PZ^{GABA} neurons counteracts the wake-promoting action of psychostimulants (Anaclet et al., 2018). The PZ is generally located dorsal and lateral from the facial nerve but its exact boundaries are not precisely defined. A recent study has shown that, in mouse, the parvicellular reticular nucleus part alpha (PCRtA), ventral from PZ, does not contain sleep-active neurons (Sakai, 2017), indicating that the PZ sleep promoting neuronal population does not include the PCRtA.

In rats, about 40% of PZ neurons are sleep-active (Alam et al., 2018) and cell body specific PZ lesions result in insomnia (Anaclet et al., 2012). More specifically, PZ^{GABA} are involved in slow-wave-sleep (SWS) control. However, cFos expression, a marker of neuronal activity, showed that about half of sleep-active neurons are GABAergic (Anaclet et al., 2012), indicating that in the PZ, non-GABAergic neurons are also involved in sleep control. Within the PZ, the only other known neuronal population is glutamatergic, expressing the vesicular glutamate transporter isoform 2 (Vglut2; *in situ* hybridization data are available in Allen Mouse Brain Atlas, Allen Institute for Brain Science[1]). We hypothesized that PZ glutamatergic neurons (PZ^{Vglut2}) are also involved in sleep control and act synergistically with sleep-active PZ^{GABA} neurons to promote SWS. To start testing this hypothesis, we chemogenetically activated PZ^{Vglut2} neurons. Specific targeting of PZ was challenging and sleep phenotypes were difficult to interpret due to the possible transfection of the neighboring parabrachial (PB) and sublaterodorsal (SLD) nuclei that are involved in wakefulness and rapid eye movement (REM) sleep, respectively (Clement et al., 2011; Fuller et al., 2011). To get around these obstacles and specifically test the involvement of PZ glutamatergic neurons in sleep-wake control, we used Phox2B, a transcription factor expressed in PZ but not PB or SLD glutamatergic neurons. Data indicate that PZ glutamatergic neurons are not involved in sleep-wake control. Additionally, we found that excitation of PB or SLD glutamatergic neurons promotes wakefulness or REM sleep, respectively, results that are complimentary to the reduction in wakefulness or REM sleep previously observed following lesion of PB or SLD, respectively (Clement et al., 2011; Fuller et al., 2011).

MATERIALS AND METHODS

Animals

In order to visualize Vglut2-, Phox2B- and Vgat-expressing neurons, Vglut2-IRES-cre [Jackson Laboratory #016963 (Vong et al., 2011)], Phox2B-IRES-cre [Jackson Laboratory #016223 (Rossi et al., 2011)] and Vgat-IRES-cre [Jackson Laboratory #016962 (Vong et al., 2011)] mice were crossed with a cre-dependent reporter mouse Flox-L10-GFP [Jackson Laboratory #24750 (Liu et al., 2014)], producing Vglut2-GFP, Phox2B-GFP and Vgat-GFP mouse lines. Thirty two adult male Vglut2-GFP mice, seven adult male Phox2B-GFP and one adult male Vgat-GFP (8–12 weeks, 20–25 g) mice were used in this study. Mice were bred at our animal facility and underwent genotyping both before and after experiments. All procedures were approved by the Institutional Animal Care and Use Committee of Beth Israel Deaconess Medical Center and of University of Massachusetts Medical School.

Surgery

Naïve mice were anesthetized with ketamine/xylazine [100 and 10 mg/kg, respectively, intraperitoneal (IP)] and then placed in a stereotaxic apparatus. To selectively express the hM3Dq receptors in glutamatergic (Vglut2+) or Phox2B-expressing neurons of the PZ, we performed bilateral injections of an adeno-associated viral (AAV; serotype 10) vector expressing the hM3Dq receptor in a cre-dependent configuration [hSyn-DIO-hM3Dq-mCherry-AAV; (Anaclet et al., 2014)] into the PZ [coordinates from Bregma: Antero-posterior = −5.6 mm, Lateral = ± 1.0 mm, Dorso-ventral = −4.2 mm, as per the mouse atlas of Paxinos and Watson (Paxinos and Franklin, 2001)] of *Vglut2-IRES-cre* ($PZ^{Vglut2-hM3Dq}$) mice, *Phox2B-IRES-cre* ($PZ^{Phox2B-hM3Dq}$) mice or non-cre expressing littermate control mice. Injections of the viral vector (60 nl) into the PZ of these mice were performed using a compressed air delivery system as previously described (Anaclet et al., 2010). After injections, mice were implanted with four EEG screw electrodes (Pinnacle Technology Inc., Catalog #8403) and two flexible electromyogram (EMG) wire electrodes (Plastics One, catalog #E363/76/SPC), previously soldered to a 6-pin connector (Heilind Electronics, catalog #853-43-006-10-001000) and the assembly was secured with dental cement. The scalp wound was closed with surgical sutures and the mouse was kept in a warm environment until resuming normal activity as previously described (Anaclet et al., 2015).

Sleep-Wake Monitoring

Three weeks after surgery, the mice were housed individually in transparent barrels in an insulated sound-proofed recording chamber maintained at an ambient temperature of 22 ± 1°C and on a 12 h light/dark cycle (lights-on at 7 A.M., Zeitgeber time: ZT0) with food and water available *ad libitum*. Mice were habituated to the recording cable for 5–7 days before starting polygraphic recording. Cortical EEG (ipsilateral fronto-parietal leads) and EMG signals were amplified (A-M System 3500, United States) and digitalized with a resolution of 500 Hz using Vital Recorder (Kissei, Japan). Mice were recorded for a 24 h baseline period followed by IP injections of saline (control injection) or Clozapine-N-oxide (CNO, NIMH Chemical Synthesis and Drug Supply Program; 0.3 mg/kg in saline). Injections were performed at 10 A.M. (10:00, ZT3, light period, time of high sleep-drive) and 7 P.M. (19:00, ZT12, beginning of the dark period, time of high wake-drive), in a randomized cross-over design, with each injection separated by a 2–3 day washout period. In each experiment, recordings were simultaneously made from an equal number (batches of 2–4) of $PZ^{Vglut2-hM3Dq}$ and $PZ^{Vglut2-wt}$ mice.

Sleep Scoring and Analysis

Using SleepSign for Animal (Kissei, Japan) assisted by spectral analysis using fast Fourier transform, polygraphic records were visually scored in 10 s epochs for wakefulness (W), SWS, and REM sleep. The percentage of time spent in wake, SWS and REM sleep were summarized for each group and each condition. The SWS to REM sleep latency is defined as the time between the onset of the first SWS episode, lasting $>$20 s, after injection and the onset of the first REM sleep episode, lasting $>$10 s.

Sleep-wake fragmentation was assessed by analyzing the distribution of each vigilance stage in different bout lengths. Vigilance stages were separated into eight bout lengths ($<$30, 40–70, 80–150, 160–310, 320–630, 640–1270, 1280–2550, and

[1] http://mouse.brain-map.org/experiment/show/73818754

>2550 s) (Mochizuki et al., 2004; Kantor et al., 2013). For each vigilance stage, the number of episodes and the percentage of the vigilance stages occurring in each bout length were used to produce a time-weighted frequency histogram.

Recordings were scored again in 5 s epochs to allow for performance of an EEG power spectrum analysis. On the basis of visual and spectral analysis, epochs containing artifacts occurring during active wake (with large movements) or containing two vigilance states were visually identified and omitted from the spectral analysis. Recordings containing wake artifacts during more than 20% of the time were removed from the spectral analysis. EEG power spectra were computed for consecutive 5 s epochs within the frequency range of 0.5–120 Hz using a fast Fourier transform routine (FFT). The data were collapsed into 0.5 Hz bins. To determine the effect of injection on sleep-wake power spectra, EEG power spectra were analyzed during the 3 h period of time post-injection, starting 10 min after injection as a previous study had shown that CNO injection significantly affected SWS amount during 3 h post-injection and SWS latency was no more than 10 min (Anaclet et al., 2014). The data were standardized by expressing each frequency bin as a percentage relative to the same bin under baseline conditions from the same mouse and from the same time of the day (same Zeitgeber time). To analyze the EEG frequency bands, power bins were summed in δ 0.5–5 Hz, θ 5–9 Hz, α 9–15 Hz, β 15–30 Hz, low γ 30–60 Hz and high γ 60–120 Hz, and expressed in percentage of baseline power band, from the same circadian time.

Statistical analysis was performed using Prism v6 (GraphPad Software, San Diego, CA, United States). Following confirmation that the data met the assumptions of the ANOVA model, two-way ANOVA followed by a *post hoc* Bonferroni test were used to compare the effects of the drug injection and time period on sleep-wake parameters, the effect of the drug injection and the distribution of vigilance episodes, or the effect of drug injection and power band on cortical EEG power density. Paired Student's *t*-test was used to compare the effects of the drug injection on SWS to REM sleep latency. Sample size and power calculations were performed *post hoc* at http://www.biomath.info, using means and standard deviations derived from our analysis. The present study was sufficiently powered to detect effect sizes.

Immunostaining and RNAscope

At the end of the behavioral experiments, mice were deeply anesthetized with ketamine/xylazine (200 and 20 mg/kg, respectively) and perfused transcardially with 20 ml of saline, followed by 100 ml of neutral phosphate-buffered formalin (4%; Thermo Fisher Scientific). Brains were removed from the skull and incubated in neutral phosphate-buffered formalin (4%; Thermo Fisher Scientific) for 2 h, followed by 20% sucrose until they sank.

For immunostaining, using a freezing microtome, brains were sectioned at 40 μm into 3 series. One series was used to label mCherry to visualize neurons transfected by hSyn-DIO-hM3Dq-mCherry-AAV. Floating brain sections were incubated overnight with the primary antiserum (1:10,000; rabbit polyclonal antibody against mCherry was raised against DsRed, catalog #632496, Clontech). The next day, sections were incubated in goat anti-rabbit biotinylated secondary antiserum (1:1,000; catalog # BA-1000, Vector Laboratories), followed by incubation in ABC reagents (1:1000; Vector Laboratories) for 90 min. Visualization reaction was in a 0.06% solution of 3,3-diaminobenzidine tetrahydrochloride (Sigma-Aldrich) in PBS plus 0.02% H_2O_2 for 2–15 min. Finally, the sections were mounted on slides, dehydrated, cleared, and coverslipped. To map the extent of hSyn-DIO-hM3Dq-mCherry-AAV transfection, immunostained neurons were visualized with a brightfield microscope (Keyence BZ-X710, Japan) and mapped (**Figures 1B**, **3A**, **4A**, **7A**).

For RNAscope, using a cryostat (Thermo Scientific, Cryostar NX70), brains were sectioned at 10 μm and mounted onto Surgipath (Leica) adhesive microscope slides, 3 slices per slide. Slides were kept at −80°C until shortly before *in situ* hybridization. Slides were first warmed to room temperature and then we performed the RNAscope hybridization using a RNAscope Multiplex Fluorescent Reagent Kit (Advanced Cell Diagnostics, Inc., Newark, CA, United States). Briefly, according to the manufacturer's instructions, target retrieval was performed at 99°C after which slices were dehydrated in 100% ethanol and air-dried. Next, sections were treated with protease inhibitor (Protease III, RNAscope) for 30 min at 40°C. After rinsing in RNAscope wash buffer, we incubated the sections in the RNAscope probes for Vglut2 (Mm-Slc17a6, catalog # 319171) and Phox2B (Mm-Phox2b-C2, catalog # 407861-C2). Additional sections were incubated in the manufacturer-supplied 2-plex positive control (catalog # 320761) and negative control (catalog # 320751) probes. Following the first 3 signal amplification steps, the fourth amplification was performed using Amp 4 Alt C-FL, such that channel 1 (Vglut2) was fluorescently labeled with Alto 550 and channel 2 (Phox2B) was labeled with Alto 647. Fluorescent images were collected with a confocal microscope (Zeiss LSM 700; **Figures 6D–P**).

Figures 6A–C, Phox2B-GFP Native GFP fluorescence images were collected with a fluorescence microscope (Keyence BZ-X710, Japan).

Whole-Cell *in vitro* Experiments

For *in vitro* electrophysiological recordings, 10–13 days old Vglut2-ires-cre (N = 17) and Phox2B-ires-cre (N = 5) mice were injected bilaterally in the PZ, SLD or PB area with hSyn-DIO-hM3Dq-mCherry-AAV (100 nl/side). At about 3 weeks of age, 250 μm thick coronal brain slices of the PZ, SLD or PB area were prepared.

Mice were deeply anesthetized (200 mg/Kg Ketamine, 20 mg/Kg Xylazine) and transcardially perfused with ice-cold *N*-methyl-D-glucamine based artificial cerebrospinal fluid (NMDG-ACSF) containing (in mM): NMDG 98, HEPES 20, Glucose 25, $NaHCO_3$ 30, Na-ascorbate 5, Na-pyruvate 3, Thiourea 2, $MgSO_4$ 10, NaH_2PO_4 1.24, KCl 2.5, $CaCl_2$ 0.5; pH adjusted to ≈7.3 with HCl 37%. The brains were quickly extracted from the skull and sliced in carbogeneted (95% O2 5% CO2) ice-cold NMDG-ACSF using a vibrating microtome (7000-SMZ2, Campden Instruments). Slices containing the area of interest were immediately transferred to a chamber with carbogented NMDG-ACSF kept at 35°C for 8 min, then moved to carbogeneted normal ACSF at room temperature containing

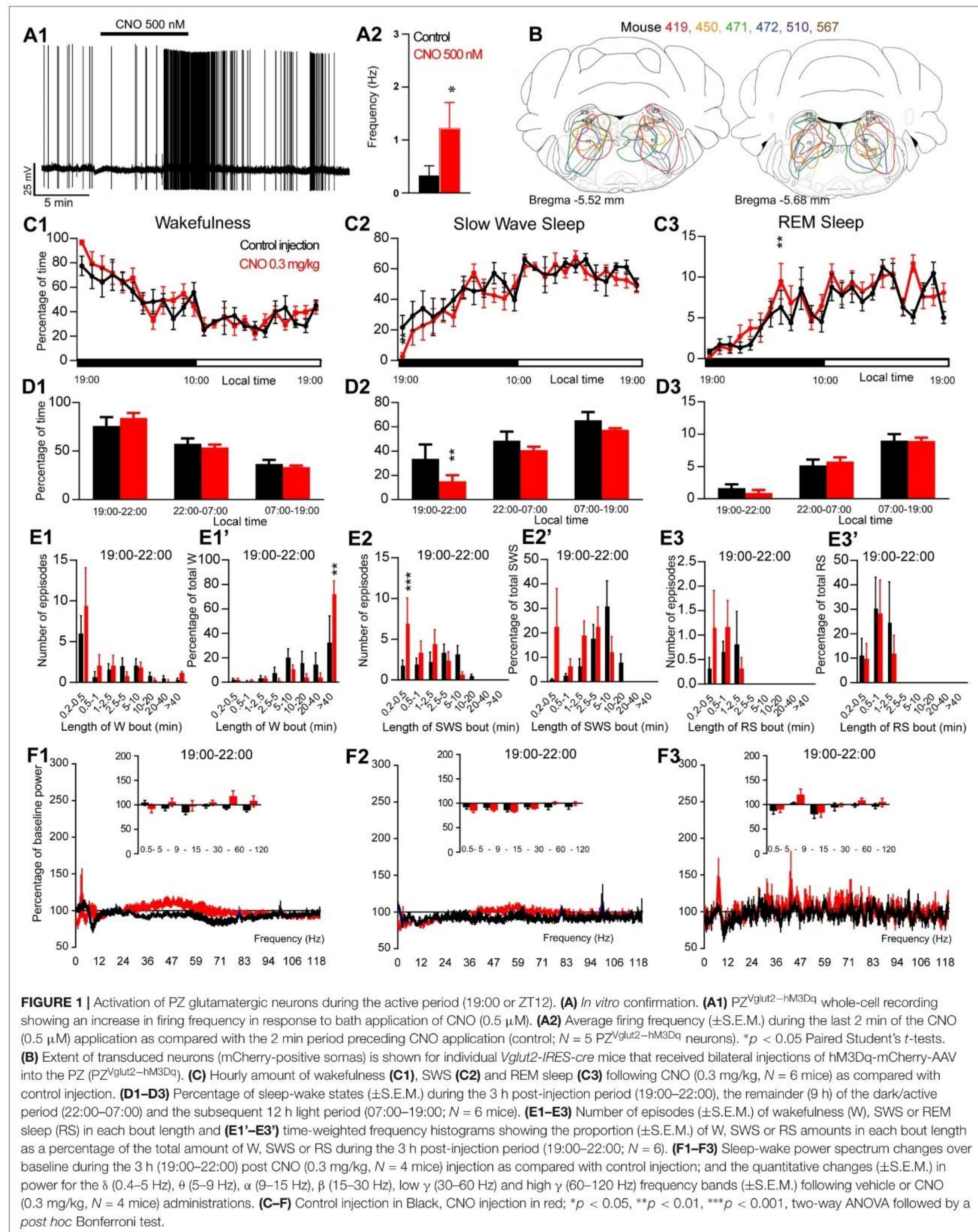

FIGURE 1 | Activation of PZ glutamatergic neurons during the active period (19:00 or ZT12). **(A)** *In vitro* confirmation. **(A1)** $PZ^{Vglut2-hM3Dq}$ whole-cell recording showing an increase in firing frequency in response to bath application of CNO (0.5 μM). **(A2)** Average firing frequency (±S.E.M.) during the last 2 min of the CNO (0.5 μM) application as compared with the 2 min period preceding CNO application (control; $N = 5$ $PZ^{Vglut2-hM3Dq}$ neurons). $^{*}p < 0.05$ Paired Student's *t*-tests. **(B)** Extent of transduced neurons (mCherry-positive somas) is shown for individual *Vglut2-IRES-cre* mice that received bilateral injections of hM3Dq-mCherry-AAV into the PZ ($PZ^{Vglut2-hM3Dq}$). **(C)** Hourly amount of wakefulness **(C1)**, SWS **(C2)** and REM sleep **(C3)** following CNO (0.3 mg/kg, $N = 6$ mice) as compared with control injection. **(D1–D3)** Percentage of sleep-wake states (±S.E.M.) during the 3 h post-injection period (19:00–22:00), the remainder (9 h) of the dark/active period (22:00–07:00) and the subsequent 12 h light period (07:00–19:00; $N = 6$ mice). **(E1–E3)** Number of episodes (±S.E.M.) of wakefulness (W), SWS or REM sleep (RS) in each bout length and **(E1'–E3')** time-weighted frequency histograms showing the proportion (±S.E.M.) of W, SWS or RS amounts in each bout length as a percentage of the total amount of W, SWS or RS during the 3 h post-injection period (19:00–22:00; $N = 6$). **(F1–F3)** Sleep-wake power spectrum changes over baseline during the 3 h (19:00–22:00) post CNO (0.3 mg/kg, $N = 4$ mice) injection as compared with control injection; and the quantitative changes (±S.E.M.) in power for the δ (0.4–5 Hz), θ (5–9 Hz), α (9–15 Hz), β (15–30 Hz), low γ (30–60 Hz) and high γ (60–120 Hz) frequency bands (±S.E.M.) following vehicle or CNO (0.3 mg/kg, $N = 4$ mice) administrations. **(C–F)** Control injection in Black, CNO injection in red; $^{*}p < 0.05$, $^{**}p < 0.01$, $^{***}p < 0.001$, two-way ANOVA followed by a *post hoc* Bonferroni test.

(in mM): NaCl 126, $NaHCO_3$ 26, Glucose 10, Na-ascorbate 1, Thiourea 2, Na-Pyruvate 3, NaH_2PO_4 1.24, KCl 2.5, $CaCl_2$ 2, $MgCl_2$ 1.3.

Recordings were guided using a combination of fluorescence and infrared differential interference contrast (IR-DIC) video microscopy using a fixed stage upright microscope (Axio Examiner.D1, Zeiss) equipped with a Nomarski immersion lens (40×/1.0) and an infrared-sensitive camera (Orca flash 4.0, Hamamatsu). Images were displayed in real time using Zen2 software (Carl Zeiss). Recordings were conducted in whole-cell mode using an EPC-10 USB amplifier and Patchmaster software (Heka).

Recordings were performed in current clamp mode using a K-gluconate based pipette solution containing (in mM): K-gluconate 120, KCl 10, $MgCl_2$ 3, HEPES 10, K-ATP, Na-GTP 0.5. After at least 10 min of stable recording, ACSF containing CNO (500 nM) was perfused into the chamber for 3–5 min before washout. Recordings were analyzed, using Patchmaster software, by comparing the last 2 min before the application of CNO to the last 2 min of the CNO application. Paired Student's t-tests were used to calculate statistical significance.

RESULTS

PZ^{Vglut2} Neurons Are Not Sleep-Promoting

To test whether activation of PZ^{Vglut2} neurons affects sleep-wake phenotype, Vglut2-IRES-Cre mice were injected into the PZ with a virus vector containing the excitatory hM3Dq receptor (AAV-mCherry-hM3Dq) to specifically express hM3Dq receptors in PZ glutamatergic neurons ($PZ^{Vglut2-hM3Dq}$ mice). First, responses of $PZ^{Vglut2-hM3Dq}$ neurons to the hM3Dq ligand, clozapine-N-oxide (CNO), were tested using whole-cell *in vitro* recordings (**Figure 1A1**). Bath application of CNO (500 nM) significantly increased firing rates in $PZ^{Vglut2-hM3Dq}$ neurons (1.2 ± 0.5 vs. 0.3 ± 0.2 Hz in control condition, $p = 0.042$; **Figure 1A2**), confirming that CNO activates PZ glutamatergic neurons. We then tested, *in vivo*, the sleep-wake phenotypes upon activation of PZ glutamatergic neurons. At the end of the behavioral studies, the injection sites were mapped using mCherry immunostaining. Of the sixteen Vglut2-IRES-Cre mice injected with AAV-mCherry-hM3Dq, six mice displayed more specific expression of mCherry bilaterally in the PZ (**Figure 1B**) and were used for the following sleep-wake analysis.

To test the effect of PZ^{Vglut2} neurons in sleep-wake control, mice were injected in a randomized cross-over design with saline or CNO (0.3 mg/kg) at the beginning of the dark/active period (19:00, ZT12) or during the light/rest period (10:00, ZT3). When injected at 19:00, CNO treatment did not significantly affect the hourly amount of wakefulness (two-way ANOVA, $F(23,115) = 1.06$, $p = 0.40$; **Figure 1C1**), SWS (two-way ANOVA, $F(23,115) = 1.02$, $p = 0.45$; **Figure 1C2**), or REM sleep (two-way ANOVA, $F(23,115) = 1.38$, $p = 0.14$; **Figure 1C3**). Because in previous studies (Anaclet et al., 2014, 2015, 2018) the effect of CNO-mediated neuronal activation or inhibition on sleep-wake cycles was most pronounced during the 3 h post-injection period, we performed a more refined analysis of this period. Neither wakefulness nor REM sleep amount and consolidation were affected by CNO injection during the 3 h post CNO injection as compared with control injection (**Figures 1D1,D3,E1,E1',E3,E3'**). However, SWS amounts were significantly decreased during the 3 h post CNO injection period as compared with control injections (15.0 ± 5.0 vs. 33.5 ± 11.9% of SWS in control condition, $p < 0.01$; **Figure 1D2**) but without change in bout length distribution (**Figure 1E2'**). This SWS decrease is associated with a significant increase in the number of very short SWS bouts (7.0 ± 3.1 vs. 1.8 ± 0.6 bouts lasting between 10 and 30 s, $p = 0.0006$; **Figure 1E2**). Wakefulness bout duration was also increased with a significant increase of the proportion of wakefulness from long bout lengths (>40 min long bouts: 72.9 ± 10.1 vs. 33.3 ± 21.1% of total wakefulness after control injection, $p = 0.003$; **Figure 1E1'**). These results indicate more labile switching between the two vigilance stages. Cortical EEG power spectral distribution was affected by the treatment in wakefulness (two-way ANOVA, $F(243,729) = 1.48$, $p < 0.0001$; **Figure 1F1**) and SWS (two-way ANOVA, $F(243,729) = 3.88$, $p < 0.0001$; **Figure 1F2**) but not in REM sleep (two-way ANOVA, $F(243,729) = 0.82$, $p = 0.97$; **Figure 1F3**). However, none of the frequency bands displayed any significant difference between CNO and control injection, in any vigilance stage (**Figures 1F1–F3**). Altogether, activation of PZ glutamatergic neurons at a time when the wake-promoting systems are active, during the active phase, did not induce SWS and showed only minimal effects on sleep-wake phenotype, indicating that PZ^{Vglut2} neurons are not sleep-promoting.

In order to test if activation of PZ^{Vglut2} neurons affects sleep-wake phenotypes differently when the sleep-promoting system is driving sleep, during the light period, CNO was injected at 10:00. CNO treatment significantly affected wakefulness (two-way ANOVA, $F(23,115) = 3.14$, $p < 0.0001$; **Figure 2A1**), SWS (two-way ANOVA, $F(23,115) = 3.12$, $p < 0.0001$; **Figure 2A2**) and REM sleep (two-way ANOVA, $F(23,115) = 2.16$, $p = 0.004$; **Figure 2A3**) hourly distribution. Wakefulness amount was significantly increased during the 4 h post CNO injection period (74.6 ± 7.5 vs. 40.3 ± 3.9% of time in control condition, $p < 0.001$; **Figure 2B1**). This wakefulness increase was at the expense of SWS (21.9 ± 6.1 vs. 53.5 ± 4.2% of time in control condition, $p < 0.001$; **Figure 2B2**). The increase in wakefulness was due to bout elongation, after CNO injection, as the mice were spending most of their wake time in bouts longer than 40 min (44.5 ± 11.2 vs. 7.2 ± 7.2% of total wakefulness after control injection, $p < 0.001$; **Figure 2C1'**), while in control condition, they were spending most of their wake time in 20–40 min long bouts (15.5 ± 8.2 vs. 44.3 ± 4.5% of total wakefulness in control condition, $p = 0.01$; **Figure 2C1'**). The number of wakefulness episodes, however, remained unchanged (**Figure 2C1**). The decrease of SWS was due to fragmentation characterized by a significant increase in the number of very short SWS bouts (13.0 ± 4.0 vs. 3.2 ± 0.6 episodes 30 s long or shorter in control condition, $p < 0.0001$; **Figure 2C2**) and a significant decrease of long SWS bouts (0.0 ± 0.0 vs. 27.8 ± 6.1% of total SWS in bouts 10–20 min long in control condition, $p < 0.0001$; **Figure 2C2'**). Interestingly, REM sleep amount displayed a trend to increase during the second part

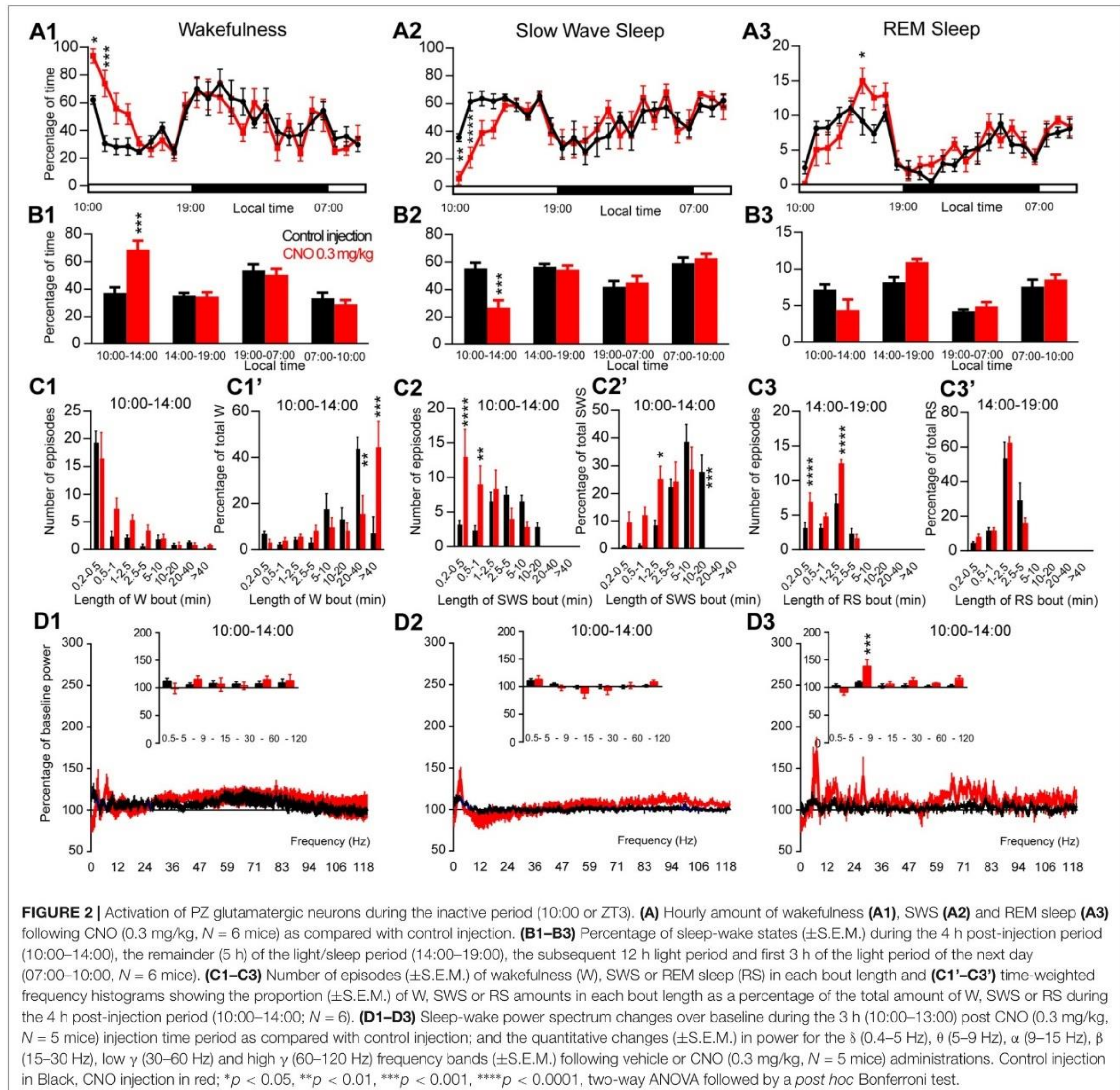

FIGURE 2 | Activation of PZ glutamatergic neurons during the inactive period (10:00 or ZT3). **(A)** Hourly amount of wakefulness **(A1)**, SWS **(A2)** and REM sleep **(A3)** following CNO (0.3 mg/kg, $N = 6$ mice) as compared with control injection. **(B1–B3)** Percentage of sleep-wake states (±S.E.M.) during the 4 h post-injection period (10:00–14:00), the remainder (5 h) of the light/sleep period (14:00–19:00), the subsequent 12 h light period and first 3 h of the light period of the next day (07:00–10:00, $N = 6$ mice). **(C1–C3)** Number of episodes (±S.E.M.) of wakefulness (W), SWS or REM sleep (RS) in each bout length and **(C1'–C3')** time-weighted frequency histograms showing the proportion (±S.E.M.) of W, SWS or RS amounts in each bout length as a percentage of the total amount of W, SWS or RS during the 4 h post-injection period (10:00–14:00; $N = 6$). **(D1–D3)** Sleep-wake power spectrum changes over baseline during the 3 h (10:00–13:00) post CNO (0.3 mg/kg, $N = 5$ mice) injection time period as compared with control injection; and the quantitative changes (±S.E.M.) in power for the δ (0.4–5 Hz), θ (5–9 Hz), α (9–15 Hz), β (15–30 Hz), low γ (30–60 Hz) and high γ (60–120 Hz) frequency bands (±S.E.M.) following vehicle or CNO (0.3 mg/kg, $N = 5$ mice) administrations. Control injection in Black, CNO injection in red; $^{*}p < 0.05$, $^{**}p < 0.01$, $^{***}p < 0.001$, $^{****}p < 0.0001$, two-way ANOVA followed by a *post hoc* Bonferroni test.

of the light period, 4 h following CNO injection (14:00–19:00; 10.3 ± 0.2 vs. 8.5 ± 0.7% of time after control injection, $p > 0.05$; **Figure 2B3**). This was associated with a significant increase in the number of episodes (10–30 s long bouts: 7.0 ± 1.3 vs. 3.3 ± 0.6 bouts after control injection, $p < 0.0001$; 10–30 s long bouts: 12.5 ± 0.6 vs. 6.8 ± 1.2 bouts after control injection, $p < 0.0001$; **Figure 2C3**). REM sleep bout length distribution, however, remained unchanged (**Figure 2C3'**). Cortical EEG power spectral distribution was not affected by the treatment in wakefulness (two-way ANOVA, $F(243,972) = 0.76$, $p = 0.996$; **Figure 2D1**). In contrast, both SWS (two-way ANOVA, $F(243,972) = 2.79$, $p < 0.0001$; **Figure 2D2**) and REM sleep (two-way ANOVA, $F(243,972) = 1.43$, $p = 0.0001$; **Figure 2D3**) cortical EEG power spectral distribution was affected by the treatment. Interestingly, during REM sleep, the theta band was significantly increased (128.1 ± 6.3 vs. 106.9 ± 3.2% of baseline theta power in control condition, $p < 0.001$; **Figure 2D3**).

Activation of SLD^{Vglut2} Neurons During the Inactive Period Enhances REM Sleep

The excitatory receptor, hM3Dq, was mostly expressed in the SLD in six Vglut2-hM3Dq mice (SLD$^{Vglut2-hM3Dq}$; **Figure 3A**). Whole-cell recording confirmed the expression of functional

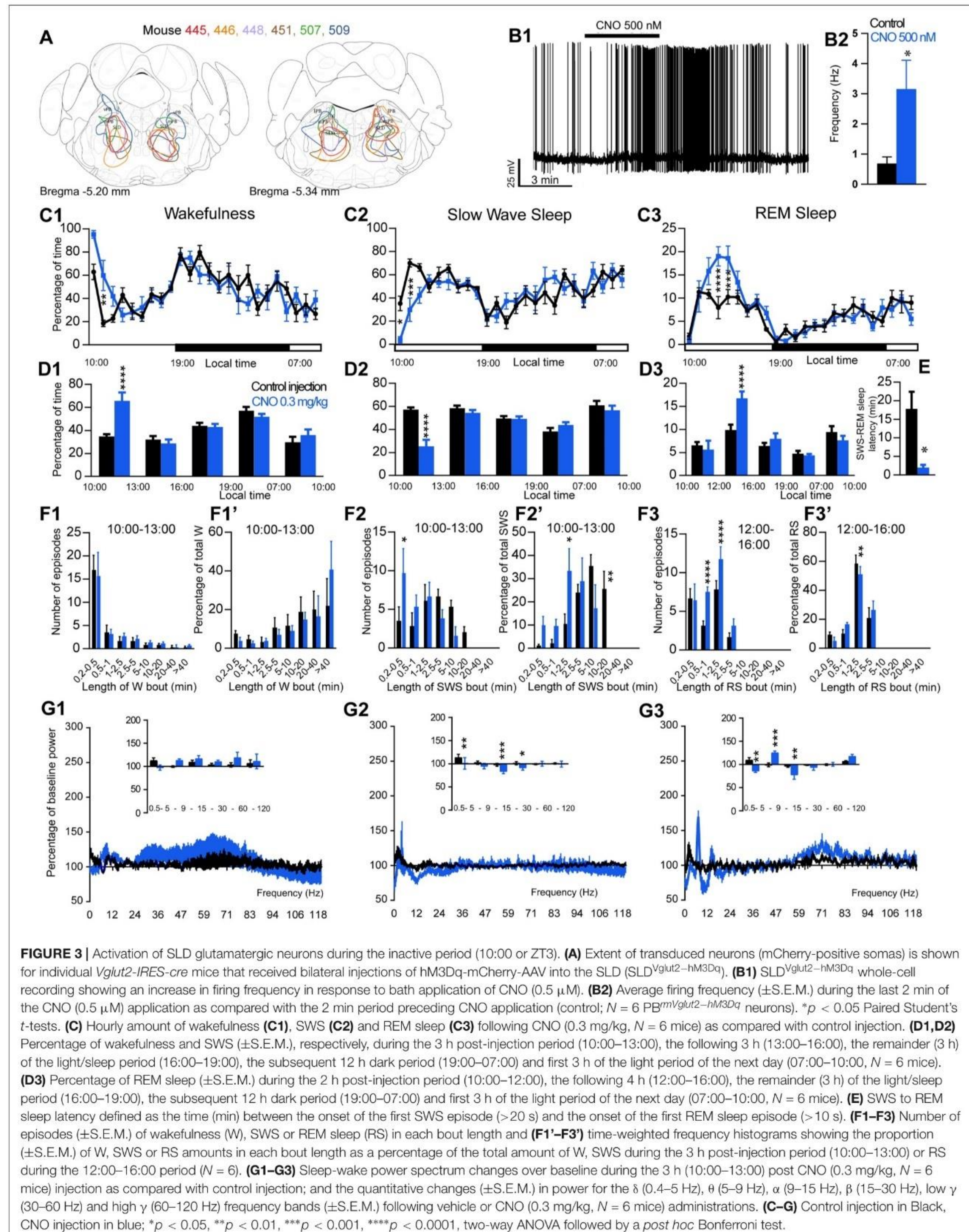

FIGURE 3 | Activation of SLD glutamatergic neurons during the inactive period (10:00 or ZT3). **(A)** Extent of transduced neurons (mCherry-positive somas) is shown for individual *Vglut2-IRES-cre* mice that received bilateral injections of hM3Dq-mCherry-AAV into the SLD ($SLD^{Vglut2-hM3Dq}$). **(B1)** $SLD^{Vglut2-hM3Dq}$ whole-cell recording showing an increase in firing frequency in response to bath application of CNO (0.5 μM). **(B2)** Average firing frequency (±S.E.M.) during the last 2 min of the CNO (0.5 μM) application as compared with the 2 min period preceding CNO application (control; $N = 6$ $PB^{rmVglut2-hM3Dq}$ neurons). $^{*}p < 0.05$ Paired Student's *t*-tests. **(C)** Hourly amount of wakefulness **(C1)**, SWS **(C2)** and REM sleep **(C3)** following CNO (0.3 mg/kg, $N = 6$ mice) as compared with control injection. **(D1,D2)** Percentage of wakefulness and SWS (±S.E.M.), respectively, during the 3 h post-injection period (10:00–13:00), the following 3 h (13:00–16:00), the remainder (3 h) of the light/sleep period (16:00–19:00), the subsequent 12 h dark period (19:00–07:00) and first 3 h of the light period of the next day (07:00–10:00, $N = 6$ mice). **(D3)** Percentage of REM sleep (±S.E.M.) during the 2 h post-injection period (10:00–12:00), the following 4 h (12:00–16:00), the remainder (3 h) of the light/sleep period (16:00–19:00), the subsequent 12 h dark period (19:00–07:00) and first 3 h of the light period of the next day (07:00–10:00, $N = 6$ mice). **(E)** SWS to REM sleep latency defined as the time (min) between the onset of the first SWS episode (>20 s) and the onset of the first REM sleep episode (>10 s). **(F1–F3)** Number of episodes (±S.E.M.) of wakefulness (W), SWS or REM sleep (RS) in each bout length and **(F1'–F3')** time-weighted frequency histograms showing the proportion (±S.E.M.) of W, SWS or RS amounts in each bout length as a percentage of the total amount of W, SWS during the 3 h post-injection period (10:00–13:00) or RS during the 12:00–16:00 period ($N = 6$). **(G1–G3)** Sleep-wake power spectrum changes over baseline during the 3 h (10:00–13:00) post CNO (0.3 mg/kg, $N = 6$ mice) injection as compared with control injection; and the quantitative changes (±S.E.M.) in power for the δ (0.4–5 Hz), θ (5–9 Hz), α (9–15 Hz), β (15–30 Hz), low γ (30–60 Hz) and high γ (60–120 Hz) frequency bands (±S.E.M.) following vehicle or CNO (0.3 mg/kg, $N = 6$ mice) administrations. **(C–G)** Control injection in Black, CNO injection in blue; $^{*}p < 0.05$, $^{**}p < 0.01$, $^{***}p < 0.001$, $^{****}p < 0.0001$, two-way ANOVA followed by a *post hoc* Bonferroni test.

hM3Dq receptors (**Figure 3B1**). CNO (500 nM) application significantly increased the firing rate of SLD neurons (3.15 ± 0.96 vs. 0.68 ± 0.23 Hz in control condition, $p = 0.032$, **Figure 3B2**). Sleep-wake analysis during the inactive phase (10:00) revealed that CNO (0.3 mg/kg, $n = 6$, 10:00) injection significantly affected wakefulness (two-way ANOVA, $F(23,115) = 2.38$, $p = 0.0014$; **Figure 3C1**), SWS (two-way ANOVA, $F(23,115) = 2.82$, $p = 0.0001$; **Figure 3C2**) and REM sleep (two-way ANOVA, $F(23,115) = 3.30$, $p < 0.0001$; **Figure 3C3**) in $SLD^{Vglut2-hM3Dq}$ mice, as compared with control injection. Wakefulness was significantly increased during the 3 h post CNO injection period (65.0 ± 8.8 vs. 34.8 ± 2.1% of time after control injection, $p < 0.0001$; **Figure 3D1**). At the same time, SWS amount was significantly decreased (25.9 ± 7.0 vs. 57.3 ± 1.8% of time after control injection, $p < 0.0001$; **Figure 3D2**). REM sleep amount remained unchanged during the 2 h post CNO injection period (6.2 ± 2.2 vs. 6.5 ± 0.7% of time after control injection, $p > 0.05$; **Figure 3D3**). However, REM sleep amount was significantly increased during the 2–6 h post-injection period (15.5 ± 1.1 vs. 9.8 ± 1.2% of time after control injection, $p < 0.0001$; **Figure 3D3**). Interestingly, the SWS to REM sleep latency was significantly decreased after CNO injection (2.0 ± 0.7 vs. 17.8 ± 4.6 min between the beginning of the first SWS episode and the beginning of the first REM sleep episode in control condition, $p = 0.018$; **Figure 3E**). The observed wakefulness increases during the 3 h post CNO injection resulted from a non-significant increase in both the number of long bouts (>40 min; **Figure 3F1**) and in the proportion of wakefulness from long bouts (>40 min; **Figure 3F1'**). SWS decrease was due to a significant decrease of the proportion of SWS from long SWS bouts (0.0 ± 0.0 vs. 26.0 ± 7.2% of total SWS from 10–20 min long bouts in control condition, $p = 0.0038$, **Figure 3F2'**), associated with a significant increase in the proportion of SWS from short SWS bouts (33.7 ± 9.2 vs. 10.8 ± 3.9% of total SWS from 1–2.5 min long bouts in control condition, $p = 0.014$, **Figure 3F2'**). At the same time, the number of very short SWS bouts (10–30 s long) were significantly increased (9.8 ± 3.0 vs. 3.5 ± 1.8 bouts in control condition, $p = 0.015$, **Figure 3F2**). The REM sleep increase 2–6 h post CNO injection was due to a significant increase in the number of medium-duration bouts (6.6 ± 1.6 vs. 3.6 ± 1.1 0.5–1 min long bouts in control condition, $p < 0.0001$; and 12.4 ± 3.0 vs. 6.8 ± 1.2 1–2.5 min long bouts in control condition, $p < 0.0001$, **Figure 3F3**) while REM sleep bout length is moderately affected (**Figure 3F3'**).

Cortical EEG power distribution was affected by CNO administration during wakefulness (two-way ANOVA, $F(243,972) = 3.16$, $p < 0.0001$; **Figure 3G1**), SWS (two-way ANOVA, $F(243,972) = 2.27$, $p < 0.0001$; **Figure 3G2**) and REM sleep (two-way ANOVA, $F(243,972) = 4.89$, $p < 0.0001$; **Figure 3G3**). During SWS, delta (101.1 ± 12.5 vs. 113.3 ± 7.4% of baseline power in control condition, $p < 0.01$), sigma (83.8 ± 4.7 vs. 98.0 ± 3.2% of baseline power in control condition, $p < 0.001$) and beta (91.9 ± 5.3 vs. 98.0 ± 3.2% of baseline power in control condition, $p < 0.05$) power bands were decreased (**Figure 3G2**). During REM sleep, both delta (86.5 ± 3.2 vs. 109.0 ± 5.9% of baseline power in control condition, $p < 0.01$) and sigma (78.1 ± 10.1 vs. 96.8 ± 3.0% of baseline power in control condition, $p < 0.01$) frequency bands were significantly decreased whereas theta (125.0 ± 3.9 vs. 99.1 ± 3.9% of baseline power in control condition, $p < 0.001$) was significantly increased (**Figure 3G3**). Similar to $PZ^{Vglut2-hM3Dq}$ mice, $SLD^{Vglut2-hM3Dq}$ did not show any sleep-wake phenotypes when CNO was injected at the beginning of the dark/active period (data not shown), indicating a time of the day difference.

Activation of PB^{Vglut2} Neurons Induces Wakefulness

The excitatory receptor, hM3Dq, was mostly expressed in the PB in five Vglut2-hM3Dq mice ($PB^{Vglut2-hM3Dq}$; **Figure 4A**). Slice electrophysiology showed that firing rates of $PB^{Vglut2-hM3Dq}$ neurons were significantly increased (1.48 ± 0.40 vs. 0.32 ± 0.04 Hz in control condition, $p = 0.042$) by bath application of CNO (500 nM; **Figures 4B1,B2**). Injection of CNO (0.3 mg/kg, 10:00) in $PB^{Vglut2-hM3Dq}$ mice significantly affected wakefulness (two-way ANOVA, $F(23,92) = 6.12$, $p < 0.0001$; **Figure 4C1**), SWS (two-way ANOVA, $F(23,92) = 6.24$, $p < 0.0001$; **Figure 4C2**) and REM sleep (two-way ANOVA, $F(23,92) = 3.44$, $p < 0.0001$; **Figure 4C3**). Wakefulness amount was significantly increased during the remaining 9 h of the light period post-injection (79.3 ± 9.5 vs. 32.4 ± 1.5% of time, $p < 0.001$; **Figure 4D1**). At the same time, both SWS (17.8 ± 7.8 vs. 59.1 ± 1.4% of time, $p < 0.001$; **Figures 4C2–D3**) and REM sleep (2.9 ± 1.7 vs. 8.5 ± 0.4% of time, $p < 0.01$; **Figures 4C3–D3**) amount were significantly decreased. No sleep rebound followed the long-lasting wakefulness increase (47.5 ± 1.1 vs. 47.7 ± 2.7% of time spent in SWS during the following dark period, 19:00–07:00, $p > 0.05$; **Figures 4C2,D2**). Wakefulness enhancement was due to a significant increase in bout length (76.7 ± 7.3 vs. 0.0 ± 0.05 of wakefulness from >40 min long bouts, $p < 0.0001$, **Figure 4E1'**), associated with a significant decrease in the number of short episodes (**Figure 4E1**). Both SWS bout number (5.6 ± 2.5 vs. 20.8 ± 2.1 5–10 min long bouts, $p = 0.0002$; **Figure 4E2**) and bout duration (3.4 ± 2.4 vs. 23.9 ± 6.6% of SWS in 10–20 min long bouts, $p = 0.025$; **Figure 4E2'**) were significantly decreased. Similarly, both REM sleep bout number (**Figure 4E3**) and bout duration (**Figure 4E3'**) were significantly decreased during the 5 h period following injection. Cortical EEG power distribution was affected by CNO injection during wakefulness (two-way ANOVA, $F(543,972) = 1.66$, $p < 0.0001$; **Figure 4F1**). PB^{Vglut2} induced wakefulness was characterized by a significant decrease in cortical EEG delta power (49.9 ± 5.2 vs. 102.1 ± 7.4% of baseline power in control condition, $p < 0.01$; **Figure 4F2**). Similar results were obtained when CNO was injected at the beginning of the active period (19:00; not shown).

CNO Does Not Affect Sleep-Wake Cycle in Control Mice

To control for non-specific actions of CNO, non-cre expressing littermate mice were used. No hM3Dq receptor transfection was seen in these control mice. Treatment did not affect the hourly distribution of wakefulness (two-way ANOVA, $F(23,92) = 1.53$, $p = 0.082$; **Figure 5A1**), SWS (two-way ANOVA, $F(23,92) = 1.56$,

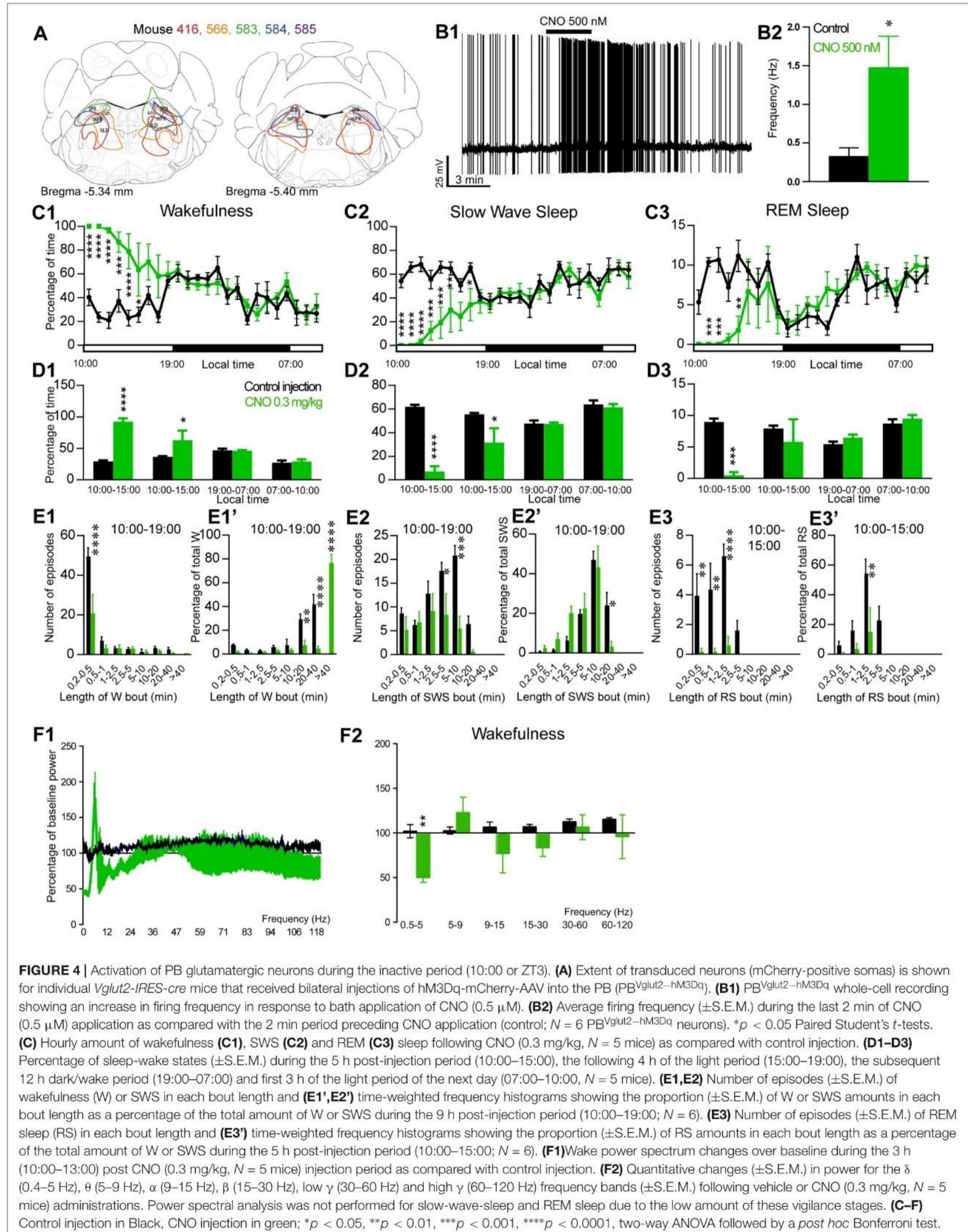

FIGURE 4 | Activation of PB glutamatergic neurons during the inactive period (10:00 or ZT3). **(A)** Extent of transduced neurons (mCherry-positive somas) is shown for individual *Vglut2-IRES-cre* mice that received bilateral injections of hM3Dq-mCherry-AAV into the PB ($PB^{Vglut2-hM3Dq}$). **(B1)** $PB^{Vglut2-hM3Dq}$ whole-cell recording showing an increase in firing frequency in response to bath application of CNO (0.5 μM). **(B2)** Average firing frequency (±S.E.M.) during the last 2 min of CNO (0.5 μM) application as compared with the 2 min period preceding CNO application (control; N = 6 $PB^{Vglut2-hM3Dq}$ neurons). $^*p < 0.05$ Paired Student's *t*-tests. **(C)** Hourly amount of wakefulness **(C1)**, SWS **(C2)** and REM **(C3)** sleep following CNO (0.3 mg/kg, N = 5 mice) as compared with control injection. **(D1–D3)** Percentage of sleep-wake states (±S.E.M.) during the 5 h post-injection period (10:00–15:00), the following 4 h of the light period (15:00–19:00), the subsequent 12 h dark/wake period (19:00–07:00) and first 3 h of the light period of the next day (07:00–10:00, N = 5 mice). **(E1,E2)** Number of episodes (±S.E.M.) of wakefulness (W) or SWS in each bout length and **(E1',E2')** time-weighted frequency histograms showing the proportion (±S.E.M.) of W or SWS amounts in each bout length as a percentage of the total amount of W or SWS during the 9 h post-injection period (10:00–19:00; N = 6). **(E3)** Number of episodes (±S.E.M.) of REM sleep (RS) in each bout length and **(E3')** time-weighted frequency histograms showing the proportion (±S.E.M.) of RS amounts in each bout length as a percentage of the total amount of W or SWS during the 5 h post-injection period (10:00–15:00; N = 6). **(F1)** Wake power spectrum changes over baseline during the 3 h (10:00–13:00) post CNO (0.3 mg/kg, N = 5 mice) injection period as compared with control injection. **(F2)** Quantitative changes (±S.E.M.) in power for the δ (0.4–5 Hz), θ (5–9 Hz), α (9–15 Hz), β (15–30 Hz), low γ (30–60 Hz) and high γ (60–120 Hz) frequency bands (±S.E.M.) following vehicle or CNO (0.3 mg/kg, N = 5 mice) administrations. Power spectral analysis was not performed for slow-wave-sleep and REM sleep due to the low amount of these vigilance stages. **(C–F)** Control injection in Black, CNO injection in green; $^*p < 0.05$, $^{**}p < 0.01$, $^{***}p < 0.001$, $^{****}p < 0.0001$, two-way ANOVA followed by a *post hoc* Bonferroni test.

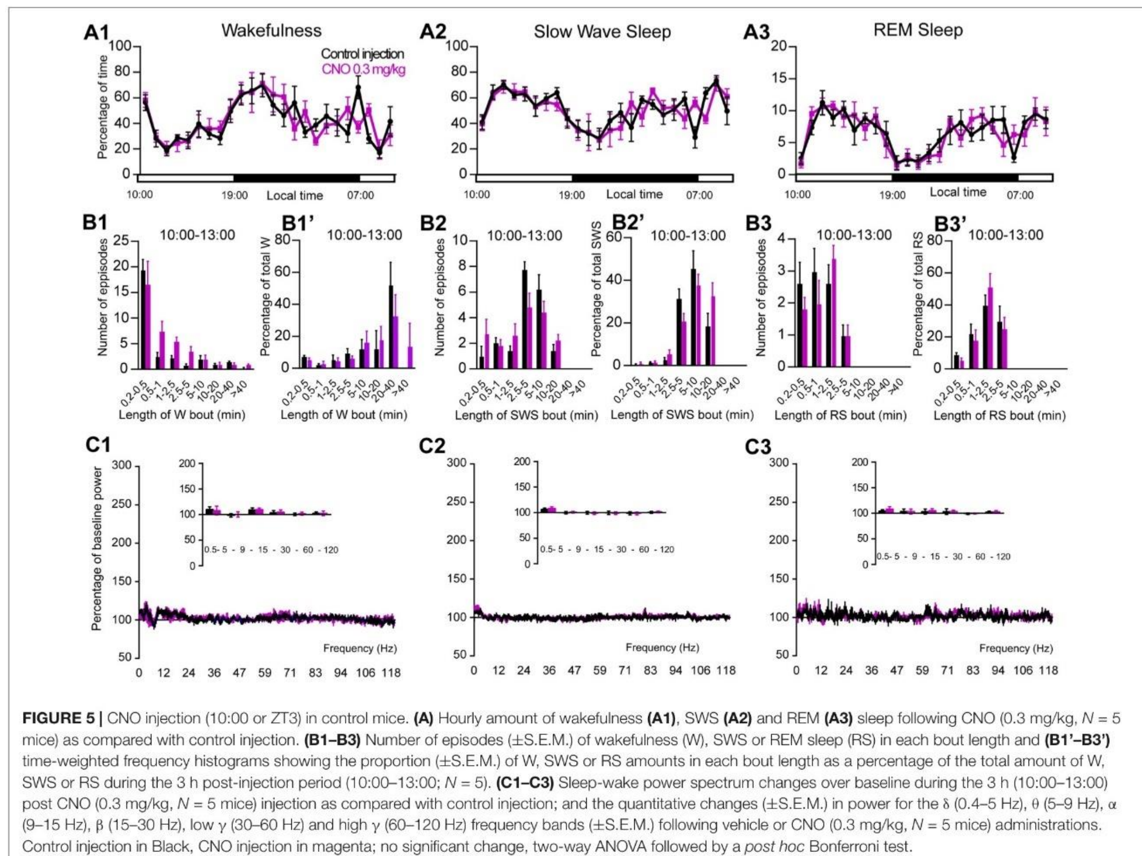

FIGURE 5 | CNO injection (10:00 or ZT3) in control mice. **(A)** Hourly amount of wakefulness **(A1)**, SWS **(A2)** and REM **(A3)** sleep following CNO (0.3 mg/kg, $N = 5$ mice) as compared with control injection. **(B1–B3)** Number of episodes (±S.E.M.) of wakefulness (W), SWS or REM sleep (RS) in each bout length and **(B1'–B3')** time-weighted frequency histograms showing the proportion (±S.E.M.) of W, SWS or RS amounts in each bout length as a percentage of the total amount of W, SWS or RS during the 3 h post-injection period (10:00–13:00; $N = 5$). **(C1–C3)** Sleep-wake power spectrum changes over baseline during the 3 h (10:00–13:00) post CNO (0.3 mg/kg, $N = 5$ mice) injection as compared with control injection; and the quantitative changes (±S.E.M.) in power for the δ (0.4–5 Hz), θ (5–9 Hz), α (9–15 Hz), β (15–30 Hz), low γ (30–60 Hz) and high γ (60–120 Hz) frequency bands (±S.E.M.) following vehicle or CNO (0.3 mg/kg, $N = 5$ mice) administrations. Control injection in Black, CNO injection in magenta; no significant change, two-way ANOVA followed by a *post hoc* Bonferroni test.

$p = 0.071$; **Figure 5A2**) or REM sleep (two-way ANOVA, $F(23,92) = 1.06$, $p = 0.4$; **Figure 5A3**). Moreover, CNO treatment did not affect the number of episodes or the episode length distribution as compared with control injection (**Figures 5B1–B3'**) in any vigilance state. Finally, the cortical EEG power distribution during wakefulness, SWS and REM sleep was similar after CNO injection, as compared with both control injection and baseline recording (**Figures 5C1–C3**). These results confirm that the sleep-wake effects seen in $PZ^{Vglut2-hM3Dq}$, $PB^{Vglut2-hM3Dq}$ and $SLD^{Vglut2-hM3Dq}$ mice is due to the specific activation of glutamatergic neurons.

Phox2B Is a Specific Marker for PZ Glutamatergic Neurons

Because chemogenetic activation of PZ^{Vglut2} neurons resulted in phenotypes resembling chemogenetic activation of PB^{Vglut2} and SLD^{Vglut2} neurons, i.e., wakefulness and REM sleep increase, respectively, we hypothesized that in the $PZ^{Vglut2-hM3Dq}$ mouse group some PB^{Vglut2} and SLD^{Vglut2} neurons were transfected and therefore responsible for the phenotypes. To specifically target PZ glutamatergic neurons we took advantage of a specific marker for PZ glutamatergic neurons, Phox2B. In the adult rat medullary and pontine regions in proximity to the PZ, Phox2B expression is restricted to the PZ, with a notable lack of expression in either the PB or the SLD (Kang et al., 2007). Moreover, Phox2B is co-localized with Vglut2 but not with Vgat or GAD67 [**Figures 6D–G**; (Stornetta et al., 2006)], suggesting that Phox2B is a specific marker for PZ glutamatergic neurons. We first confirmed the presence of Phox2B expression in PZ (**Figure 6A**) of mouse using Phox2B-GFP mice. No GFP positive neurons were seen in either the PB or the SLD (**Figures 6B,C**), indicating that Phox2B is specific for PZ glutamatergic neurons. Neurons of the locus coeruleus were GFP positive (LC; **Figures 6A,B**), which is consistent with previous studies showing that Phox2B is necessary for the differentiation of central noradrenergic and adrenergic neurons (Pattyn et al., 2000; Huber et al., 2005). We then assessed the extent of co-localization between Vglut2 and Phox2B in PZ. In each of the slices containing the PZ ($n = 12$ from 4 mice), Vglut2 co-localized exclusively with Phox2B and Phox2B was found primarily lateral to the facial nerve, in the entire PZ area (**Figures 6H–K**). Higher magnification photomicrographs show the cellular details of Vglut2/Phox2B co-localization

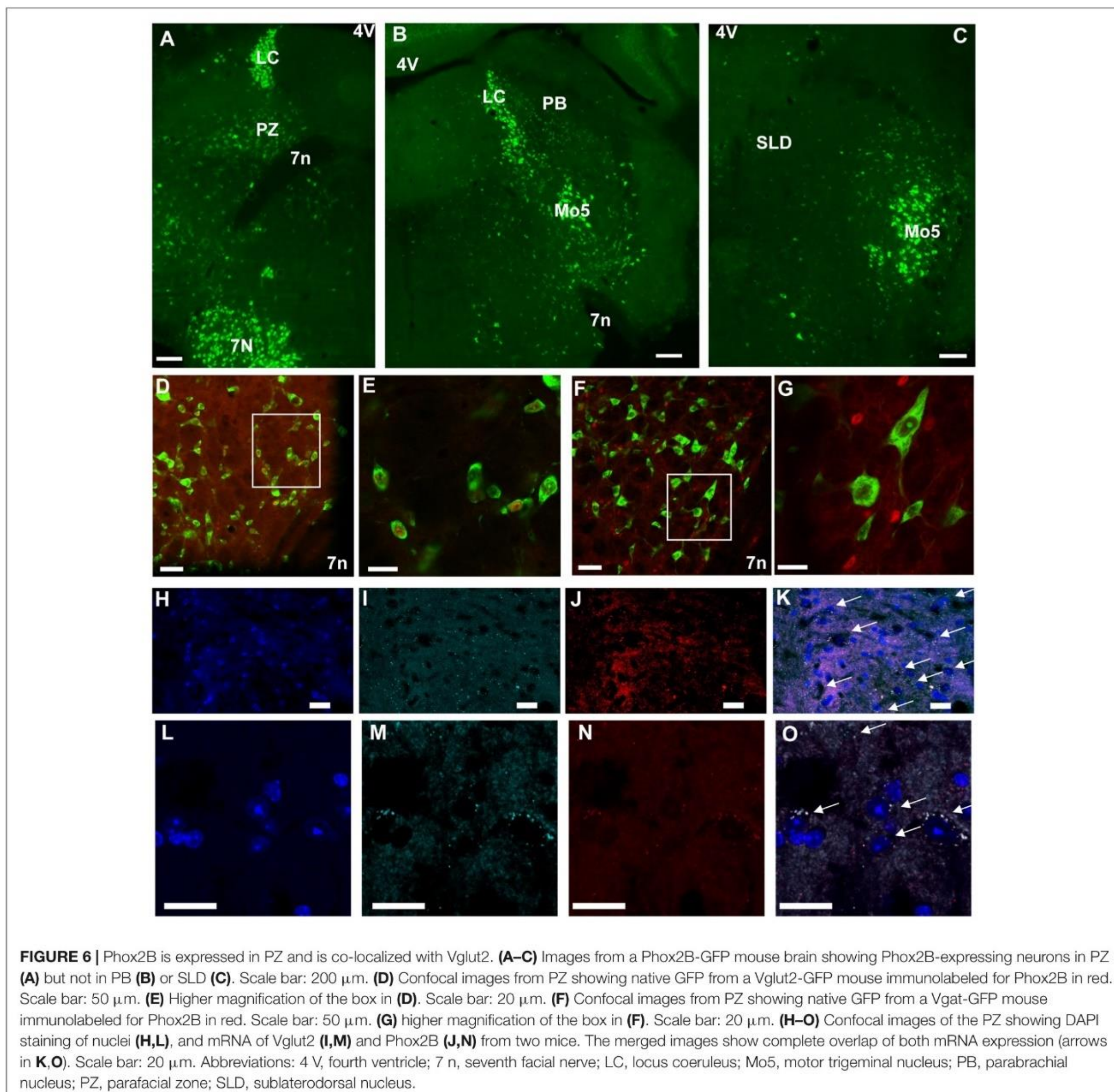

FIGURE 6 | Phox2B is expressed in PZ and is co-localized with Vglut2. **(A–C)** Images from a Phox2B-GFP mouse brain showing Phox2B-expressing neurons in PZ **(A)** but not in PB **(B)** or SLD **(C)**. Scale bar: 200 μm. **(D)** Confocal images from PZ showing native GFP from a Vglut2-GFP mouse immunolabeled for Phox2B in red. Scale bar: 50 μm. **(E)** Higher magnification of the box in **(D)**. Scale bar: 20 μm. **(F)** Confocal images from PZ showing native GFP from a Vgat-GFP mouse immunolabeled for Phox2B in red. Scale bar: 50 μm. **(G)** higher magnification of the box in **(F)**. Scale bar: 20 μm. **(H–O)** Confocal images of the PZ showing DAPI staining of nuclei **(H,L)**, and mRNA of Vglut2 **(I,M)** and Phox2B **(J,N)** from two mice. The merged images show complete overlap of both mRNA expression (arrows in **K**,**O**). Scale bar: 20 μm. Abbreviations: 4 V, fourth ventricle; 7 n, seventh facial nerve; LC, locus coeruleus; Mo5, motor trigeminal nucleus; PB, parabrachial nucleus; PZ, parafacial zone; SLD, sublaterodorsal nucleus.

Figures 6L–O). Therefore, Phox2B is a specific marker for PZ glutamatergic neurons and Phox2B-IRES-cre mice can be used to specifically activate PZ glutamatergic neurons and study their role in sleep-wake control.

Activation of PZ^{Phox2B} Neurons Does Not Affect Sleep-Wake Cycle

To assess the involvement of PZ glutamatergic neurons, five Phox2B-IRES-Cre mice were injected into the PZ with AAV-hM3Dq-mCherry (**Figure 7A**). Three of the five cases also showed partial expression in the LC. Whole-cell *in vitro* recording (**Figure 7B1**) confirmed that bath application of CNO (500 nM) significantly increased firing rate in $PZ^{Phox2B-hM3Dq}$ neurons (3.9 ± 1.8 vs. 1.4 ± 1.2 Hz in control condition, $p = 0.028$; **Figure 7B2**). CNO injection was successful in four of the five $PZ^{Phox2B-hM3Dq}$ mice (one mouse displayed an atypical adverse reaction to the injection). CNO treatment during the light period (10:00) did not affect the hourly amounts of wakefulness (two-way ANOVA, $F(23,69) = 1.26$, $p = 0.23$; **Figure 7C1**), SWS (two-way ANOVA, $F(23,69) = 1.21$, $p = 0.27$; **Figure 7C2**) or REM sleep (two-way ANOVA, $F(23,69) = 0.92$, $p = 0.57$; **Figure 7C3**). In order to study the qualitative aspects of the sleep-wake cycle following activation of PZ^{Phox2B} neurons, we studied fragmentation (**Figures 7D1–D3'**) and cortical EEG

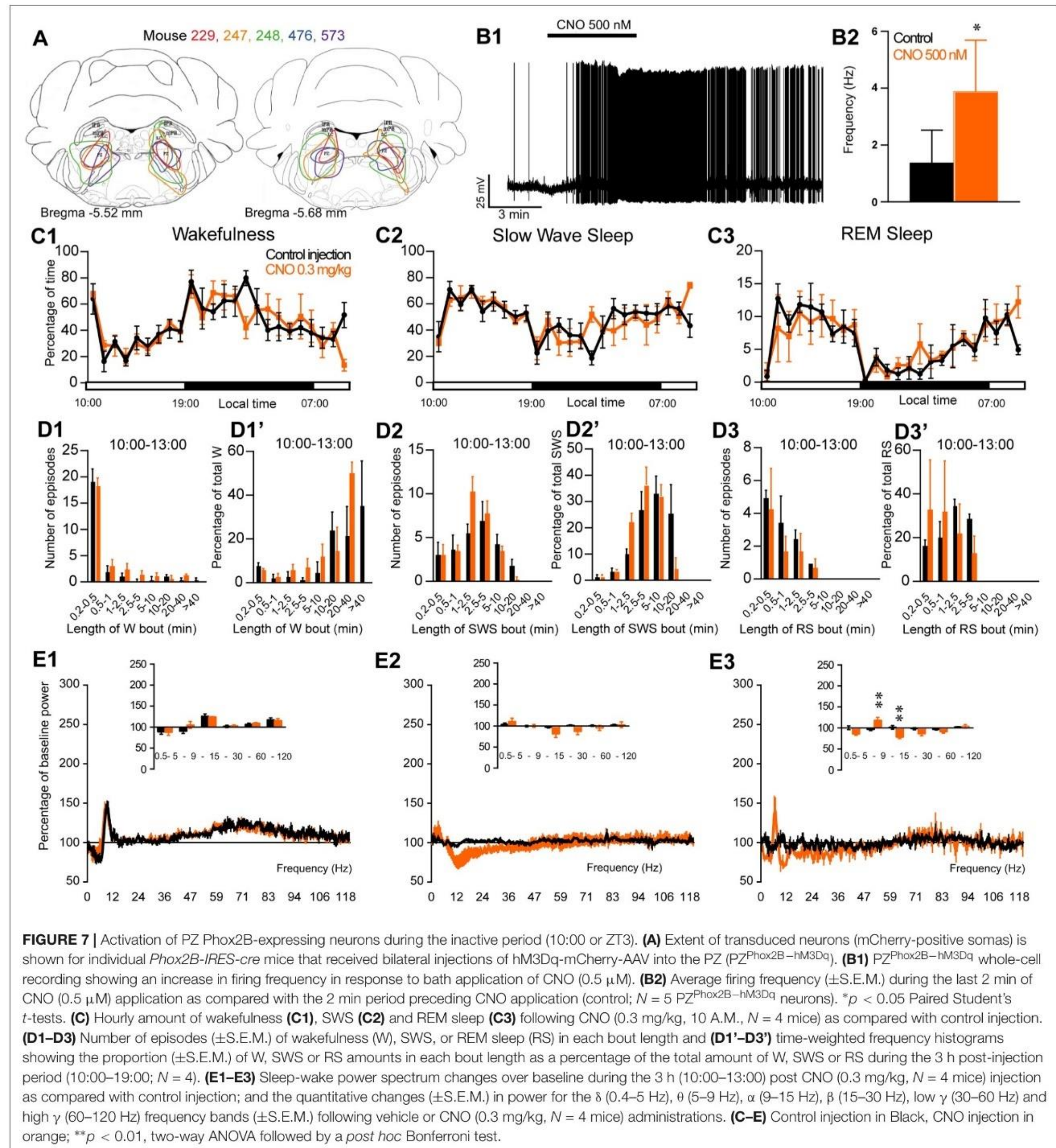

FIGURE 7 | Activation of PZ Phox2B-expressing neurons during the inactive period (10:00 or ZT3). **(A)** Extent of transduced neurons (mCherry-positive somas) is shown for individual *Phox2B-IRES-cre* mice that received bilateral injections of hM3Dq-mCherry-AAV into the PZ ($PZ^{Phox2B-hM3Dq}$). **(B1)** $PZ^{Phox2B-hM3Dq}$ whole-cell recording showing an increase in firing frequency in response to bath application of CNO (0.5 μM). **(B2)** Average firing frequency (±S.E.M.) during the last 2 min of CNO (0.5 μM) application as compared with the 2 min period preceding CNO application (control; $N = 5$ $PZ^{Phox2B-hM3Dq}$ neurons). $^{*}p < 0.05$ Paired Student's *t*-tests. **(C)** Hourly amount of wakefulness **(C1)**, SWS **(C2)** and REM sleep **(C3)** following CNO (0.3 mg/kg, 10 A.M., $N = 4$ mice) as compared with control injection. **(D1–D3)** Number of episodes (±S.E.M.) of wakefulness (W), SWS, or REM sleep (RS) in each bout length and **(D1'–D3')** time-weighted frequency histograms showing the proportion (±S.E.M.) of W, SWS or RS amounts in each bout length as a percentage of the total amount of W, SWS or RS during the 3 h post-injection period (10:00–19:00; $N = 4$). **(E1–E3)** Sleep-wake power spectrum changes over baseline during the 3 h (10:00–13:00) post CNO (0.3 mg/kg, $N = 4$ mice) injection as compared with control injection; and the quantitative changes (±S.E.M.) in power for the δ (0.4–5 Hz), θ (5–9 Hz), α (9–15 Hz), β (15–30 Hz), low γ (30–60 Hz) and high γ (60–120 Hz) frequency bands (±S.E.M.) following vehicle or CNO (0.3 mg/kg, $N = 4$ mice) administrations. **(C–E)** Control injection in Black, CNO injection in orange; $^{**}p < 0.01$, two-way ANOVA followed by a *post hoc* Bonferroni test.

power distribution (**Figures 7E1–E3**) of the three vigilance stages during the 3 h post-injection time period. The number of sleep-wake episodes and episode length distribution were similar between CNO and control injections (**Figures 7D1–D3**). Treatment did not affect the cortical EEG power distribution during wakefulness and SWS. However, during REM sleep, the theta frequency band was significantly increased (118.4 ± 6.8 vs. 96.5 ± 2.5% of baseline power in control condition, $p < 0.01$; **Figure 7D3**) while the sigma frequency band was significantly decreased (78.4 ± 3.8 vs. 101.6 2.5% of baseline power in control condition, $p < 0.01$; **Figure 7D3**). These results indicate that activation of $PZ^{Phox2B-hM3Dq}$ during the light, inactive, period does not affect the sleep-wake cycle but could be involved in cortical EEG activation during REM sleep. Similar results were

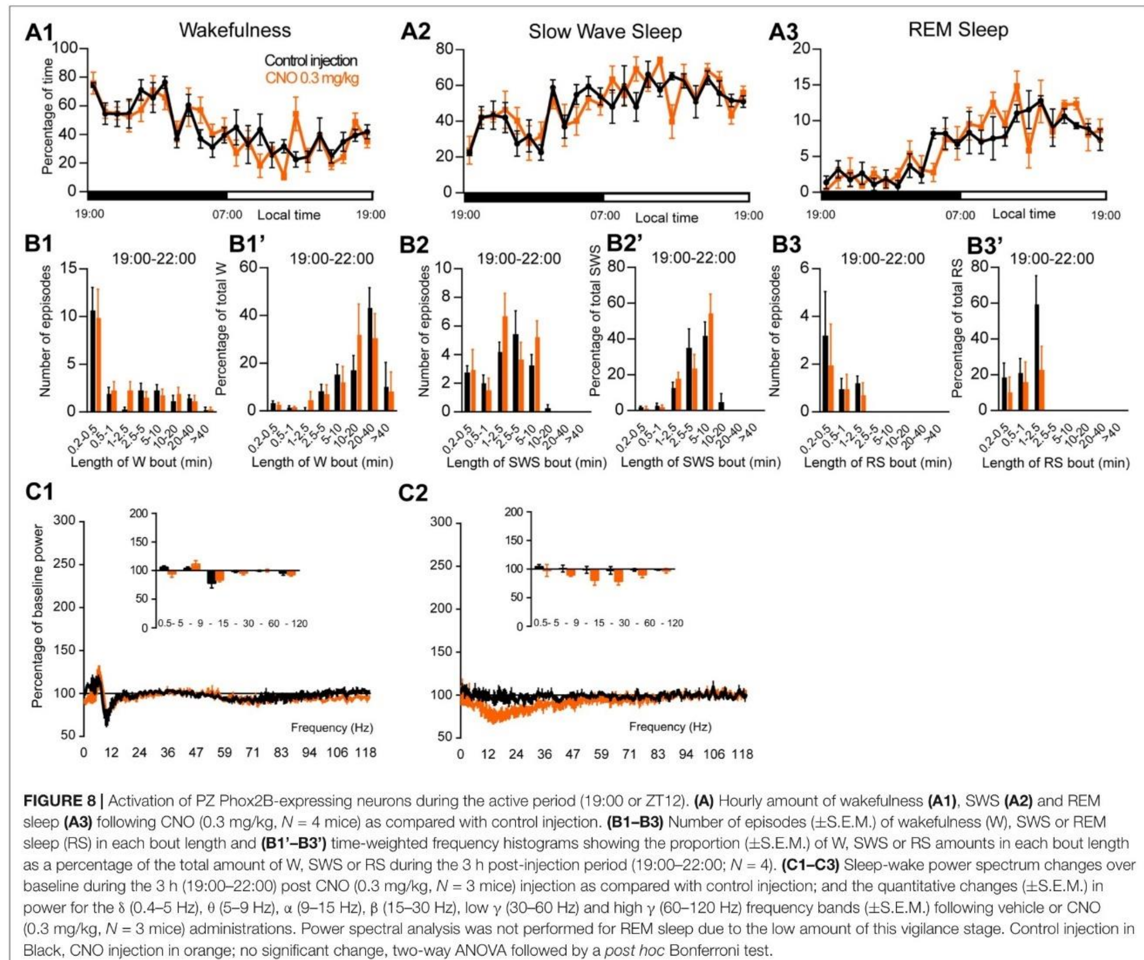

FIGURE 8 | Activation of PZ Phox2B-expressing neurons during the active period (19:00 or ZT12). **(A)** Hourly amount of wakefulness **(A1)**, SWS **(A2)** and REM sleep **(A3)** following CNO (0.3 mg/kg, $N = 4$ mice) as compared with control injection. **(B1–B3)** Number of episodes (±S.E.M.) of wakefulness (W), SWS or REM sleep (RS) in each bout length and **(B1'–B3')** time-weighted frequency histograms showing the proportion (±S.E.M.) of W, SWS or RS amounts in each bout length as a percentage of the total amount of W, SWS or RS during the 3 h post-injection period (19:00–22:00; $N = 4$). **(C1–C3)** Sleep-wake power spectrum changes over baseline during the 3 h (19:00–22:00) post CNO (0.3 mg/kg, $N = 3$ mice) injection as compared with control injection; and the quantitative changes (±S.E.M.) in power for the δ (0.4–5 Hz), θ (5–9 Hz), α (9–15 Hz), β (15–30 Hz), low γ (30–60 Hz) and high γ (60–120 Hz) frequency bands (±S.E.M.) following vehicle or CNO (0.3 mg/kg, $N = 3$ mice) administrations. Power spectral analysis was not performed for REM sleep due to the low amount of this vigilance stage. Control injection in Black, CNO injection in orange; no significant change, two-way ANOVA followed by a *post hoc* Bonferroni test.

obtained when CNO was administrated at the beginning of the active period (19:00; **Figure 8**).

DISCUSSION

To test the contribution of PZ glutamatergic neurons in sleep-wake control, we chemogenetically activated Vglut2-expressing neurons. Based on the sleep-wake phenotype and anatomical confirmation of the injection sites, the mice were separated in three groups: (1) one group, with targeted neuronal transfection mainly in the PZ, displayed increased wakefulness followed by a trend to increased REM sleep during the rest period but not during the active period; (2) a second group, with transfections that included the SLD, displayed a shorter wake increase followed by a significant increase in REM sleep amount; and (3) the third group, which had significant PB transfection, displayed a prominent and long lasting increase in wakefulness, independent of the time of day the injections were performed. Thus, due to the difficulty in targeting only glutamatergic PZ neurons while avoiding glutamatergic neurons in surrounding areas, the role of PZ^{Vglut2} neurons in sleep-wake control was still unclear. CNO did not affect the sleep-wake cycle in control mice not expressing the hM3Dq receptor, confirming that the phenotypes seen in Vglut2 transfected mice were specifically due to the activation of glutamatergic neurons. To test the specific role of PZ glutamatergic neurons in sleep-wake control, we took advantage of Phox2B, a transcription factor expressed by a subset of brainstem glutamatergic neurons. We first confirmed that Phox2B is a specific marker for PZ glutamatergic neurons in mice. Because chemogenetic activation of PZ^{Phox2B} neurons did not affect sleep-wake phenotypes, we can conclude that PZ glutamatergic neurons are not sufficient to influence the sleep-wake cycle.

The absence of a sleep-wake phenotype in control and $PZ^{Phox2B-hM3Dq}$ mice after CNO injection provides additional

evidence that CNO, at the dose used in our studies, does not affect the baseline sleep-wake cycle. A recent study had shown that clozapine, a metabolite of CNO, but not CNO, crosses the blood brain barrier and binds chemogenetic receptors with high affinity in rats (Gomez et al., 2017). This finding was subsequently challenged by the observation that both clozapine and CNO cross the blood brain barrier in mice, and that unbound CNO is present in the brain at concentrations sufficient to activate DREADDs, albeit at a higher initial dose than we typically use (Jendryka et al., 2019). We had previously shown that, at a dose of 0.3 mg/kg, CNO does not affect sleep-wake quantity and quality in Vgat-IRES-cre mice (Anaclet et al., 2014), nor does it interfere with the wake-promoting actions of armodafinil and caffeine (Anaclet et al., 2018). In the present study, we confirm the absence of non-specific actions of CNO on the sleep-wake cycle, using two different mouse strains, Vglut2-IRES-cre and Phox2B-IRES-cre mice. Additionally, we confirmed that CNO is able to directly activate $PZ^{Vglut2-hM3Dq}$, $PB^{Vglut2-hM3Dq}$, and $SLD^{Vglut2-hM3Dq}$ neurons *in vitro*, where the short application duration (few minutes) and the absence of hepatic metabolism make back-conversion to clozapine highly unlikely. In summary, CNO was able to activate glutamatergic neurons expressing hM3Dq chemogenetic receptor and did not result in non-specific sleep-wake phenotypes.

Phox2B Is a Specific Marker for PZ Glutamatergic Neurons

The transcription factor Phox2B has been studied for its involvement in the control of breathing and autonomic regulation. Phox2B mutations have been implicated in congenital central hypoventilation syndrome (Moreira et al., 2016). Phox2B-expressing neurons located in the medullary retrotrapezoid nucleus (RTN), ventral from the facial nucleus, are sensitive to hypoxia (Onimaru et al., 2008), hypercapnic acidosis and serotonin (Wu et al., 2019). Phox2B is necessary for the differentiation of central noradrenergic and adrenergic neurons (Pattyn et al., 2000; Huber et al., 2005). Phox2B is expressed in PZ in adult rats (Kang et al., 2007) but these neurons have no known physiological function. In the present study, we showed that, in PZ, Phox2B is highly co-localized with Vglut2 and therefore, is a specific marker for PZ glutamatergic neurons. Phox2B is also highly co-localized with LC noradrenergic neurons, known to be wake-promoting. However, in this study, the three mice showing partial expression of hM3Dq receptors in LC, did not display an increase in wake amount following CNO injection. It is possible that either the partial coverage of LC was not enough to promote wakefulness or LC noradrenergic neurons were not activated by the chemogenetic ligand. *In vitro* recordings of $LC^{Phox2B-hM3Dq}$ neurons would be necessary to answer this question.

The Role of PZ Glutamatergic Neurons in Sleep-Wake Control

A previous study has suggested that some PZ non-GABAergic neurons are sleep-active (Anaclet et al., 2012). Because glutamatergic neurons are the only other neuronal population identified in PZ thus far, we tested if chemogenetic activation of PZ glutamatergic neurons affects sleep-wake phenotypes. Specific targeting of PZ glutamatergic neurons using Vglut2-cre mice was challenging. Of the over 29 injected mice, only six displayed hM3Dq expression mainly in PZ ($PZ^{Vglut2-hM3Dq}$). Five mice displayed hM3Dq expression mainly in PB ($PB^{Vglut2-hM3Dq}$) and six in SLD ($SLD^{Vglut2-hM3Dq}$). The remaining mice included seven showing expression of hM3Dq at multiple sites, and five died after surgery or during the sleep recordings. These last two mouse groups were excluded from the study.

Chemogenetic activation of $PZ^{Vglut2-hM3Dq}$ neurons at the beginning of the mouse active phase (19:00) had limited impact on the sleep-wake cycle. On the other hand, chemogenetic activation of $PZ^{Vglut2-hM3Dq}$ neurons during the mouse rest phase (10:00) resulted in an early wake enhancement followed by an increase in REM sleep amount. Because these phenotypes are reminiscent of the phenotypes observed in $PB^{Vglut2-hM3Dq}$ and $SLD^{Vglut2-hM3Dq}$ mice, we hypothesized that they were due to the inadvertent transfection of PB and SLD neurons. In other words, in the $PZ^{Vglut2-hM3Dq}$ group, transfection would not be restricted to PZ. To test this hypothesis and definitively confirm the role of PZ^{Vglut2} neurons in sleep-wake control, we took advantage of Phox2B, a specific marker for PZ^{Vglut2} neurons. Using Phox2B-cre mice to specifically target PZ^{Vglut2} neurons and not neighboring PB and SLD, we showed that PZ^{Vglut2} neurons are not sufficient to affect the sleep-wake cycle at any time of the day. These results indicate that PZ glutamatergic neurons have no role in sleep or wake induction and/or maintenance. It remains, however, to be tested whether PZ^{Vglut2} neurons are necessary for normal sleep-wake cycle control, using inhibitory chemogenetic receptors and/or cell body specific lesion.

A New Mouse Model for REM Sleep Enhancement

Rostral to the PZ and PB, the SLD contains Vglut2-expressing neurons that are specifically active during REM sleep recovery (Clement et al., 2011). The SLD contains a large proportion of neurons with tonic discharge patterns immediately prior to and during REM sleep (Sakai, 2015). Cell body specific SLD lesions, knockout of glutamatergic transmission and genetic inactivation significantly reduce REM sleep amount and result in REM sleep without muscle atonia (Lu et al., 2006; Krenzer et al., 2011; Valencia Garcia et al., 2017). In the present study, we show for the first time that chemogenetic activation of SLD^{Vglut2} neurons results in increased REM sleep amount and reduced SWS to REM sleep latency. Moreover, cortical EEG theta power is significantly enhanced during REM sleep. These data provide a new and unique model of REM sleep enhancement. Such a model will permit probing of the specific role of REM sleep in other neurophysiological functions, such as memory consolidation. However, specific targeting of SLD glutamatergic neurons is challenging due to the close proximity of PB wake-promoting glutamatergic neurons (Fuller et al., 2011). A specific marker for SLD glutamatergic neurons would be very useful.

Additional Evidence for the Importance of PB in Wakefulness

In close proximity to PZ, just dorsal, lateral and rostral, the PB is a critical brainstem wake-promoting system. Following lesions of both PB and precoeruleus (PC), rats can no longer sustain cortical activation and become comatose (Fuller et al., 2011). Since this seminal study, the role of PB glutamatergic neurons in wakefulness has been refined. Specific lesions of medial PB result in hypersomnolence (Kaur et al., 2013). Glutamatergic neurons located in the external lateral PB are activated by hypoxia and are a key component of the vitally important circuitry regulating arousal from sleep apnea episodes (Kaur et al., 2017). In the present study we show that chemogenetic activation of medial PB results in long lasting wake enhancement. Moreover, CNO induced wakefulness was characterized by a decreased delta frequency band power. Because the delta band is considered a marker of EEG synchronization and is more prominent during quiet wakefulness, this result indicates a more active wake state induced by activation of PB^{Vglut2} neurons. Finally, no sleep rebound was seen after the wake enhancement. This is in accordance with previous studies using chemogenetics to specifically activate wake-promoting neuronal populations (Anaclet et al., 2015; Venner et al., 2016; Pedersen et al., 2017) and indicates that chemogenetic activation of wake-promoting neuronal populations does not enhance the homeostatic drive for sleep. All together, these results confirm the strong wake-promoting action of PB glutamatergic neurons.

CONCLUSION

This study shows, for the first time, that PZ glutamatergic neurons are not sufficient to affect the sleep-wake cycle in mouse. However, chemogenetic activation of PB or SLD glutamatergic neurons results in wake or REM sleep enhancement, respectively. Finally, Phox2B is a specific marker for PZ glutamatergic neurons. All together, these results provide a better understanding on how the brain regulates sleep-wake cycles, forming a framework for future studies characterizing the sleep-promoting subpopulation of the PZ.

DATA AVAILABILITY

The raw data supporting the conclusions of this manuscript will be made available by the authors, without undue reservation, to any qualified researcher.

ETHICS STATEMENT

All procedures were approved by the Institutional Animal Care and Use Committee of Beth Israel Deaconess Medical Center and of University of Massachusetts Medical School.

AUTHOR CONTRIBUTIONS

EE performed the immunostaining and analyzed the sleep data. LF performed and analyzed the *in vitro* experiments. HG performed and analyzed the *in situ* hybridization experiments and wrote the manuscript. CA performed the surgeries and the *in vivo* experiments, and wrote the manuscript.

FUNDING

This research was funded by the National Institutes of Health grants K99MH103399 (CA) and R00MH103399 (CA), Coins for Alzheimer's Research Trust (CART) fund and by the University of Massachusetts Medical School startup funds. The latter were used to fund the open access publication fees.

ACKNOWLEDGMENTS

We are grateful to Quan Hue Ha, Minh Ha, Myriam Debryune, Rebecca Broadhurst, and Tilar Martin for superb technical assistance. We thank Dr. Patrick Fuller for his support.

REFERENCES

Alam, M. A., Kostin, A., Siegel, J., McGinty, D., Szymusiak, R., and Alam, M. N. (2018). "Characteristics of sleep-active neurons in the medullary parafacial zone in rats". *Sleep* 41:zsy130. doi: 10.1093/sleep/zsy130

Anaclet, C., Griffith, K., and Fuller, P. M. (2018). Activation of the GABAergic parafacial zone maintains sleep and counteracts the wake-promoting action of the psychostimulants armodafinil and caffeine. *Neuropsychopharmacology* 43, 415–425. doi: 10.1038/npp.2017.152

Anaclet, C., Ferrari, L., Arrigoni, E., Bass, C. E., Saper, C. B., Lu, J., et al. (2014). The GABAergic parafacial zone is a medullary slow wave sleep-promoting center. *Nat. Neurosci.* 17, 1217–1224. doi: 10.1038/nn.3789

Anaclet, C., and Fuller, P. M. (2017). Brainstem regulation of slow-wave-sleep. *Curr. Opin. Neurobiol.* 44, 139–143. doi: 10.1016/j.conb.2017.04.004

Anaclet, C., Lin, J. S., Vetrivelan, R., Krenzer, M., Vong, L., Fuller, P. M., et al. (2012). Identification and characterization of a sleep-active cell group in the rostral medullary brainstem. *J. Neurosci.* 32, 17970–17976. doi: 10.1523/JNEUROSCI.0620-12.2012

Anaclet, C., Pedersen, N. P., Ferrari, L. L., Venner, A., Bass, C. E., Arrigoni, E., et al. (2015). Basal forebrain control of wakefulness and cortical rhythms. *Nat. Commun.* 6:8744. doi: 10.1038/ncomms9744

Anaclet, C., Pedersen, N. P., Fuller, P. M., and Lu, J. (2010). Brainstem circuitry regulating phasic activation of trigeminal motoneurons during REM sleep. *PLoS One* 5:e8788. doi: 10.1371/journal.pone.0008788

Clement, O., Sapin, E., Berod, A., Fort, P., and Luppi, P. H. (2011). Evidence that neurons of the sublaterodorsal tegmental nucleus triggering paradoxical (REM) sleep are glutamatergic. *Sleep* 34, 419–423. doi: 10.1093/sleep/34.4.419

Fuller, P. M., Sherman, D., Pedersen, N. P., Saper, C. B., and Lu, J. (2011). Reassessment of the structural basis of the ascending arousal system. *J. Comp. Neurol.* 519, 933–956. doi: 10.1002/cne.22559

Gomez, J. L., Bonaventura, J., Lesniak, W., Mathews, W. B., Rodriguez, L. A., and Ellis, R. J. (2017). Chemogenetics revealed: dREADD occupancy and activation via converted clozapine. *Science* 357, 503–507. doi: 10.1126/science.aan2475

Huber, K., Karch, N., Ernsberger, U., Goridis, C., and Unsicker, K. (2005). The role of Phox2B in chromaffin cell development. *Dev. Biol.* 279, 501–508. doi: 10.1016/j.ydbio.2005.01.007

Jendryka, M., Palchaudhuri, M., Ursu, D., Liss, B., Katzel, D., Nissen, W., et al. (2019). Pharmacokinetic and pharmacodynamic actions of clozapine-N-oxide, clozapine, and compound 21 in DREADD-based chemogenetics in mice. *Sci. Rep.* 9:4522. doi: 10.1038/s41598-019-41088-2

Kang, B. J., Chang, D. A., Mackay, D. D., West, G. H., Moreira, T. S., Takakura, A. C., et al. (2007). Central nervous system distribution of the transcription factor Phox2b in the adult rat. *J. Comp. Neurol.* 503, 627–641. doi: 10.1002/cne.21409

Kantor, S., Mochizuki, T., Lops, S. N., Ko, B., Clain, E., Clark, E., et al. (2013). Orexin gene therapy restores the timing and maintenance of wakefulness in narcoleptic mice. *Sleep* 36, 1129–1138. doi: 10.5665/sleep.2870

Kaur, S., Pedersen, N. P., Yokota, S., Hur, E. E., Fuller, P. M., Lazarus, M., et al. (2013). Glutamatergic signaling from the parabrachial nucleus plays a critical role in hypercapnic arousal. *.J. Neurosci.* 33, 7627–7640. doi: 10.1523/JNEUROSCI.0173-13.2013

Kaur, S., Wang, J. L., Ferrari, L., Thankachan, S., Kroeger, D., Venner, A., et al. (2017). A Genetically defined circuit for arousal from sleep during hypercapnia. *Neuron* 96, 1153.e5–1167e5. doi: 10.1016/j.neuron.2017.10.009

Krenzer, M., Anaclet, C., Vetrivelan, R., Wang, N., Vong, L., Lowell, B. B., et al. (2011). Brainstem and spinal cord circuitry regulating REM sleep and muscle atonia. *PLoS One* 6:e24998. doi: 10.1371/journal.pone.0024998

Liu, J., Krautzberger, A. M., Sui, S. H., Hofmann, O. M., Chen, Y., Baetscher, M., et al. (2014). Cell-specific translational profiling in acute kidney injury. *J. Clin. Invest.* 124, 1242–1254. doi: 10.1172/JCI72126

Lu, J., Sherman, D., Devor, M., and Saper, C. B. (2006). A putative flip-flop switch for control of REM sleep. *Nature* 441, 589–594. doi: 10.1038/nature04767

Mochizuki, T., Crocker, A., McCormack, S., Yanagisawa, M., Sakurai, T., and Scammell, T. E. (2004). Behavioral state instability in orexin knock-out mice. *J. Neurosci.* 24, 6291–6300. doi: 10.1523/jneurosci.0586-04.2004

Moreira, T. S., Takakura, A. C., Czeisler, C., and Otero, J. J. (2016). Respiratory and autonomic dysfunction in congenital central hypoventilation syndrome. *J. Neurophysiol.* 116, 742–752. doi: 10.1152/jn.00026.2016

Onimaru, H., Ikeda, K., and Kawakami, K. (2008). CO_2-sensitive preinspiratory neurons of the parafacial respiratory group express Phox2b in the neonatal rat. *J. Neurosci.* 28, 12845–12850. doi: 10.1523/JNEUROSCI.3625-08.2008

Pattyn, A., Goridis, C., and Brunet, J. F. (2000). Specification of the central noradrenergic phenotype by the homeobox gene Phox2b. *Mol. Cell. Neurosci.* 15, 235–243. doi: 10.1006/mcne.1999.0826

Paxinos, G. T., and Franklin, K. B. J. (2001). *The Mouse Brain in Stereotaxic Coordinates*, 2 Edn. San Diego: Academic.

Pedersen, N. P., Ferrari, L., Venner, A., Wang, J. L., Abbott, S. B. G., Vujovic, N., et al. (2017). Supramammillary glutamate neurons are a key node of the arousal system. *Nat. Commun.* 8:1405. doi: 10.1038/s41467-017-01004-6

Rossi, J., Balthasar, N., Olson, D., Scott, M., Berglund, E., Lee, C. E., et al. (2011). Melanocortin-4 receptors expressed by cholinergic neurons regulate energy balance and glucose homeostasis. *Cell Metab.* 13, 195–204. doi: 10.1016/j.cmet.2011.01.010

Sakai, K. (2015). Paradoxical (rapid eye movement) sleep-on neurons in the laterodorsal pontine tegmentum in mice. *Neuroscience* 310, 455–471. doi: 10.1016/j.neuroscience.2015.09.063

Sakai, K. (2017). Are there sleep-promoting neurons in the mouse parafacial zone? *Neuroscience* 367, 98–109. doi: 10.1016/j.neuroscience.2017.10.026

Stornetta, R. L., Moreira, T. S., Takakura, A. C., Kang, B. J., Chang, D. A., West, G. H., et al. (2006). Expression of Phox2b by brainstem neurons involved in chemosensory integration in the adult rat. *J. Neurosci.* 26, 10305–10314. doi: 10.1523/JNEUROSCI.2917-06.2006

Valencia Garcia, S., Libourel, P. A., Lazarus, M., Grassi, D., Luppi, P. H., and Fort, P. (2017). Genetic inactivation of glutamate neurons in the rat sublaterodorsal tegmental nucleus recapitulates REM sleep behaviour disorder. *Brain* 140, 414–428. doi: 10.1093/brain/aww310

Venner, A., Anaclet, C., Broadhurst, R. Y., Saper, C. B., and Fuller, P. M. (2016). A Novel Population of wake-promoting GABAergic neurons in the ventral lateral hypothalamus. *Curr. Biol.* 26, 2137–2143. doi: 10.1016/j.cub.2016.05.078

Vong, L., Ye, C., Yang, Z., Choi, B., Chua, S Jr, and Lowell, B. B. (2011). Leptin action on GABAergic neurons prevents obesity and reduces inhibitory tone to POMC neurons. *Neuron* 71, 142–154. doi: 10.1016/j.neuron.2011.05.028

Wu, Y., Proch, K. L., Teran, F. A., Lechtenberg, R. J., Kothari, H., and Richerson, G. B. (2019). Chemosensitivity of Phox2b-expressing retrotrapezoid neurons is mediated in part by input from 5-HT neurons. *J. Physiol.* 597, 2741–2766. doi: 10.1113/JP277052

Conflict of Interest Statement: The authors declare that the research was conducted in the absence of any commercial or financial relationships that could be construed as a potential conflict of interest.

Copyright © 2019 Erickson, Ferrari, Gompf and Anaclet. This is an open-access article distributed under the terms of the Creative Commons Attribution License (CC BY). The use, distribution or reproduction in other forums is permitted, provided the original author(s) and the copyright owner(s) are credited and that the original publication in this journal is cited, in accordance with accepted academic practice. No use, distribution or reproduction is permitted which does not comply with these terms.

Bibliography

Abo-Zahhad, M., Ahmed, S., & Seha, S. N. (2015). A New EEG Acquisition Protocol for Biometric Identification Using Eye Blinking Signals. *International Journal of Intelligent Systems and Applications (IJISA)*, *07*, 48-54. https://doi.org/10.5815/ijisa.2015.06.05

Adamantidis, A. R., Zhang, F., Aravanis, A. M., Deisseroth, K., & de Lecea, L. (2007). Neural substrates of awakening probed with optogenetic control of hypocretin neurons. *Nature*, *450*(7168), 420-424. https://doi.org/10.1038/nature06310

Alam, M. N., Szymusiak, R., Gong, H., King, J., & McGinty, D. (1999). Adenosinergic modulation of rat basal forebrain neurons during sleep and waking: neuronal recording with microdialysis. *J Physiol*, *521*(3), 679-690. https://doi.org/10.1111/j.1469-7793.1999.00679.x

Aldabal, L., & Bahammam, A. S. (2011). Metabolic, endocrine, and immune consequences of sleep deprivation. *The open respiratory medicine journal*, *5*, 31-43. https://doi.org/10.2174/1874306401105010031

American Academy of Sleep, M. (2014). *International classification of sleep disorders* (3 ed.). American Academy of Sleep Medicine.

American Psychiatric Association. (2013). Sleep-Wake Disorders. In Emmanuel (Ed.), *Diagnostic and Statistical Manual of Mental Disorders* (5th ed.). https://doi.org/10.1176/appi.books.9780890425596.dsm12

Anaclet, C., De Luca, R., Venner, A., Malyshevskaya, O., Lazarus, M., Arrigoni, E., & Fuller, P. M. (2018). Genetic Activation, Inactivation, and Deletion Reveal a Limited And Nuanced Role for Somatostatin-Containing Basal Forebrain Neurons in Behavioral State Control. *J Neurosci*, *38*(22), 5168-5181. https://doi.org/10.1523/JNEUROSCI.2955-17.2018

Anaclet, C., Ferrari, L., Arrigoni, E., Bass, C. E., Saper, C. B., Lu, J., & Fuller, P. M. (2014). The GABAergic parafacial zone is a medullary slow wave sleep-promoting center. *Nat Neurosci*, *17*(9), 1217-1224. https://doi.org/10.1038/nn.3789

Anaclet, C., & Fuller, P. M. (2017). Brainstem regulation of slow-wave-sleep. *Curr Opin Neurobiol*, *44*, 139-143. https://doi.org/10.1016/j.conb.2017.04.004

Anaclet, C., Griffith, K., & Fuller, P. M. (2018). Activation of the GABAergic Parafacial Zone Maintains Sleep and Counteracts the Wake-Promoting Action of the Psychostimulants Armodafinil and Caffeine. *Neuropsychopharmacology*, *43*(2), 415-425. https://doi.org/10.1038/npp.2017.152

Anaclet, C., Lin, J. S., Vetrivelan, R., Krenzer, M., Vong, L., Fuller, P. M., & Lu, J. (2012). Identification and characterization of a sleep-active cell group in the rostral medullary brainstem. *J Neurosci*, *32*(50), 17970-17976. https://doi.org/10.1523/JNEUROSCI.0620-12.2012

Anaclet, C., Pedersen, N. P., Ferrari, L. L., Venner, A., Bass, C. E., Arrigoni, E., & Fuller, P. M. (2015). Basal forebrain control of wakefulness and cortical rhythms. *Nat Commun*, *6*, 8744. https://doi.org/10.1038/ncomms9744

Arnal, P. J., Sauvet, F., Leger, D., van Beers, P., Bayon, V., Bougard, C., Rabat, A., Millet, G. Y., & Chennaoui, M. (2015). Benefits of Sleep Extension on Sustained Attention and Sleep Pressure Before and During Total Sleep Deprivation and Recovery. *Sleep*, *38*(12), 1935-1943. https://doi.org/10.5665/sleep.5244

Babson, K. A., Trainor, C. D., Feldner, M. T., & Blumenthal, H. (2010). A test of the effects of acute sleep deprivation on general and specific self-reported anxiety and depressive symptoms: An experimental extension. *Journal of Behavior Therapy and Experimental Psychiatry*, *41*(3), 297-303. https://doi.org/https://doi.org/10.1016/j.jbtep.2010.02.008

Baglioni, C., Spiegelhalder, K., Lombardo, C., & Riemann, D. (2010). Sleep and emotions: A focus on insomnia. *Sleep Med Rev*, *14*(4), 227-238. https://doi.org/https://doi.org/10.1016/j.smrv.2009.10.007

Basheer, R., Bauer, A., Elmenhorst, D., Ramesh, V., & McCarley, R. W. (2007). Sleep deprivation upregulates A1 adenosine receptors in the rat basal forebrain. *Neuroreport*, *18*(18), 1895-1899. https://doi.org/10.1097/WNR.0b013e3282f262f6

Basheer, R., Porkka-Heiskanen, T., Strecker, R. E., Thakkar, M. M., & McCarley, R. W. (2000). Adenosine as a biological signal mediating sleepiness following prolonged wakefulness. *Biol Signals Recept*, *9*(6), 319-327. https://doi.org/10.1159/000014655

Basheer, R., Strecker, R. E., Thakkar, M. M., & McCarley, R. W. (2004). Adenosine and sleep-wake regulation. *Prog Neurobiol*, *73*(6), 379-396. https://doi.org/10.1016/j.pneurobio.2004.06.004

Benington, J. H., Kodali, S. K., & Heller, H. C. (1995). Stimulation of A1 adenosine receptors mimics the electroencephalographic effects of sleep deprivation. *Brain Research*, *692*(1), 79-85. https://doi.org/https://doi.org/10.1016/0006-8993(95)00590-M

Bentley, P., Vuilleumier, P., Thiel, C. M., Driver, J., & Dolan, R. J. (2003). Cholinergic enhancement modulates neural correlates of selective attention and emotional processing. *Neuroimage*, *20*(1), 58-70. https://doi.org/10.1016/s1053-8119(03)00302-1

Blunden, S., & Galland, B. (2014). The complexities of defining optimal sleep: empirical and theoretical considerations with a special emphasis on children. *Sleep Med Rev*, *18*(5), 371-378. https://doi.org/10.1016/j.smrv.2014.01.002

Boissard, R., Fort, P., Gervasoni, D., Barbagli, B., & Luppi, P. H. (2003). Localization of the GABAergic and non-GABAergic neurons projecting to the sublaterodorsal nucleus and potentially gating paradoxical sleep onset. *Eur J Neurosci*, *18*(6), 1627-1639. https://doi.org/10.1046/j.1460-9568.2003.02861.x

Borbély, A. A. (1982). A two process model of sleep regulation. *Hum Neurobiol*, *1*(3), 195-204.
Borbély, A. A., Daan, S., Wirz-Justice, A., & Deboer, T. (2016). The two-process model of sleep regulation: a reappraisal. *J Sleep Res*, *25*(2), 131-143. https://doi.org/10.1111/jsr.12371
Borea, P. A., Gessi, S., Merighi, S., & Varani, K. (2016). Adenosine as a Multi-Signalling Guardian Angel in Human Diseases: When, Where and How Does it Exert its Protective Effects? *Trends in Pharmacological Sciences*, *37*(6), 419-434. https://doi.org/10.1016/j.tips.2016.02.006
Borodovitsyna, O., Flamini, M., & Chandler, D. (2017). Noradrenergic Modulation of Cognition in Health and Disease. *Neural Plasticity*, *2017*, 6031478. https://doi.org/10.1155/2017/6031478
Boyce, R., Glasgow, S. D., Williams, S., & Adamantidis, A. (2016). Causal evidence for the role of REM sleep theta rhythm in contextual memory consolidation. *Science*, *352*(6287), 812-816. https://doi.org/10.1126/science.aad5252
Breton-Provencher, V., & Sur, M. (2019). Active control of arousal by a locus coeruleus GABAergic circuit. *Nature Neuroscience*, *22*(2), 218-228. https://doi.org/10.1038/s41593-018-0305-z
Brzezinski, J. A. t., Brown, N. L., Tanikawa, A., Bush, R. A., Sieving, P. A., Vitaterna, M. H., Takahashi, J. S., & Glaser, T. (2005). Loss of circadian photoentrainment and abnormal retinal electrophysiology in Math5 mutant mice. *Invest Ophthalmol Vis Sci*, *46*(7), 2540-2551. https://doi.org/10.1167/iovs.04-1123
Burgess, C. R., & Scammell, T. E. (2012). Narcolepsy: neural mechanisms of sleepiness and cataplexy. *The Journal of neuroscience : the official journal of the Society for Neuroscience*, *32*(36), 12305-12311. https://doi.org/10.1523/JNEUROSCI.2630-12.2012
Butcher, L. L., Oh, J. D., & Woolf, N. J. (1993). Cholinergic neurons identified by in situ hybridization histochemistry. *Prog Brain Res*, *98*, 1-8. https://doi.org/10.1016/s0079-6123(08)62377-8
Cappuccio, F. P., Cooper, D., D'Elia, L., Strazzullo, P., & Miller, M. A. (2011). Sleep duration predicts cardiovascular outcomes: a systematic review and meta-analysis of prospective studies. *European Heart Journal*, *32*(12), 1484-1492. https://doi.org/10.1093/eurheartj/ehr007
Cappuccio, F. P., D'Elia, L., Strazzullo, P., & Miller, M. A. (2010). Quantity and Quality of Sleep and Incidence of Type 2 Diabetes. *A systematic review and meta-analysis*, *33*(2), 414-420. https://doi.org/10.2337/dc09-1124
Carskadon, M. A., & Dement, W. C. (2005). Chapter 2 - Normal Human Sleep: An Overview. In M. H. Kryger, T. Roth, & W. C. Dement (Eds.), *Principles and Practice of Sleep Medicine (Fourth Edition)* (pp. 13-23). W.B. Saunders. https://doi.org/https://doi.org/10.1016/B0-72-160797-7/50009-4
Carter, M. E., Adamantidis, A., Ohtsu, H., Deisseroth, K., & de Lecea, L. (2009). Sleep homeostasis modulates hypocretin-mediated sleep-to-wake

transitions. *J Neurosci*, *29*(35), 10939-10949. https://doi.org/10.1523/jneurosci.1205-09.2009

Carter, M. E., Brill, J., Bonnavion, P., Huguenard, J. R., Huerta, R., & de Lecea, L. (2012). Mechanism for Hypocretin-mediated sleep-to-wake transitions. *Proceedings of the National Academy of Sciences*, *109*(39), E2635-E2644. https://doi.org/10.1073/pnas.1202526109

Chamberlin, N. L., Arrigoni, E., Chou, T. C., Scammell, T. E., Greene, R. W., & Saper, C. B. (2003). Effects of adenosine on gabaergic synaptic inputs to identified ventrolateral preoptic neurons. *Neuroscience*, *119*(4), 913-918. https://doi.org/https://doi.org/10.1016/S0306-4522(03)00246-X

Chen, K.-S., Xu, M., Zhang, Z., Chang, W.-C., Gaj, T., Schaffer, D. V., & Dan, Y. (2018). A Hypothalamic Switch for REM and Non-REM Sleep. *Neuron*, *97*(5), 1168-1176.e1164. https://doi.org/10.1016/j.neuron.2018.02.005

Chen, L., Yin, D., Wang, T.-X., Guo, W., Dong, H., Xu, Q., Luo, Y.-J., Cherasse, Y., Lazarus, M., Qiu, Z.-l., Lu, J., Qu, W.-M., & Huang, Z.-L. (2016). Basal Forebrain Cholinergic Neurons Primarily Contribute to Inhibition of Electroencephalogram Delta Activity, Rather Than Inducing Behavioral Wakefulness in Mice. *Neuropsychopharmacology*, *41*(8), 2133-2146. https://doi.org/10.1038/npp.2016.13

Chen, M. C., Vetrivelan, R., Guo, C.-N., Chang, C., Fuller, P. M., & Lu, J. (2017). Ventral medullary control of rapid eye movement sleep and atonia. *Experimental Neurology*, *290*, 53-62. https://doi.org/https://doi.org/10.1016/j.expneurol.2017.01.002

Cho, J. R., Treweek, J. B., Robinson, J. E., Xiao, C., Bremner, L. R., Greenbaum, A., & Gradinaru, V. (2017). Dorsal Raphe Dopamine Neurons Modulate Arousal and Promote Wakefulness by Salient Stimuli. *Neuron*, *94*(6), 1205-1219.e1208. https://doi.org/10.1016/j.neuron.2017.05.020

Chowdhury, S., Matsubara, T., Miyazaki, T., Ono, D., Fukatsu, N., Abe, M., Sakimura, K., Sudo, Y., & Yamanaka, A. (2019). GABA neurons in the ventral tegmental area regulate non-rapid eye movement sleep in mice. *Elife*, *8*. https://doi.org/10.7554/eLife.44928

Cirelli, C. (2005). A molecular window on sleep: changes in gene expression between sleep and wakefulness. *Neuroscientist*, *11*(1), 63-74. https://doi.org/10.1177/1073858404270900

Cirelli, C., Gutierrez, C. M., & Tononi, G. (2004). Extensive and Divergent Effects of Sleep and Wakefulness on Brain Gene Expression. *Neuron*, *41*(1), 35-43. https://doi.org/https://doi.org/10.1016/S0896-6273(03)00814-6

Corbit, L. H., & Janak, P. H. (2010). Posterior dorsomedial striatum is critical for both selective instrumental and Pavlovian reward learning. *Eur J Neurosci*, *31*(7), 1312-1321. https://doi.org/10.1111/j.1460-9568.2010.07153.x

Daan, S., Beersma, D. G., & Borbély, A. A. (1984). Timing of human sleep: recovery process gated by a circadian pacemaker. *Am J Physiol*, *246*(2 Pt 2), R161-183. https://doi.org/10.1152/ajpregu.1984.246.2.R161

Dang-Vu, T. T., Schabus, M., Desseilles, M., Albouy, G., Boly, M., Darsaud, A., Gais, S., Rauchs, G., Sterpenich, V., Vandewalle, G., Carrier, J., Moonen, G., Balteau, E., Degueldre, C., Luxen, A., Phillips, C., & Maquet, P. (2008). Spontaneous neural activity during human slow wave sleep. *Proceedings of the National Academy of Sciences*, *105*(39), 15160-15165. https://doi.org/10.1073/pnas.0801819105

Darwent, D., Ferguson, S. A., Sargent, C., Paech, G. M., Williams, L., Zhou, X., Matthews, R. W., Dawson, D., Kennaway, D. J., & Roach, G. D. (2010). Contribution of core body temperature, prior wake time, and sleep stages to cognitive throughput performance during forced desynchrony. *Chronobiology International*, *27*(5), 898-910. https://doi.org/10.3109/07420528.2010.488621

Dautan, D., Hacioğlu Bay, H., Bolam, J. P., Gerdjikov, T. V., & Mena-Segovia, J. (2016). Extrinsic Sources of Cholinergic Innervation of the Striatal Complex: A Whole-Brain Mapping Analysis [Original Research]. *Frontiers in Neuroanatomy*, *10*(1). https://doi.org/10.3389/fnana.2016.00001

David, F., Schmiedt, J. T., Taylor, H. L., Orban, G., Di Giovanni, G., Uebele, V. N., Renger, J. J., Lambert, R. C., Leresche, N., & Crunelli, V. (2013). Essential thalamic contribution to slow waves of natural sleep. *The Journal of neuroscience : the official journal of the Society for Neuroscience*, *33*(50), 19599-19610. https://doi.org/10.1523/JNEUROSCI.3169-13.2013

de Lecea, L., Kilduff, T. S., Peyron, C., Gao, X., Foye, P. E., Danielson, P. E., Fukuhara, C., Battenberg, E. L., Gautvik, V. T., Bartlett, F. S., 2nd, Frankel, W. N., van den Pol, A. N., Bloom, F. E., Gautvik, K. M., & Sutcliffe, J. G. (1998). The hypocretins: hypothalamus-specific peptides with neuroexcitatory activity. *Proc Natl Acad Sci U S A*, *95*(1), 322-327. https://doi.org/10.1073/pnas.95.1.322

Dibner, C., Schibler, U., & Albrecht, U. (2010). The mammalian circadian timing system: organization and coordination of central and peripheral clocks. *Annu Rev Physiol*, *72*, 517-549. https://doi.org/10.1146/annurev-physiol-021909-135821

Dijk, D.-J. (1995). EEG slow waves and sleep spindles: windows on the sleeping brain. *Behav Brain Res*, *69*(1), 109-116. https://doi.org/https://doi.org/10.1016/0166-4328(95)00007-G

Dijk, D. J., & Archer, S. N. (2010). PERIOD3, circadian phenotypes, and sleep homeostasis. *Sleep Med Rev*, *14*(3), 151-160. https://doi.org/10.1016/j.smrv.2009.07.002

Dittrich, L., Morairty, S. R., Warrier, D. R., & Kilduff, T. S. (2015). Homeostatic sleep pressure is the primary factor for activation of cortical nNOS/NK1 neurons. *Neuropsychopharmacology*, *40*(3), 632-639. https://doi.org/10.1038/npp.2014.212

Drew, V. J., Lee, J. M., & Kim, T. (2018). Optogenetics: Solving the Enigma of Sleep. *Sleep Med Res*, *9*(1), 1-10. https://doi.org/10.17241/smr.2018.00178

Dringenberg, H. C. (2019). Preface: Sleep Research in the 21st Century—Advances and Challenges. In H. C. Dringenberg (Ed.), *Handbook of Behavioral Neuroscience* (Vol. 30, pp. xvii). Elsevier. https://doi.org/https://doi.org/10.1016/B978-0-12-813743-7.10000-3

Dworak, M., Kim, T., McCarley, R. W., & Basheer, R. (2017). Creatine supplementation reduces sleep need and homeostatic sleep pressure in rats. *J Sleep Res*, *26*(3), 377-385. https://doi.org/10.1111/jsr.12523

Eastridge, B. J., Hamilton, E. C., O'Keefe, G. E., Rege, R. V., Valentine, R. J., Jones, D. J., Tesfay, S., & Thal, E. R. (2003). Effect of sleep deprivation on the performance of simulated laparoscopic surgical skill. *The American Journal of Surgery*, *186*(2), 169-174. https://doi.org/https://doi.org/10.1016/S0002-9610(03)00183-1

Eban-Rothschild, A., Rothschild, G., Giardino, W. J., Jones, J. R., & de Lecea, L. (2016). VTA dopaminergic neurons regulate ethologically relevant sleep-wake behaviors. *Nat Neurosci*, *19*(10), 1356-1366. https://doi.org/10.1038/nn.4377

Elmenhorst, D., Elmenhorst, E.-M., Hennecke, E., Kroll, T., Matusch, A., Aeschbach, D., & Bauer, A. (2017). Recovery sleep after extended wakefulness restores elevated A₁ adenosine receptor availability in the human brain. *Proceedings of the National Academy of Sciences*, *114*(16), 4243-4248. https://doi.org/10.1073/pnas.1614677114

Elmenhorst, D., Meyer, P. T., Winz, O. H., Matusch, A., Ermert, J., Coenen, H. H., Basheer, R., Haas, H. L., Zilles, K., & Bauer, A. (2007). Sleep Deprivation Increases A₁ Adenosine Receptor Binding in the Human Brain: A Positron Emission Tomography Study. *The Journal of Neuroscience*, *27*(9), 2410-2415. https://doi.org/10.1523/jneurosci.5066-06.2007

Erickson, E. T. M., Ferrari, L. L., Gompf, H. S., & Anaclet, C. (2019). Differential Role of Pontomedullary Glutamatergic Neuronal Populations in Sleep-Wake Control. *Front Neurosci*, *13*, 755. https://doi.org/10.3389/fnins.2019.00755

Everson, C. A., Bergmann, B. M., & Rechtschaffen, A. (1989). Sleep deprivation in the rat: III. Total sleep deprivation. *Sleep*, *12*(1), 13-21. https://doi.org/10.1093/sleep/12.1.13

Fan, Y., Chen, P., Raza, M. U., Szebeni, A., Szebeni, K., Ordway, G. A., Stockmeier, C. A., & Zhu, M.-Y. (2018). Altered Expression of Phox2 Transcription Factors in the Locus Coeruleus in Major Depressive Disorder Mimicked by Chronic Stress and Corticosterone Treatment In Vivo and In Vitro. *Neuroscience*, *393*, 123-137. https://doi.org/10.1016/j.neuroscience.2018.09.038

Fang, Z., & Rao, H. (2017). Imaging homeostatic sleep pressure and circadian rhythm in the human brain. *Journal of thoracic disease*, *9*(5), E495-E498. https://doi.org/10.21037/jtd.2017.03.168

Fernandez-Mendoza, J., & Vgontzas, A. N. (2013). Insomnia and its impact on physical and mental health. *Current psychiatry reports*, *15*(12), 418-418. https://doi.org/10.1007/s11920-013-0418-8

Fink, A. M., Bronas, U. G., & Calik, M. W. (2018). Autonomic regulation during sleep and wakefulness: a review with implications for defining the pathophysiology of neurological disorders. *Clinical autonomic research : official journal of the Clinical Autonomic Research Society*, *28*(6), 509-518. https://doi.org/10.1007/s10286-018-0560-9

Forget, D., Morin, C. M., & Bastien, C. H. (2011). The role of the spontaneous and evoked k-complex in good-sleeper controls and in individuals with insomnia. *Sleep*, *34*(9), 1251-1260. https://doi.org/10.5665/SLEEP.1250

Friedman, L., Bergmann, B. M., & Rechtschaffen, A. (1979). Effects of sleep deprivation on sleepiness, sleep intensity, and subsequent sleep in the rat. *Sleep*, *1*(4), 369-391. https://doi.org/10.1093/sleep/1.4.369

Fuller, P. M., Yamanaka, A., & Lazarus, M. (2015). How genetically engineered systems are helping to define, and in some cases redefine, the neurobiological basis of sleep and wake. *Temperature*, *2*(3), 406-417. https://doi.org/10.1080/23328940.2015.1075095

Funk, C. M., Peelman, K., Bellesi, M., Marshall, W., Cirelli, C., & Tononi, G. (2017). Role of Somatostatin-Positive Cortical Interneurons in the Generation of Sleep Slow Waves. *The Journal of Neuroscience*, *37*(38), 9132-9148. https://doi.org/10.1523/jneurosci.1303-17.2017

Gallopin, T., Luppi, P. H., Cauli, B., Urade, Y., Rossier, J., Hayaishi, O., Lambolez, B., & Fort, P. (2005). The endogenous somnogen adenosine excites a subset of sleep-promoting neurons via A2A receptors in the ventrolateral preoptic nucleus. *Neuroscience*, *134*(4), 1377-1390. https://doi.org/https://doi.org/10.1016/j.neuroscience.2005.05.045

Garbarg, M., Barbin, G., Feger, J., & Schwartz, J.-C. (1974). Histaminergic Pathway in Rat Brain Evidenced by Lesions of the Medial Forebrain Bundle. *Science*, *186*(4166), 833-835. https://doi.org/10.1126/science.186.4166.833

Gass, N., Porkka-Heiskanen, T., & Kalinchuk, A. V. (2009). The role of the basal forebrain adenosine receptors in sleep homeostasis. *Neuroreport*, *20*(11), 1013-1018. https://doi.org/10.1097/WNR.0b013e32832d5859

Gompf, H. S., & Anaclet, C. (2020). The neuroanatomy and neurochemistry of sleep-wake control. *Curr Opin Physiol*, *15*, 143-151. https://doi.org/10.1016/j.cophys.2019.12.012

Gompf, H. S., Mathai, C., Fuller, P. M., Wood, D. A., Pedersen, N. P., Saper, C. B., & Lu, J. (2010). Locus Ceruleus and Anterior Cingulate Cortex Sustain Wakefulness in a Novel Environment. *The Journal of Neuroscience*, *30*(43), 14543-14551. https://doi.org/10.1523/jneurosci.3037-10.2010

Grandner, M. A. (2017). Sleep, Health, and Society. *Sleep Med Clin*, *12*(1), 1-22. https://doi.org/10.1016/j.jsmc.2016.10.012

Gritti, I., Mainville, L., & Jones, B. E. (1993). Codistribution of GABA- with acetylcholine-synthesizing neurons in the basal forebrain of the rat. *Journal of Comparative Neurology*, *329*(4), 438-457. https://doi.org/10.1002/cne.903290403

Gritti, I., Mainville, L., & Jones, B. E. (1994). Projections of GABAergic and cholinergic basal forebrain and GABAergic preoptic-anterior hypothalamic neurons to the posterior lateral hypothalamus of the rat. *Journal of Comparative Neurology*, *339*(2), 251-268. https://doi.org/10.1002/cne.903390206

Gritti, I., Mainville, L., Mancia, M., & Jones, B. E. (1997). GABAergic and other noncholinergic basal forebrain neurons, together with cholinergic neurons, project to the mesocortex and isocortex in the rat. *J Comp Neurol*, *383*(2), 163-177.

Hattar, S., Liao, H. W., Takao, M., Berson, D. M., & Yau, K. W. (2002). Melanopsin-containing retinal ganglion cells: architecture, projections, and intrinsic photosensitivity. *Science*, *295*(5557), 1065-1070. https://doi.org/10.1126/science.1069609

Hayashi, Y., Kashiwagi, M., Yasuda, K., Ando, R., Kanuka, M., Sakai, K., & Itohara, S. (2015). Cells of a common developmental origin regulate REM/non-REM sleep and wakefulness in mice. *Science*, *350*(6263), 957-961. https://doi.org/10.1126/science.aad1023

Henny, P., & Jones, B. E. (2008). Projections from basal forebrain to prefrontal cortex comprise cholinergic, GABAergic and glutamatergic inputs to pyramidal cells or interneurons. *The European journal of neuroscience*, *27*(3), 654-670. https://doi.org/10.1111/j.1460-9568.2008.06029.x

Hernan, A. E., Schevon, C. A., Worrell, G. A., Galanopoulou, A. S., Kahane, P., de Curtis, M., Ikeda, A., Quilichini, P., Williamson, A., Garcia-Cairasco, N., Scott, R. C., & Timofeev, I. (2017). Methodological standards and functional correlates of depth in vivo electrophysiological recordings in control rodents. A TASK1-WG3 report of the AES/ILAE Translational Task Force of the ILAE. *Epilepsia*, *58*(S4), 28-39. https://doi.org/10.1111/epi.13905

Honjoh, S., Sasai, S., Schiereck, S. S., Nagai, H., Tononi, G., & Cirelli, C. (2018). Regulation of cortical activity and arousal by the matrix cells of the ventromedial thalamic nucleus. *Nature Communications*, *9*(1), 2100. https://doi.org/10.1038/s41467-018-04497-x

Hsieh, K. C., Gvilia, I., Kumar, S., Uschakov, A., McGinty, D., Alam, M. N., & Szymusiak, R. (2011). c-Fos expression in neurons projecting from the preoptic and lateral hypothalamic areas to the ventrolateral periaqueductal gray in relation to sleep states. *Neuroscience*, *188*, 55-67. https://doi.org/10.1016/j.neuroscience.2011.05.016

Huang, Z. L., Qu, W. M., Eguchi, N., Chen, J. F., Schwarzschild, M. A., Fredholm, B. B., Urade, Y., & Hayaishi, O. (2005). Adenosine A2A, but not

A1, receptors mediate the arousal effect of caffeine. *Nat Neurosci*, *8*(7), 858-859. https://doi.org/10.1038/nn1491

Imeri, L., & Opp, M. R. (2009). How (and why) the immune system makes us sleep. *Nature Reviews Neuroscience*, *10*(3), 199-210. https://doi.org/10.1038/nrn2576

Jones, B. E., & Yang, T.-Z. (1985). The efferent projections from the reticular formation and the locus coeruleus studied by anterograde and retrograde axonal transport in the rat. *Journal of Comparative Neurology*, *242*(1), 56-92. https://doi.org/10.1002/cne.902420105

Kang, B. J., Chang, D. A., Mackay, D. D., West, G. H., Moreira, T. S., Takakura, A. C., Gwilt, J. M., Guyenet, P. G., & Stornetta, R. L. (2007). Central nervous system distribution of the transcription factor Phox2b in the adult rat. *J Comp Neurol*, *503*(5), 627-641. https://doi.org/10.1002/cne.21409

Kantor, S., Mochizuki, T., Lops, S. N., Ko, B., Clain, E., Clark, E., Yamamoto, M., & Scammell, T. E. (2013). Orexin gene therapy restores the timing and maintenance of wakefulness in narcoleptic mice. *Sleep*, *36*(8), 1129-1138. https://doi.org/10.5665/sleep.2870

Kaur, S., Pedersen, N. P., Yokota, S., Hur, E. E., Fuller, P. M., Lazarus, M., Chamberlin, N. L., & Saper, C. B. (2013). Glutamatergic Signaling from the Parabrachial Nucleus Plays a Critical Role in Hypercapnic Arousal. *The Journal of Neuroscience*, *33*(18), 7627-7640. https://doi.org/10.1523/jneurosci.0173-13.2013

Kaur, S., Wang, J. L., Ferrari, L., Thankachan, S., Kroeger, D., Venner, A., Lazarus, M., Wellman, A., Arrigoni, E., Fuller, P. M., & Saper, C. B. (2017). A Genetically Defined Circuit for Arousal from Sleep during Hypercapnia. *Neuron*, *96*(5), 1153-1167.e1155. https://doi.org/10.1016/j.neuron.2017.10.009

Killgore, W. D. S. (2010). Effects of sleep deprivation on cognition. In G. A. Kerkhof & H. P. A. v. Dongen (Eds.), *Prog Brain Res* (Vol. 185, pp. 105-129). Elsevier. https://doi.org/https://doi.org/10.1016/B978-0-444-53702-7.00007-5

Kim, T., Thankachan, S., McKenna, J. T., McNally, J. M., Yang, C., Choi, J. H., Chen, L., Kocsis, B., Deisseroth, K., Strecker, R. E., Basheer, R., Brown, R. E., & McCarley, R. W. (2015). Cortically projecting basal forebrain parvalbumin neurons regulate cortical gamma band oscillations. *Proceedings of the National Academy of Sciences*, *112*(11), 3535-3540. https://doi.org/10.1073/pnas.1413625112

Kodani, S., Soya, S., & Sakurai, T. (2017). Excitation of GABAergic Neurons in the Bed Nucleus of the Stria Terminalis Triggers Immediate Transition from Non-Rapid Eye Movement Sleep to Wakefulness in Mice. *The Journal of Neuroscience*, *37*(30), 7164-7176. https://doi.org/10.1523/jneurosci.0245-17.2017

Köhler, C., Swanson, L. W., Haglund, L., & Wu, J. Y. (1985). The cytoarchitecture, histochemistry and projections of the tuberomammillary

nucleus in the rat. *Neuroscience*, *16*(1), 85-110. https://doi.org/10.1016/0306-4522(85)90049-1

Kroeger, D., Absi, G., Gagliardi, C., Bandaru, S. S., Madara, J. C., Ferrari, L. L., Arrigoni, E., Münzberg, H., Scammell, T. E., Saper, C. B., & Vetrivelan, R. (2018). Galanin neurons in the ventrolateral preoptic area promote sleep and heat loss in mice. *Nature Communications*, *9*(1), 4129. https://doi.org/10.1038/s41467-018-06590-7

Kroeger, D., Bandaru, S. S., Madara, J. C., & Vetrivelan, R. (2019). Ventrolateral periaqueductal gray mediates rapid eye movement sleep regulation by melanin-concentrating hormone neurons. *Neuroscience*, *406*, 314-324. https://doi.org/https://doi.org/10.1016/j.neuroscience.2019.03.020

Kroeger, D., Ferrari, L. L., Petit, G., Mahoney, C. E., Fuller, P. M., Arrigoni, E., & Scammell, T. E. (2017). Cholinergic, Glutamatergic, and GABAergic Neurons of the Pedunculopontine Tegmental Nucleus Have Distinct Effects on Sleep/Wake Behavior in Mice. *The Journal of Neuroscience*, *37*(5), 1352-1366. https://doi.org/10.1523/jneurosci.1405-16.2016

Kudo, T., Konno, K., Uchigashima, M., Yanagawa, Y., Sora, I., Minami, M., & Watanabe, M. (2014). GABAergic neurons in the ventral tegmental area receive dual GABA/enkephalin-mediated inhibitory inputs from the bed nucleus of the stria terminalis. *Eur J Neurosci*, *39*(11), 1796-1809. https://doi.org/10.1111/ejn.12503

Kumar, S., Rai, S., Hsieh, K.-C., McGinty, D., Alam, M. N., & Szymusiak, R. (2013). Adenosine A(2A) receptors regulate the activity of sleep regulatory GABAergic neurons in the preoptic hypothalamus. *American journal of physiology. Regulatory, integrative and comparative physiology*, *305*(1), R31-R41. https://doi.org/10.1152/ajpregu.00402.2012

Landrigan, C. P. (2008). Driving drowsy. *Journal of clinical sleep medicine : JCSM : official publication of the American Academy of Sleep Medicine*, *4*(6), 536-537.

Lazarus, M., Shen, H.-Y., Cherasse, Y., Qu, W.-M., Huang, Z.-L., Bass, C. E., Winsky-Sommerer, R., Semba, K., Fredholm, B. B., Boison, D., Hayaishi, O., Urade, Y., & Chen, J.-F. (2011). Arousal Effect of Caffeine Depends on Adenosine A_{2A} Receptors in the Shell of the Nucleus Accumbens. *The Journal of Neuroscience*, *31*(27), 10067-10075. https://doi.org/10.1523/jneurosci.6730-10.2011

Lesku, J. A., Aulsebrook, A. E., Kelly, M. L., & Tisdale, R. K. (2019). Chapter 20 - Evolution of Sleep and Adaptive Sleeplessness. In H. C. Dringenberg (Ed.), *Handbook of Behavioral Neuroscience* (Vol. 30, pp. 299-316). Elsevier. https://doi.org/https://doi.org/10.1016/B978-0-12-813743-7.00020-7

Lesku, J. A., & Ly, L. M. T. (2017). Sleep Origins: Restful Jellyfish Are Sleeping Jellyfish. *Current Biology*, *27*(19), R1060-R1062. https://doi.org/https://doi.org/10.1016/j.cub.2017.08.024

Lesku, J. A., Vyssotski, A. L., Martinez-Gonzalez, D., Wilzeck, C., & Rattenborg, N. C. (2011). Local sleep homeostasis in the avian brain: convergence of sleep function in mammals and birds? *Proceedings of the Royal Society B: Biological Sciences*, *278*(1717), 2419-2428. https://doi.org/doi:10.1098/rspb.2010.2316

Li, X., Yu, B., Sun, Q., Zhang, Y., Ren, M., Zhang, X., Li, A., Yuan, J., Madisen, L., Luo, Q., Zeng, H., Gong, H., & Qiu, Z. (2018). Generation of a whole-brain atlas for the cholinergic system and mesoscopic projectome analysis of basal forebrain cholinergic neurons. *Proceedings of the National Academy of Sciences*, *115*(2), 415-420. https://doi.org/10.1073/pnas.1703601115

Liang, C.-L., Quang Nguyen, T., & Marks, G. A. (2014). Inhibitory and excitatory amino acid neurotransmitters are utilized by the projection from the dorsal deep mesencephalic nucleus to the sublaterodorsal nucleus REM sleep induction zone. *Brain Research*, *1567*, 1-12. https://doi.org/10.1016/j.brainres.2014.04.016

Lima, S. L., Rattenborg, N. C., Lesku, J. A., & Amlaner, C. J. (2005). Sleeping under the risk of predation. *Animal Behaviour*, *70*(4), 723-736. https://doi.org/https://doi.org/10.1016/j.anbehav.2005.01.008

Lin, L., Faraco, J., Li, R., Kadotani, H., Rogers, W., Lin, X., Qiu, X., de Jong, P. J., Nishino, S., & Mignot, E. (1999). The Sleep Disorder Canine Narcolepsy Is Caused by a Mutation in the Hypocretin (Orexin) Receptor 2 Gene. *Cell*, *98*(3), 365-376. https://doi.org/10.1016/S0092-8674(00)81965-0

Liu, J., Krautzberger, A. M., Sui, S. H., Hofmann, O. M., Chen, Y., Baetscher, M., Grgic, I., Kumar, S., Humphreys, B., Hide, W. A., & McMahon, A. P. (2014). Cell-specific translational profiling in acute kidney injury. *The Journal of Clinical Investigation*, *124*(3), 1242-1254. https://doi.org/10.1172/JCI72126

Liu, K., Kim, J., Kim, D. W., Zhang, Y. S., Bao, H., Denaxa, M., Lim, S.-A., Kim, E., Liu, C., Wickersham, I. R., Pachnis, V., Hattar, S., Song, J., Brown, S. P., & Blackshaw, S. (2017). Lhx6-positive GABA-releasing neurons of the zona incerta promote sleep. *Nature*, *548*(7669), 582-587. https://doi.org/10.1038/nature23663

Liu, N., Fu, C., Yu, H., Wang, Y., Shi, L., Hao, Y., Yuan, F., Zhang, X., & Wang, S. (2020). Respiratory Control by Phox2b-expressing Neurons in a Locus Coeruleus-preBötzinger Complex Circuit. *Neurosci Bull*. https://doi.org/10.1007/s12264-020-00519-1

Liu, Y. W., Li, J., & Ye, J. H. (2010). Histamine regulates activities of neurons in the ventrolateral preoptic nucleus. *J Physiol*, *588*(Pt 21), 4103-4116. https://doi.org/10.1113/jphysiol.2010.193904

Liu, Z.-W., & Gao, X.-B. (2007). Adenosine Inhibits Activity of Hypocretin/Orexin Neurons by the A1 Receptor in the Lateral Hypothalamus: A Possible

Sleep-Promoting Effect. *Journal of Neurophysiology*, *97*(1), 837-848. https://doi.org/10.1152/jn.00873.2006

Loddo, G., Calandra-Buonaura, G., Sambati, L., Giannini, G., Cecere, A., Cortelli, P., & Provini, F. (2017). The Treatment of Sleep Disorders in Parkinson's Disease: From Research to Clinical Practice. *Frontiers in neurology*, *8*, 42-42. https://doi.org/10.3389/fneur.2017.00042

Lu, J., Sherman, D., Devor, M., & Saper, C. B. (2006). A putative flip-flop switch for control of REM sleep. *Nature*, *441*(7093), 589-594. https://doi.org/10.1038/nature04767

Luo, Y.-J., Li, Y.-D., Wang, L., Yang, S.-R., Yuan, X.-S., Wang, J., Cherasse, Y., Lazarus, M., Chen, J.-F., Qu, W.-M., & Huang, Z.-L. (2018). Nucleus accumbens controls wakefulness by a subpopulation of neurons expressing dopamine D1 receptors. *Nature Communications*, *9*(1), 1576. https://doi.org/10.1038/s41467-018-03889-3

Luppi, P. H., Aston-Jones, G., Akaoka, H., Chouvet, G., & Jouvet, M. (1995). Afferent projections to the rat locus coeruleus demonstrated by retrograde and anterograde tracing with cholera-toxin B subunit and Phaseolus vulgaris leucoagglutinin. *Neuroscience*, *65*(1), 119-160. https://doi.org/https://doi.org/10.1016/0306-4522(94)00481-J

Ma, C., Zhong, P., Liu, D., Barger, Z. K., Zhou, L., Chang, W.-C., Kim, B., & Dan, Y. (2019). Sleep Regulation by Neurotensinergic Neurons in a Thalamo-Amygdala Circuit. *Neuron*, *103*(2), 323-334.e327. https://doi.org/https://doi.org/10.1016/j.neuron.2019.05.015

Ma, Q. D. Y., Ji, C., Xie, H., Yin, K., Ma, Z., & Bian, C. (2018). Transitions in physiological coupling between heartbeat and pulse across sleep stages. *Physiol Meas*, *39*(3), 034006. https://doi.org/10.1088/1361-6579/aab024

Mátyás, F., Komlósi, G., Babiczky, Á., Kocsis, K., Barthó, P., Barsy, B., Dávid, C., Kanti, V., Porrero, C., Magyar, A., Szűcs, I., Clasca, F., & Acsády, L. (2018). A highly collateralized thalamic cell type with arousal-predicting activity serves as a key hub for graded state transitions in the forebrain. *Nature Neuroscience*, *21*(11), 1551-1562. https://doi.org/10.1038/s41593-018-0251-9

McDonald, A. J., Muller, J. F., & Mascagni, F. (2011). Postsynaptic targets of GABAergic basal forebrain projections to the basolateral amygdala. *Neuroscience*, *183*, 144-159. https://doi.org/10.1016/j.neuroscience.2011.03.027

Méndez, M., & Radtke, R. A. (2001). Interactions Between Sleep and Epilepsy. *Journal of Clinical Neurophysiology*, *18*(2), 106-127. https://journals.lww.com/clinicalneurophys/Fulltext/2001/03000/Interactions_Between_Sleep_and_Epilepsy.3.aspx

Mesulam, M. M., Mufson, E. J., Levey, A. I., & Wainer, B. H. (1983). Cholinergic innervation of cortex by the basal forebrain: cytochemistry and cortical connections of the septal area, diagonal band nuclei, nucleus basalis

(substantia innominata), and hypothalamus in the rhesus monkey. *J Comp Neurol*, *214*(2), 170-197. https://doi.org/10.1002/cne.902140206

Methippara, M. M., Kumar, S., Alam, M. N., Szymusiak, R., & McGinty, D. (2005). Effects on sleep of microdialysis of adenosine A1 and A2a receptor analogs into the lateral preoptic area of rats. *American journal of physiology. Regulatory, integrative and comparative physiology*, *289*(6), R1715-1723. https://doi.org/10.1152/ajpregu.00247.2005

Mitrofanis, J. (2005). Some certainty for the "zone of uncertainty"? Exploring the function of the zona incerta. *Neuroscience*, *130*(1), 1-15. https://doi.org/10.1016/j.neuroscience.2004.08.017

Mochizuki, T., Crocker, A., McCormack, S., Yanagisawa, M., Sakurai, T., & Scammell, T. E. (2004). Behavioral state instability in orexin knock-out mice. *J Neurosci*, *24*(28), 6291-6300. https://doi.org/10.1523/JNEUROSCI.0586-04.2004

Morairty, S. R., Dittrich, L., Pasumarthi, R. K., Valladao, D., Heiss, J. E., Gerashchenko, D., & Kilduff, T. S. (2013). A role for cortical nNOS/NK1 neurons in coupling homeostatic sleep drive to EEG slow wave activity. *Proc Natl Acad Sci U S A*, *110*(50), 20272-20277. https://doi.org/10.1073/pnas.1314762110

Morairty, S., Rainnie, D., McCarley, R., & Greene, R. (2004). Disinhibition of ventrolateral preoptic area sleep-active neurons by adenosine: a new mechanism for sleep promotion. *Neuroscience*, *123*(2), 451-457. https://doi.org/https://doi.org/10.1016/j.neuroscience.2003.08.066

Moreira, T. S., Takakura, A. C., Czeisler, C., & Otero, J. J. (2016). Respiratory and autonomic dysfunction in congenital central hypoventilation syndrome. *J Neurophysiol*, *116*(2), 742-752. https://doi.org/10.1152/jn.00026.2016

Moruzzi, G., & Magoun, H. W. (1949). Brain stem reticular formation and activation of the EEG. *Electroencephalography and Clinical Neurophysiology*, *1*(1), 455-473. https://doi.org/https://doi.org/10.1016/0013-4694(49)90219-9

Neckelmann, D., & Ursin, R. (1993). Sleep stages and EEG power spectrum in relation to acoustical stimulus arousal threshold in the rat. *Sleep*, *16*(5), 467-477.

Neske, G. T., & Connors, B. W. (2016). Distinct Roles of SOM and VIP Interneurons during Cortical Up States. *Front Neural Circuits*, *10*, 52. https://doi.org/10.3389/fncir.2016.00052

Nobuta, H., Cilio, M. R., Danhaive, O., Tsai, H. H., Tupal, S., Chang, S. M., Murnen, A., Kreitzer, F., Bravo, V., Czeisler, C., Gokozan, H. N., Gygli, P., Bush, S., Weese-Mayer, D. E., Conklin, B., Yee, S. P., Huang, E. J., Gray, P. A., Rowitch, D., & Otero, J. J. (2015). Dysregulation of locus coeruleus development in congenital central hypoventilation syndrome. *Acta Neuropathol*, *130*(2), 171-183. https://doi.org/10.1007/s00401-015-1441-0

Oishi, Y., Huang, Z.-L., Fredholm, B. B., Urade, Y., & Hayaishi, O. (2008). Adenosine in the tuberomammillary nucleus inhibits the histaminergic

system via A₁ receptors and promotes non-rapid eye movement sleep. *Proceedings of the National Academy of Sciences*, *105*(50), 19992-19997. https://doi.org/10.1073/pnas.0810926105

Oishi, Y., Xu, Q., Wang, L., Zhang, B.-J., Takahashi, K., Takata, Y., Luo, Y.-J., Cherasse, Y., Schiffmann, S. N., de Kerchove d'Exaerde, A., Urade, Y., Qu, W.-M., Huang, Z.-L., & Lazarus, M. (2017). Slow-wave sleep is controlled by a subset of nucleus accumbens core neurons in mice. *Nature Communications*, *8*(1), 734. https://doi.org/10.1038/s41467-017-00781-4

Okada, H., Iwase, S., Mano, T., Sugiyama, Y., & Watanabe, T. (1991). Changes in muscle sympathetic nerve activity during sleep in humans. *Neurology*, *41*(12), 1961-1961. https://doi.org/10.1212/wnl.41.12.1961

Okamura, H., Yamaguchi, S., & Yagita, K. (2002). Molecular machinery of the circadian clock in mammals. *Cell Tissue Res*, *309*(1), 47-56. https://doi.org/10.1007/s00441-002-0572-5

Ostlund, S. B., Wassum, K. M., Murphy, N. P., Balleine, B. W., & Maidment, N. T. (2011). Extracellular dopamine levels in striatal subregions track shifts in motivation and response cost during instrumental conditioning. *J Neurosci*, *31*(1), 200-207. https://doi.org/10.1523/jneurosci.4759-10.2011

Pattyn, A., Morin, X., Cremer, H., Goridis, C., & Brunet, J. F. (1997). Expression and interactions of the two closely related homeobox genes Phox2a and Phox2b during neurogenesis. *Development*, *124*(20), 4065-4075.

Paxinos, G., & Franklin, K. B. (2001). *The mouse brain in stereotaxic coordinates* (2nd ed.). Academic Press.

Pedersen, N. P., Ferrari, L., Venner, A., Wang, J. L., Abbott, S. B. G., Vujovic, N., Arrigoni, E., Saper, C. B., & Fuller, P. M. (2017). Supramammillary glutamate neurons are a key node of the arousal system. *Nature Communications*, *8*(1), 1405. https://doi.org/10.1038/s41467-017-01004-6

Peever, J., & Fuller, P. M. (2017). The Biology of REM Sleep. *Current Biology*, *27*(22), R1237-R1248. https://doi.org/https://doi.org/10.1016/j.cub.2017.10.026

Peyron, C., Tighe, D. K., van den Pol, A. N., de Lecea, L., Heller, H. C., Sutcliffe, J. G., & Kilduff, T. S. (1998). Neurons Containing Hypocretin (Orexin) Project to Multiple Neuronal Systems. *The Journal of Neuroscience*, *18*(23), 9996-10015. https://doi.org/10.1523/jneurosci.18-23-09996.1998

Pfeffer, M., Korf, H. W., & Wicht, H. (2018). Synchronizing effects of melatonin on diurnal and circadian rhythms. *Gen Comp Endocrinol*, *258*, 215-221. https://doi.org/10.1016/j.ygcen.2017.05.013

Porkka-Heiskanen, T., Strecker, R. E., Thakkar, M., Bjorkum, A. A., Greene, R. W., & McCarley, R. W. (1997). Adenosine: a mediator of the sleep-inducing effects of prolonged wakefulness. *Science*, *276*(5316), 1265-1268. https://doi.org/10.1126/science.276.5316.1265

Pudovkina, O. L., Kawahara, Y., de Vries, J., & Westerink, B. H. (2001). The release of noradrenaline in the locus coeruleus and prefrontal cortex

studied with dual-probe microdialysis. *Brain Res*, *906*(1-2), 38-45. https://doi.org/10.1016/s0006-8993(01)02553-7

Qiu, M.-H., Zhong, Z.-G., Chen, M. C., & Lu, J. (2019). Nigrostriatal and mesolimbic control of sleep–wake behavior in rat. *Brain Structure and Function*, *224*(7), 2525-2535. https://doi.org/10.1007/s00429-019-01921-w

Radulovacki, M., Virus, R. M., Djuricic-Nedelson, M., & Green, R. D. (1984). Adenosine analogs and sleep in rats. *J Pharmacol Exp Ther*, *228*(2), 268-274.

Rainnie, D., Grunze, H., McCarley, R., & Greene, R. (1994). Adenosine inhibition of mesopontine cholinergic neurons: implications for EEG arousal. *Science*, *263*(5147), 689-692. https://doi.org/10.1126/science.8303279

Rajaratnam, S. M. W., & Arendt, J. (2001). Health in a 24-h society. *The Lancet*, *358*(9286), 999-1005. https://doi.org/https://doi.org/10.1016/S0140-6736(01)06108-6

Reppert, S. M., Weaver, D. R., Stehle, J. H., & Rivkees, S. A. (1991). Molecular cloning and characterization of a rat A1-adenosine receptor that is widely expressed in brain and spinal cord. *Mol Endocrinol*, *5*(8), 1037-1048. https://doi.org/10.1210/mend-5-8-1037

Reichert, S., Pavón Arocas, O., & Rihel, J. (2019). The Neuropeptide Galanin Is Required for Homeostatic Rebound Sleep following Increased Neuronal Activity. *Neuron*, *104*(2), 370-384.e375. https://doi.org/10.1016/j.neuron.2019.08.010

Ren, S., Wang, Y., Yue, F., Cheng, X., Dang, R., Qiao, Q., Sun, X., Li, X., Jiang, Q., Yao, J., Qin, H., Wang, G., Liao, X., Gao, D., Xia, J., Zhang, J., Hu, B., Yan, J., Wang, Y., Xu, M., Han, Y., Tang, X., Chen, X., He, C., & Hu, Z. (2018). The paraventricular thalamus is a critical thalamic area for wakefulness. *Science*, *362*(6413), 429-434. https://doi.org/10.1126/science.aat2512

Reppert, S. M., & Weaver, D. R. (2002). Coordination of circadian timing in mammals. *Nature*, *418*(6901), 935-941. https://doi.org/10.1038/nature00965

Ronzoni, G., Del Arco, A., Mora, F., & Segovia, G. (2016). Enhanced noradrenergic activity in the amygdala contributes to hyperarousal in an animal model of PTSD. *Psychoneuroendocrinology*, *70*, 1-9. https://doi.org/10.1016/j.psyneuen.2016.04.018

Rossi, J., Balthasar, N., Olson, D., Scott, M., Berglund, E., Lee, C. E., Choi, M. J., Lauzon, D., Lowell, B. B., & Elmquist, J. K. (2011). Melanocortin-4 receptors expressed by cholinergic neurons regulate energy balance and glucose homeostasis. *Cell Metab*, *13*(2), 195-204. https://doi.org/10.1016/j.cmet.2011.01.010

Roth, T., Coulouvrat, C., Hajak, G., Lakoma, M. D., Sampson, N. A., Shahly, V., Shillington, A. C., Stephenson, J. J., Walsh, J. K., & Kessler, R. C. (2011). Prevalence and Perceived Health Associated with Insomnia Based on DSM-IV-TR; International Statistical Classification of Diseases and

Related Health Problems, Tenth Revision; and Research Diagnostic Criteria/International Classification of Sleep Disorders, Second Edition Criteria: Results from the America Insomnia Survey. *Biological Psychiatry*, *69*(6), 592-600. https://doi.org/https://doi.org/10.1016/j.biopsych.2010.10.023

Sack, R. L., Lewy, A. J., & Hughes, R. J. (1998). Use of melatonin for sleep and circadian rhythm disorders. *Ann Med*, *30*(1), 115-121. https://doi.org/10.3109/07853899808999393

Sakai, K. (2017). Are there Sleep-promoting Neurons in the Mouse Parafacial Zone? *Neuroscience*, *367*, 98-109. https://doi.org/10.1016/j.neuroscience.2017.10.026

Sakai, K. (2018). Single unit activity of periaqueductal gray and deep mesencephalic nucleus neurons involved in sleep stage switching in the mouse. *European Journal of Neuroscience*, *47*(9), 1110-1126. https://doi.org/10.1111/ejn.13888

Sakurai, T., Amemiya, A., Ishii, M., Matsuzaki, I., Chemelli, R. M., Tanaka, H., Williams, S. C., Richardson, J. A., Kozlowski, G. P., Wilson, S., Arch, J. R. S., Buckingham, R. E., Haynes, A. C., Carr, S. A., Annan, R. S., McNulty, D. E., Liu, W.-S., Terrett, J. A., Elshourbagy, N. A., Bergsma, D. J., & Yanagisawa, M. (1998). Orexins and Orexin Receptors: A Family of Hypothalamic Neuropeptides and G Protein-Coupled Receptors that Regulate Feeding Behavior. *Cell*, *92*(4), 573-585. https://doi.org/10.1016/S0092-8674(00)80949-6

Salamone, J. D. (1994). The involvement of nucleus accumbens dopamine in appetitive and aversive motivation. *Behav Brain Res*, *61*(2), 117-133. https://doi.org/10.1016/0166-4328(94)90153-8

Salamone, J. D., & Correa, M. (2009). Dopamine/adenosine interactions involved in effort-related aspects of food motivation. *Appetite*, *53*(3), 422-425. https://doi.org/https://doi.org/10.1016/j.appet.2009.07.018

Saper, C. B. (1982). Reciprocal parabrachial-cortical connections in the rat. *Brain Research*, *242*(1), 33-40. https://doi.org/https://doi.org/10.1016/0006-8993(82)90493-0

Saper, C. B., & Loewy, A. D. (1980). Efferent connections of the parabrachial nucleus in the rat. *Brain Res*, *197*(2), 291-317. https://doi.org/10.1016/0006-8993(80)91117-8

Sapin, E., Lapray, D., Bérod, A., Goutagny, R., Léger, L., Ravassard, P., Clément, O., Hanriot, L., Fort, P., & Luppi, P. H. (2009). Localization of the brainstem GABAergic neurons controlling paradoxical (REM) sleep. *PLoS One*, *4*(1), e4272. https://doi.org/10.1371/journal.pone.0004272

Sara, S. J. (2009). The locus coeruleus and noradrenergic modulation of cognition. *Nature Reviews Neuroscience*, *10*(3), 211-223. https://doi.org/10.1038/nrn2573

Satoh, S., Matsumura, Hitoshi, Koike, N., Tokunaga, Yoshimitsu, Maeda, T., & Hayaishi, O. (1999). Region-dependent difference in the sleep-promoting

potency of an adenosine A2A receptor agonist. *European Journal of Neuroscience*, *11*(5), 1587-1597. https://doi.org/10.1046/j.1460-9568.1999.00569.x

Scammell, T. E., Gerashchenko, D. Y., Mochizuki, T., McCarthy, M. T., Estabrooke, I. V., Sears, C. A., Saper, C. B., Urade, Y., & Hayaishi, O. (2001). An adenosine A2a agonist increases sleep and induces Fos in ventrolateral preoptic neurons. *Neuroscience*, *107*(4), 653-663. https://doi.org/https://doi.org/10.1016/S0306-4522(01)00383-9

Schwarz, L. A., Miyamichi, K., Gao, X. J., Beier, K. T., Weissbourd, B., DeLoach, K. E., Ren, J., Ibanes, S., Malenka, R. C., Kremer, E. J., & Luo, L. (2015). Viral-genetic tracing of the input–output organization of a central noradrenaline circuit. *Nature*, *524*(7563), 88-92. https://doi.org/10.1038/nature14600

Scullin, M. K., & Bliwise, D. L. (2015). Sleep, cognition, and normal aging: integrating a half century of multidisciplinary research. *Perspect Psychol Sci*, *10*(1), 97-137. https://doi.org/10.1177/1745691614556680

Sherin, J. E., Elmquist, J. K., Torrealba, F., & Saper, C. B. (1998). Innervation of histaminergic tuberomammillary neurons by GABAergic and galaninergic neurons in the ventrolateral preoptic nucleus of the rat. *J Neurosci*, *18*(12), 4705-4721.

Sheth, S., Brito, R., Mukherjea, D., Rybak, L. P., & Ramkumar, V. (2014). Adenosine receptors: expression, function and regulation. *International journal of molecular sciences*, *15*(2), 2024-2052. https://doi.org/10.3390/ijms15022024

Shi, L., Chen, S. J., Ma, M. Y., Bao, Y. P., Han, Y., Wang, Y. M., Shi, J., Vitiello, M. V., & Lu, L. (2018). Sleep disturbances increase the risk of dementia: A systematic review and meta-analysis. *Sleep Med Rev*, *40*, 4-16. https://doi.org/10.1016/j.smrv.2017.06.010

Shi, S., Millius, A., & Ueda, H. R. (2019). Chapter 12 - Genes and Ion Channels in the Circadian and Homeostatic Regulation of Sleep. In H. C. Dringenberg (Ed.), *Handbook of Behavioral Neuroscience* (Vol. 30, pp. 181-193). Elsevier. https://doi.org/https://doi.org/10.1016/B978-0-12-813743-7.00012-8

Shiromani, P. J., & Peever, J. H. (2017). New Neuroscience Tools That Are Identifying the Sleep-Wake Circuit. *Sleep*, *40*(4). https://doi.org/10.1093/sleep/zsx032

Siclari, F., Bernardi, G., Cataldi, J., & Tononi, G. (2018). Dreaming in NREM Sleep: A High-Density EEG Study of Slow Waves and Spindles. *J Neurosci*, *38*(43), 9175-9185. https://doi.org/10.1523/jneurosci.0855-18.2018

Siegel, J. M. (2005). Clues to the functions of mammalian sleep. *Nature*, *437*(7063), 1264-1271. https://doi.org/10.1038/nature04285

Smith, K. S., Berridge, K. C., & Aldridge, J. W. (2011). Disentangling pleasure from incentive salience and learning signals in brain reward circuitry. *Proc*

Natl Acad Sci U S A, *108*(27), E255-264. https://doi.org/10.1073/pnas.1101920108

Sokoloff, G., Uitermarkt, B. D., & Blumberg, M. S. (2015). REM sleep twitches rouse nascent cerebellar circuits: Implications for sensorimotor development. *Developmental Neurobiology*, *75*(10), 1140-1153. https://doi.org/10.1002/dneu.22177

Steinberg, E. E., Keiflin, R., Boivin, J. R., Witten, I. B., Deisseroth, K., & Janak, P. H. (2013). A causal link between prediction errors, dopamine neurons and learning. *Nat Neurosci*, *16*(7), 966-973. https://doi.org/10.1038/nn.3413

Steriade, M., Timofeev, I., & Grenier, F. (2001). Natural Waking and Sleep States: A View From Inside Neocortical Neurons. *Journal of Neurophysiology*, *85*(5), 1969-1985. https://doi.org/10.1152/jn.2001.85.5.1969

Takata, Y., Oishi, Y., Zhou, X.-Z., Hasegawa, E., Takahashi, K., Cherasse, Y., Sakurai, T., & Lazarus, M. (2018). Sleep and Wakefulness Are Controlled by Ventral Medial Midbrain/Pons GABAergic Neurons in Mice. *The Journal of Neuroscience*, *38*(47), 10080-10092. https://doi.org/10.1523/jneurosci.0598-18.2018

Taylor, S. R., Badurek, S., Dileone, R. J., Nashmi, R., Minichiello, L., & Picciotto, M. R. (2014). GABAergic and glutamatergic efferents of the mouse ventral tegmental area. *The Journal of comparative neurology*, *522*(14), 3308-3334. https://doi.org/10.1002/cne.23603

Thakkar, M. M., Engemann, S. C., Walsh, K. M., & Sahota, P. K. (2008). Adenosine and the homeostatic control of sleep: Effects of A1 receptor blockade in the perifornical lateral hypothalamus on sleep–wakefulness. *Neuroscience*, *153*(4), 875-880. https://doi.org/https://doi.org/10.1016/j.neuroscience.2008.01.017

Thakkar, M. M., Winston, S., & McCarley, R. W. (2003). A₁ Receptor and Adenosinergic Homeostatic Regulation of Sleep-Wakefulness: Effects of Antisense to the A₁ Receptor in the Cholinergic Basal Forebrain. *The Journal of Neuroscience*, *23*(10), 4278-4287. https://doi.org/10.1523/jneurosci.23-10-04278.2003

Timofeev, I., Bazhenov, M., Seigneur, J., & Sejnowski, T. (2012). Neuronal Synchronization and Thalamocortical Rhythms in Sleep, Wake and Epilepsy. In J. L. Noebels, M. Avoli, M. A. Rogawski, R. W. Olsen, & A. V. Delgado-Escueta (Eds.), *Jasper's Basic Mechanisms of the Epilepsies*. National Center for Biotechnology Information (US) Copyright © 2012, Michael A Rogawski, Antonio V Delgado-Escueta, Jeffrey L Noebels, Massimo Avoli and Richard W Olsen.

Timofeev, I., & Steriade, M. (1996). Low-frequency rhythms in the thalamus of intact-cortex and decorticated cats. *Journal of Neurophysiology*, *76*(6), 4152-4168. https://doi.org/10.1152/jn.1996.76.6.4152

Tiveron, M. C., Hirsch, M. R., & Brunet, J. F. (1996). The expression pattern of the transcription factor Phox2 delineates synaptic pathways of the autonomic nervous system. *J Neurosci*, *16*(23), 7649-7660.

Tobler, I., & Borbély, A. A. (1985). Effect of rest deprivation on motor activity of fish. *Journal of Comparative Physiology A*, *157*(6), 817-822. https://doi.org/10.1007/BF01350078

Tobler, I., Borbély, A. A., & Groos, G. (1983). The effect of sleep deprivation on sleep in rats with suprachiasmatic lesions. *Neurosci Lett*, *42*(1), 49-54. https://doi.org/10.1016/0304-3940(83)90420-2

Valencia Garcia, S., Brischoux, F., Clément, O., Libourel, P.-A., Arthaud, S., Lazarus, M., Luppi, P.-H., & Fort, P. (2018). Ventromedial medulla inhibitory neuron inactivation induces REM sleep without atonia and REM sleep behavior disorder. *Nature Communications*, *9*(1), 504. https://doi.org/10.1038/s41467-017-02761-0

Van Dongen, H. P., Maislin, G., Mullington, J. M., & Dinges, D. F. (2003). The cumulative cost of additional wakefulness: dose-response effects on neurobehavioral functions and sleep physiology from chronic sleep restriction and total sleep deprivation. *Sleep*, *26*(2), 117-126. https://doi.org/10.1093/sleep/26.2.117

Venner, A., Anaclet, C., Broadhurst, R. Y., Saper, C. B., & Fuller, P. M. (2016). A Novel Population of Wake-Promoting GABAergic Neurons in the Ventral Lateral Hypothalamus. *Curr Biol*, *26*(16), 2137-2143. https://doi.org/10.1016/j.cub.2016.05.078

Venner, A., Todd, W. D., Fraigne, J., Bowrey, H., Eban-Rothschild, A., Kaur, S., & Anaclet, C. (2019). Newly identified sleep-wake and circadian circuits as potential therapeutic targets. *Sleep*, *42*(5). https://doi.org/10.1093/sleep/zsz023

Virus, R. M., Ticho, S., Pilditch, M., & Radulovacki, M. (1990). A comparison of the effects of caffeine, 8-cyclopentyltheophylline, and alloxazine on sleep in rats. Possible roles of central nervous system adenosine receptors. *Neuropsychopharmacology*, *3*(4), 243-249.

Wagner, U., Gais, S., & Born, J. (2001). Emotional memory formation is enhanced across sleep intervals with high amounts of rapid eye movement sleep. *Learn Mem*, *8*(2), 112-119. https://doi.org/10.1101/lm.36801

Waterhouse, J., Fukuda, Y., & Morita, T. (2012). Daily rhythms of the sleep-wake cycle. *Journal of Physiological Anthropology*, *31*(1), 5. https://doi.org/10.1186/1880-6805-31-5

Weber, F., Hoang Do, J. P., Chung, S., Beier, K. T., Bikov, M., Saffari Doost, M., & Dan, Y. (2018). Regulation of REM and Non-REM Sleep by Periaqueductal GABAergic Neurons. *Nature Communications*, *9*(1), 354. https://doi.org/10.1038/s41467-017-02765-w

Wyatt, J. K., Ritz-De Cecco, A., Czeisler, C. A., & Dijk, D. J. (1999). Circadian temperature and melatonin rhythms, sleep, and neurobehavioral function

in humans living on a 20-h day. *Am J Physiol*, *277*(4 Pt 2), R1152-1163. https://doi.org/10.1152/ajpregu.1999.277.4.r1152

Yamaguchi, H., Hopf, F. W., Li, S.-B., & de Lecea, L. (2018). In vivo cell type-specific CRISPR knockdown of dopamine beta hydroxylase reduces locus coeruleus evoked wakefulness. *Nature Communications*, *9*(1), 5211. https://doi.org/10.1038/s41467-018-07566-3

Yamanaka, A., Beuckmann, C. T., Willie, J. T., Hara, J., Tsujino, N., Mieda, M., Tominaga, M., Yagami, K., Sugiyama, F., Goto, K., Yanagisawa, M., & Sakurai, T. (2003). Hypothalamic orexin neurons regulate arousal according to energy balance in mice. *Neuron*, *38*(5), 701-713. https://doi.org/10.1016/s0896-6273(03)00331-3

Yang, S.-R., Hu, Z.-Z., Luo, Y.-J., Zhao, Y.-N., Sun, H.-X., Yin, D., Wang, C.-Y., Yan, Y.-D., Wang, D.-R., Yuan, X.-S., Ye, C.-B., Guo, W., Qu, W.-M., Cherasse, Y., Lazarus, M., Ding, Y.-Q., & Huang, Z.-L. (2018). The rostromedial tegmental nucleus is essential for non-rapid eye movement sleep. *PLOS Biology*, *16*(4), e2002909. https://doi.org/10.1371/journal.pbio.2002909

Yu, X., Li, W., Ma, Y., Tossell, K., Harris, J. J., Harding, E. C., Ba, W., Miracca, G., Wang, D., Li, L., Guo, J., Chen, M., Li, Y., Yustos, R., Vyssotski, A. L., Burdakov, D., Yang, Q., Dong, H., Franks, N. P., & Wisden, W. (2019). GABA and glutamate neurons in the VTA regulate sleep and wakefulness. *Nature Neuroscience*, *22*(1), 106-119. https://doi.org/10.1038/s41593-018-0288-9

Yuan, X.-S., Wang, L., Dong, H., Qu, W.-M., Yang, S.-R., Cherasse, Y., Lazarus, M., Schiffmann, S. N., d'Exaerde, A. d. K., Li, R.-X., & Huang, Z.-L. (2017). Striatal adenosine A2A receptor neurons control active-period sleep via parvalbumin neurons in external globus pallidus. *Elife*, *6*, e29055. https://doi.org/10.7554/eLife.29055

Zhang, Z., Liu, W.-Y., Diao, Y.-P., Xu, W., Zhong, Y.-H., Zhang, J.-Y., Lazarus, M., Liu, Y.-Y., Qu, W.-M., & Huang, Z.-L. (2019). Superior Colliculus GABAergic Neurons Are Essential for Acute Dark Induction of Wakefulness in Mice. *Current Biology*, *29*(4), 637-644.e633. https://doi.org/10.1016/j.cub.2018.12.031

Zhang, Z., Zhong, P., Hu, F., Barger, Z., Ren, Y., Ding, X., Li, S., Weber, F., Chung, S., Palmiter, R. D., & Dan, Y. (2019). An Excitatory Circuit in the Perioculomotor Midbrain for Non-REM Sleep Control. *Cell*, *177*(5), 1293-1307.e1216. https://doi.org/10.1016/j.cell.2019.03.041

Zitting, K. M., Vujovic, N., Yuan, R. K., Isherwood, C. M., Medina, J. E., Wang, W., Buxton, O. M., Williams, J. S., Czeisler, C. A., & Duffy, J. F. (2018). Human Resting Energy Expenditure Varies with Circadian Phase. *Curr Biol*, *28*(22), 3685-3690.e3683. https://doi.org/10.1016/j.cub.2018.10.005